


January 2013

# Evaluating CFRP-Masonry Bond Using Thermal Imaging

Joseph Christopher Ross

University of South Florida, josep.ross@gmail.com

Follow this and additional works at: <http://scholarcommons.usf.edu/etd>

 Part of the [Civil Engineering Commons](#), and the [Materials Science and Engineering Commons](#)

## Scholar Commons Citation

Ross, Joseph Christopher, "Evaluating CFRP-Masonry Bond Using Thermal Imaging" (2013). *Graduate Theses and Dissertations*.  
<http://scholarcommons.usf.edu/etd/4838>

This Thesis is brought to you for free and open access by the Graduate School at Scholar Commons. It has been accepted for inclusion in Graduate Theses and Dissertations by an authorized administrator of Scholar Commons. For more information, please contact [scholarcommons@usf.edu](mailto:scholarcommons@usf.edu).

Evaluating CFRP-Masonry Bond

Using Thermal Imaging

by

Joseph C. Ross

A thesis submitted in partial fulfillment  
of the requirements for the degree of  
Master of Science in Civil Engineering  
Department of Civil and Environmental Engineering  
College of Engineering  
University of South Florida

Co-Major Professor: Rajan Sen, Ph.D.  
Co-Major Professor: Austin Mullins, Ph.D.  
Michael Stokes, Ph.D.

Date of Approval:  
October 18, 2013

Keywords: epoxy, thermocouple, pull-off testing, masonry strengthening, infrared thermography

Copyright © 2013, Joseph C. Ross

## DEDICATION

I would like to thank my family. My brother, David, was good enough to be my unofficial research assistant to help me perform some of the tests included in this study at strange hours of the night or whenever we were both off of work. My wife, Sarah, has also been especially supportive and has encouraged me to finish this research. This paper would not have been published without her encouragement.

## ACKNOWLEDGMENTS

I would like to thank first and foremost Dr. Rajan Sen for offering me this opportunity to perform research. Dr. Sen has been very supportive and helpful in all stages of this research and has been particularly understanding of my commitments to my employer by allowing me to work at a slower pace. I would also like to thank Dr. Gray Mullins and Danny Winters for the technical advice they offered and the valuable knowledge of instrumentation they provided. Many of the testing arrangements as well as the equipment itself were provided to me by Dr. Sen, Dr. Mullins and Danny Winters. Indeed, there would be no data to analyze or to write about without their input in this regard. Additionally, I would like to thank Howard Kliger for offering advice on epoxy properties. Lastly, I would like to thank Dr. Sen, Dr. Mullins and Dr. Michael Stokes for serving on my committee.



## TABLE OF CONTENTS

LIST OF TABLES .....	iii
LIST OF FIGURES .....	iv
ABSTRACT .....	xii
1. INTRODUCTION .....	1
1.1 Introduction to the Masonry Walls at USF .....	1
1.2 Construction Industry Background .....	2
1.3 Masonry Background .....	3
1.4 Introduction to Ground Subsidence .....	4
1.5 CFRP Background .....	5
1.6 Infrared Thermography Overview .....	5
1.7 Scope .....	6
1.8 Organization of Thesis .....	7
2. TESTING AND EQUIPMENT USED .....	9
2.1 Thermocouple Temperature Measurements .....	9
2.2 Infrared Camera .....	10
2.3 Thermal Scanner .....	11
2.4 Infrared Thermography .....	12
2.4.1 Background .....	12
2.4.2 Light .....	13
2.4.3 Active and Passive Thermography .....	13
2.4.4 Ideal Conditions and Potential Sources of Error .....	15
3. MATERIAL PROPERTIES .....	18
3.1 Carbon-Fiber Reinforced Polymers .....	18
4. TEMPERATURE DATA .....	21
4.1 Introduction .....	21
4.2 Validity of the Data .....	22
4.3 Historical Temperature Data .....	23
4.4 Other Historical Factors .....	24
5. THERMOCOUPLE RESULTS .....	30
5.1 Thermocouple Arrangement .....	30

5.2 Testing Results for Arrangement 1 .....	31
5.3 Testing Results for Arrangement 2 .....	34
6. THERMAL IMAGING RESULTS.....	47
6.1 Method of Thermography.....	47
6.2 Day 1.....	49
6.3 Day 2.....	51
7. THERMAL SCANNER RESULTS.....	66
7.1 Scanning Setup .....	66
7.2 Scan of Wall 2 .....	67
7.3 Scan of Wall 3 .....	70
8. RECOMMENDATIONS AND PREDICTIONS.....	79
8.1 General Predictions.....	79
8.2 Limitations.....	79
8.3 Pull-Off Testing.....	81
9. CONCLUSION .....	86
REFERENCES .....	91
APPENDICES .....	93
Appendix A: Wall 2 Thermal Imaging .....	94
Appendix B: Wall 2 Thermocouple Temperature Contours.....	132
Appendix C: Scanner Contours .....	140
Appendix D: Historical Thermal Stresses.....	141
Appendix E: Correction Factors .....	143
Appendix F: Wall Scan Overlays .....	145
ABOUT THE AUTHOR .....	END PAGE

## LIST OF TABLES

Table 1: Week 1 Comparison of Temperature Data .....	26
Table 2: Week 2 Comparison of Temperature Data .....	27
Table 3: Sunrise and Sunsets for 8/11/12 to 8/18/12 .....	42
Table 4: Corresponding Opposite Thermocouples on Wall 2 Double-Sided Arrangement .....	44
Table 5: Explanation of Wall 2 Scan Annotations.....	74
Table 6: Explanation of Wall 3 Scan Annotations.....	77
Table 7: Pull-Off Recommendations Wall 2. ....	83
Table 8: Pull-Off Recommendations Wall 3. ....	85

## LIST OF FIGURES

Figure 1: Plan View of Masonry Walls at USF .....	7
Figure 2: Photograph of Masonry Walls at USF .....	8
Figure 3a: Photograph of Thermocouple on Masonry Wall .....	16
Figure 3b: Photograph of Thermal Scanner .....	17
Figure 4: Historical Maximum and Minimum Temperatures for Tampa, FL. ....	27
Figure 5: Historical Daily Reversals in Temperature. ....	28
Figure 6: Bell Curve of Historical Temperature Differentials.....	28
Figure 7: Historical Rainfall in Tampa, FL .....	29
Figure 8: Historical Relative Humidity in Tampa, FL.....	29
Figure 9: Thermocouple Arrangement #1 on Wall 2 Elevation (Looking South).....	36
Figure 10: Thermocouples Installed on Wall 2.....	37
Figure 11: Wall 2 North Side Data Summary 3/31/12 to 4/7/12 (Looking South).....	37
Figure 12: Daily Behavior of Thermocouple Position 4 on North Side of Wall 2 .....	38
Figure 13: All Thermocouples Data on North Side of Wall 2.....	39
Figure 14: North Side of Wall 2 Temperature Data on 4/4/12 1:00 PM .....	40
Figure 15: Thermal Contours on North Side of Wall 2 at 1:00 PM 4/4/12 .....	40
Figure 16: Passive Heat Variation on North Side of Wall 2 on 10/17/13 at 10:31 AM.....	41
Figure 17: Overhanging End of Walls .....	41
Figure 18: North Side of Wall 2 Thermocouple Summary 8/11/12 to 8/18/12 .....	42

Figure 19: South Side of Wall 2 Thermocouple Summary 8/11/12 to 8/18/12 .....	43
Figure 20: Plan View of Double-Sided Thermocouple Arrangement on Wall 2 .....	43
Figure 21: North Side of Wall 2 8/16/12 at 1:00 PM .....	44
Figure 22: South Side of Wall 2 8/16/12 at 1:00 PM .....	45
Figure 23: Contour North Side of Wall 2 8/16/12 1:00 PM (Looking South).....	45
Figure 24: Contour South Side of Wall 2 8/16/12 1:00PM (Looking South).....	46
Figure 25: Double-Sided Temperatures on Wall 2 .....	46
Figure 26: Thermal Camera Display during Operation on 7/30/11 at 11:49 AM .....	54
Figure 27: Global Thermal Image of Wall 2 at 2:07 PM (North Side).....	54
Figure 28: Color Thermal Image of Wall 2 .....	55
Figure 29: Wall 2 Global Photo .....	55
Figure 30: Thermal Image Location 2 10:32 AM (Wall 2 on the North Side).....	56
Figure 31: Color Thermal Image at Location 2 .....	56
Figure 32: Wall 2 Location 2 Photo (North Side).....	57
Figure 33: Thermal Image Location 6 1:19 PM (North Side of Wall 2) .....	57
Figure 34: Color Thermal Image at Location 6 .....	58
Figure 35: Location 6 Photo (North Side of Wall 2) .....	58
Figure 36: Thermal Image Location 16 1:54 PM (North Side of Wall 2) .....	59
Figure 37: Color Thermal Image at Location 16 .....	59
Figure 38: Location 16 Photo (North Side of Wall 2) .....	60
Figure 39: Hot Spot 1 on 4/28/12 at 12:39 PM (North Side of Wall 2) .....	60
Figure 40: Color Thermal Image of Hot Spot 1 .....	61
Figure 41: Hot Spot 2 on 4/28/12 at 1:00 PM (North Side of Wall 2) .....	61

Figure 42: Color Thermal Image of Hot Spot 2.....	62
Figure 43: Wall 2 at Location 15 near Where Hot Spots 1 and 2 were Found.....	62
Figure 44: Location of Hot Spots Found on Wall 2 with Thermal Camera .....	63
Figure 45: Global Image of North Side of Wall 3 on 4/28/12 at 1:08 PM.....	63
Figure 46: Color Thermal Image of Wall 3 .....	64
Figure 47: Global Photo of Wall 3.....	64
Figure 48: Tear in Fabric on North Side of Wall 3.....	65
Figure 49: Thermal Scanner Setup on Wall 3.....	72
Figure 50: Relative Position of IR Sensors on Adjacent Scans .....	72
Figure 51: Wall 2 Thermal Scans (on North Side).....	73
Figure 52: Elevation of North Side of Walls Denoting Coordinate System Used in Tables.....	73
Figure 53: Wall 2 Thermal Scan Results Prior to Post Processing.....	74
Figure 54: Thermal Scan Results on Wall 2 after Post Processing.....	74
Figure 55: Hot Spots from Thermal Camera on Wall 2 (North Side of Wall) .....	75
Figure 56: Scanning Results on Wall 2 (North Side of Wall) .....	76
Figure 57: Wall 3 Thermal Scans (on North Side of Wall).....	76
Figure 58: Wall 3 Scan Results Prior to Post Processing .....	77
Figure 59: Wall 3 Scan Results after Post Processing .....	77
Figure 60: Results on Wall 3 .....	78
Figure 61: General Predictions on CFRP Bond on Walls 2 and 3.....	83
Figure 62: Wall 2 Pull-Off Recommendations (North Side Elevation Shown).....	83
Figure 63: Wall 3 Pull-Off Recommendations (North Side Elevation Shown).....	84
Figure 64: The Two Walls Investigated.....	90

Figure A1: Global View of Wall 2 at 2:07 PM.....	94
Figure A2: Color Thermal Image of Wall 2 .....	94
Figure A3: Wall 2 .....	95
Figure A4: Thermal Image at Location 1 at 10:17 AM (North Side of Wall 2).....	95
Figure A5: Color Thermal Image at Location 1 .....	96
Figure A6: Photo at Location 1 (North Side of Wall 2) .....	96
Figure A7: Thermal Image at Location 2 at 10:32 AM (North Side of Wall 2).....	97
Figure A8: Color Thermal Image at Location 2 .....	97
Figure A9: Photo at Location 2 (North Side of Wall 2) .....	98
Figure A10: Thermal Image at Location 3 at 10:43 AM (North Side of Wall 2).....	98
Figure A11: Color Thermal Image at Location 3 .....	99
Figure A12: Photo at Location 3 (North Side of Wall 2) .....	99
Figure A13: Thermal Image at Location 4 at 11:00 AM (North Side of Wall 2).....	100
Figure A14: Color Thermal Image at Location 4 .....	100
Figure A15: Photo at Location 4 (North Side of Wall 2) .....	101
Figure A16: Thermal Image at Location 5 at 12:57 PM (North Side of Wall 2) .....	101
Figure A17: Color Thermal Image at Location 5 .....	102
Figure A18: Photo at Location 5 (North Side of Wall 2) .....	102
Figure A19: Thermal Image at Location 6 at 1:19 PM (North Side of Wall 2) .....	103
Figure A20: Color Thermal Image at Location 6 .....	103
Figure A21: Photo at Location 6 (North Side of Wall 2) .....	104
Figure A22: Thermal Image at Location 7 at 1:41 PM (North Side of Wall 2) .....	104
Figure A23: Color Thermal Image at Location 7 .....	105

Figure A24: Photo at Location 7 (North Side of Wall 2) .....	105
Figure A25: Thermal Image at Location 8 at 1:51 PM (North Side of Wall 2) .....	106
Figure A26: Color Thermal Image at Location 8 .....	106
Figure A27: Photo at Location 8 (North Side of Wall 2) .....	107
Figure A28: Thermal Image at Location 9 at 10:24 AM (North Side of Wall 2).....	107
Figure A29: Color Thermal Image at Location 9 .....	108
Figure A30: Photo at Location 9 (North Side of Wall 2) .....	108
Figure A31: Thermal Image at Location 10 at 10:34 AM (North Side of Wall 2).....	109
Figure A32: Color Thermal Image at Location 10 .....	109
Figure A33: Photo at Location 10 (North Side of Wall 2) .....	110
Figure A34: Thermal Image at Location 11 at 10:47 AM (North Side of Wall 2).....	110
Figure A35: Color Thermal Image at Location 11 .....	111
Figure A36: Photo at Location 11 (North Side of Wall 2) .....	111
Figure A37: Thermal Image at Location 12 at 11:07 AM (North Side of Wall 2).....	112
Figure A38: Color Thermal Image at Location 12 .....	112
Figure A39: Photo at Location 12 (North Side of Wall 2) .....	113
Figure A40: Thermal Image at Location 13 at 1:02 PM (North Side of Wall 2) .....	113
Figure A41: Color Thermal Image at Location 13 .....	114
Figure A42: Photo at Location 13 (North Side of Wall 2) .....	114
Figure A43: Thermal Image at Location 14 at 1:23 PM (North Side of Wall 2) .....	115
Figure A44: Color Thermal Image at Location 14 .....	115
Figure A45: Photo at Location 14 (North Side of Wall 2) .....	116
Figure A46: Thermal Image at Location 15 at 1:44 PM (North Side of Wall 2) .....	116



Figure A47: Color Thermal Image at Location 15 .....	117
Figure A48: Photo at Location 15 (North Side of Wall 2) .....	117
Figure A49: Thermal Image at Location 16 at 1:54 PM (North Side of Wall 2) .....	118
Figure A50: Color Thermal Image at Location 16 .....	118
Figure A51: Photo at Location 16 (North Side of Wall 2) .....	119
Figure A52: Thermal Image at Location 17 at 10:30 AM (North Side of Wall 2).....	119
Figure A53: Color Thermal Image at Location 17 .....	120
Figure A54: Photo at Location 17 (North Side of Wall 2) .....	120
Figure A55: Thermal Image at Location 18 at 10:39 AM (North Side of Wall 2).....	121
Figure A56: Color Image at Location 18 .....	121
Figure A57: Photo at Location 18 (North Side of Wall 2) .....	122
Figure A58: Thermal Image at Location 19 at 10:51 AM (North Side of Wall 2).....	122
Figure A59: Color Image at Location 19 .....	123
Figure A60: Photo at Location 19 (North Side of Wall 2) .....	123
Figure A61: Thermal Image at Location 20 at 11:10 AM (North Side of Wall 2).....	124
Figure A62: Color Thermal Image at Location 20 .....	124
Figure A63: Photo at Location 20 (North Side of Wall 2) .....	125
Figure A64: Thermal Image at Location 21 at 1:06 PM (North Side of Wall 2) .....	125
Figure A65: Color Thermal Image at Location 21 .....	126
Figure A66: Photo at Location 21 (North Side of Wall 2) .....	126
Figure A67: Thermal Image at Location 22 at 1:34 PM (North Side of Wall 2) .....	127
Figure A68: Color Thermal Image at Location 22 .....	127
Figure A69: Photo at Location 22 (North Side of Wall 2) .....	128

Figure A70: Thermal Image at Location 23 at 1:47 PM (North Side of Wall 2) .....	128
Figure A71: Color Thermal Image at Location 23 .....	129
Figure A72: Photo at Location 23 (North Side of Wall 2) .....	129
Figure A73: Thermal Image at Location 24 at 1:58 PM (North Side of Wall 2) .....	130
Figure A74: Color Thermal Image at Location 24 .....	130
Figure A75: Photo at Location 24 (North Side of Wall 2) .....	131
Figure A76: Detailed Contour of Wall 2 North Side 4/4/12 at 1:00 PM (Looking South) .....	132
Figure A77: Wall 2 North Side Mean Contour 3/31/12 to 4/7/12 (Looking South).....	132
Figure A78: Wall 2 North Side Median Contour 3/31/12 to 4/7/12 (Looking South) .....	133
Figure A79: Wall 2 North Side Mode Contour 3/31/12 to 4/7/12 (Looking South) .....	133
Figure A80: Wall 2 North Side Max Contour 3/31/12 to 4/7/12 (Looking South) .....	134
Figure A81: Wall 2 North Side Min Contour 3/31/12 to 4/7/12 (Looking South).....	134
Figure A82: Wall 2 North Side Average Contour 8/11/12 to 8/18/12 (Looking South) .....	135
Figure A83: Wall 2 South Side Average Contour 8/11/12 to 8/18/12 (Looking South) .....	135
Figure A84: Wall 2 North Side Median Contour 8/11/12 to 8/18/12 (Looking South) .....	136
Figure A85: Wall 2 South Side Median Contour 8/11/12 to 8/18/12 (Looking South) .....	136
Figure A86: Wall 2 North Side Mode Contour 8/11/12 to 8/18/12 (Looking South) .....	137
Figure A87: Wall 2 South Side Mode Contour 8/11/12 to 8/18/12 (Looking South) .....	137
Figure A88: Wall 2 North Side Max Contour 8/11/12 to 8/18/12 (Looking South) .....	138
Figure A89: Wall 2 South Side Max Contour 8/11/12 to 8/18/12 (Looking South) .....	138
Figure A90: Wall 2 North Side Min Contour 8/11/12 to 8/18/12 (Looking South).....	139
Figure A91: Wall 2 South Side Min Contour 8/11/12 to 8/18/12 (Looking South).....	139
Figure A92: Contour of Thermal Scanner Data (Wall 2) .....	140

Figure A93: Contour of Thermal Scanner Data (Wall 3) .....	140
Figure A94: Scan Rate Corrections .....	143
Figure A95: Wall 2 Scan Overlay (Looking South) .....	145
Figure A96: Wall 3 Scan Overlay (Looking South) .....	145

## ABSTRACT

This study presents results from non-destructive testing to evaluate the degradation of the CFRP-masonry bond using thermal imaging. The goal of the research was to identify locations where there was evidence of bond deterioration that could subsequently be verified through destructive pull-off testing.

Four full-scale masonry walls were built outdoors at the University of South Florida in 1995 to evaluate the effectiveness of CFRP for repairing settlement damage. Two of the settlement-damaged walls were repaired using single layer, commercially available unidirectional CFRP systems that used Tonen (wall 3) and Henkel (wall 2) epoxies. These two walls were the subject of this investigation.

Before non-destructive tests were initiated, historical site data on temperature, humidity and rainfall variation was compiled. Over seventeen years, the walls experienced ambient temperatures as high as 98°F and as low as 25°F. The average rainfall in Tampa is about 34 inches and the annual average high humidity is around 87%. Because of the high temperature and humidity, the CFRP-masonry bond was exposed to a particularly aggressive environment.

Three types of thermal evaluation were carried out: thermocouple monitoring and both passive (solar) and active (localized heating) infrared thermal imaging. Twenty-four thermocouples were used to observe the spatial variations in temperature on the wall. Data showed that the surface temperatures of the wall are uneven with one end being hotter than the other. Measurements indicated that the wall temperatures went as high as 103°F during the week

of data collection in late March and early April of 2012. In contrast, the highest ambient temperature over the same period was 92°F. The high temperature experienced by the wall is below the glass transition temperature for the epoxies, which ranges from 140°F to 180°F.

A FLIR Tau 320 thermal imaging camera was used to identify localized de-bonding. Solar radiation heated the walls and the goal of thermal imaging was to detect hot spots which are indicative of de-bonding. Although this technique is ideal for exterior applications, initial attempts were unsuccessful. Once de-bonds were located by sounding, the camera was capable of confirming two hot spots on wall 2.

A thermal scanner built by the university from a series of ten Omega OS137 thermal sensors was used to obtain more complete thermal images of the walls. This scanner had a heating element which supplied heat and allowed for active thermography. The scanner detected 16 hot spots not seen with the thermal camera. Ten of the twelve spots on wall 2 are concentrated on a region of the wall which experienced the highest daily changes in temperature, which indicates that higher thermal and environmental cycling has caused greater de-bond.

Based on the number of hot spots found using both active and passive thermography the Toner epoxy is performing better than the Henkel epoxy. In general, the bond has endured; however, there are a few localized areas that have de-bonded. Pull-off tests are recommended on walls 2 and 3. Five locations in regions suspected to have poor bond and five locations in regions suspected to have good bond are identified for each wall.

## 1. INTRODUCTION

### 1.1 Introduction to the Masonry Walls at USF

In 1995 the Structural Research Group of the Department of Civil and Environmental Engineering at the University of South Florida (USF) set out to determine the feasibility of using CFRP to rehabilitate masonry walls damaged by ground subsidence. This was done as part of a Master's Thesis by Alfred Hartley, Jr. with Dr. Rajan Sen as his major advisor. These walls were loaded before and after the installation of the CFRP material. Only the two middle walls had CFRP installed. The CFRP provided the walls with a measurable increase in strength of between 56 to 72% when compared to the wall before the installation of CFRP [1]. The walls were built in March of 1995 just outside of the soils lab at the USF campus. They have been largely abandoned since the original testing was completed and have been subject to typical Florida weathering.

There are a total of four walls tied together by one common perpendicular wall. The walls are approximately 20 feet long. A portion of the walls rests on foundations that sit directly on soil, while the rest overhangs on steel beams. The elevated portions of the walls sit approximately 2'-8" above ground level. The walls are 8'-0" tall. Figure 1 shows the walls in plan. The filled in squares denote masonry cells that have been grouted solid and contain steel reinforcement [1]. Only the two center walls have CFRP strengthening. These walls have only one layer of CFRP reinforcement. This CFRP was bonded to the masonry with two different adhesive systems—one was from the Tonen Company of Japan and used Primer FP-NS and

Resin FR-E3P, the other was from the Henkel Company of Kankakee, IL and used Primer 13-283/13-284 and Resin 13-285/13-286. In Figure 1, North is up. The walls are constructed from standard 7 5/8" x 7 5/8" x 15 5/8" masonry blocks (nominally 8" x 8" x 16").

## 1.2 Construction Industry Background

Structures designed with Concrete Masonry Units (CMU) are built according to the building codes adopted or developed by the Authorities Having Jurisdiction (AHJs). These are the agencies that have power to regulate the construction within their boundaries. In general, most AHJs simply adopt the most recent revision of the International Building Code (IBC) published by the International Code Council (ICC) based in Washington, DC. Some jurisdictions, such as the state Florida, take the IBC as a starting point and make changes, additions, and removals they feel address issues specific to their locale. Florida uses the Florida Building Code, which uses the IBC as a model.

The latest building code put out by the ICC is IBC 2012. It only becomes effective and legally binding once AHJs begin adopting it, and that takes time. At the time of this publication, most places in the United States are still under either IBC 2006 or IBC 2009, depending on how quick the corresponding AHJ is to adopt new codes. The IBC presents two main types of requirements: structural and non-structural. In the building code are guidelines and requirements on good structural engineering practice. It sets the standards and expectations for design professionals on wind design, seismic design, steel design, concrete design, masonry design, wood design, and aluminum design. To do this it references other codes published by the American Society of Civil Engineers (ASCE), American Institute of Steel Construction (AISC), American Concrete Institute (ACI), the American Wood Council of the American Forest & Paper Association, and the Aluminum Association. These agencies constitute the main governing

bodies that recommend standards on their material or subject of expertise that are eventually adopted into structural engineering practice. The IBC also sets some of its own standards on these various issues.

The organization most relevant to masonry construction is ACI in partnership with The Masonry Society (TMS), and the Structural Engineering Institute (SEI, a division of ASCE). The standard they publish is known as “Building Code Requirements for Masonry Structures”, ACI 530, TMS 402 or ASCE 5. The latest is ACI 530-11, although since most places are using IBC 2006 or IBC 2009, ACI 530-05 and ACI 530-08 are currently the effective versions of this document as those are the editions referenced by those codes.

ACI 530 has essential data on the design of masonry buildings. It has the latest testing and technical data and recommended procedures for design. It also has essential data on masonry materials. The way that masonry is constructed today is heavily influenced by these codes and standards.

The corresponding organization for Fiber Reinforced Polymers (FRP) is also ACI. They publish the “Guide for the Design and Construction of Externally Bonded FRP Systems for Strengthening Concrete Structures”, ACI 440.2R. The 2008 edition of this publication is the latest. FRP systems are still relatively new and the information contained in ACI 440.2R is the state-of-the-art in FRP knowledge and design.

### **1.3 Masonry Background**

Generally, a masonry materials assembly consists of the masonry blocks themselves made out of concrete; mortar, which is used to bind individual blocks to each other; steel, which is placed in cells of the CMU with size and spacing determined by the engineer to reinforce against wind as well as other weights the structure needs to support; and grout, used to fill the



cells that contain steel reinforcement. Openings in the walls for doors and windows require lintels to catch the blocks above the opening. Masonry walls are tied to the foundation (usually concrete footings) by steel bars to provide structural integrity. The walls at USF were built out of Grade C90-90 blocks [1].

#### **1.4 Introduction to Ground Subsidence**

Ground subsidence can occur due to a number of causes and it affects many residential buildings throughout the United States. Ground subsidence can be a result of a sinkhole or soil settlement. In Florida, sinkholes are caused by water eating away at the limestone beneath the soil. Once limestone is eaten away, a hole develops and the soil above the limestone collapses into the hole. Sinkholes are not always big, but they can be. Soil subsidence results from the soil settling due to the added weight of a structure that was not always present. There is always some degree of settlement, but it does not become a problem unless it goes beyond a certain point. The worst type of settlement is differential settlement, where different positions of a structure settle at different rates. This is usually the type of subsidence that causes structural problems. Geotechnical engineers are trained in detecting issues relating to ground subsidence before it becomes an issue; however, having a geotechnical investigation of a residential site is often optional, and is often the first thing to get omitted in order to save on costs. Even when it is done, one can never be absolutely certain of what is under the ground since it is only feasible to do a handful of representative samples for a given site. Generally, unless a residential building will be built in soil that is obviously poor, or will be built near a flood zone (where deep foundations are generally required), the soil quality often goes unchecked.

## 1.5 CFRP Background

The CFRP used in the construction of the walls at USF were Tonen Forca carbon fiber tow sheets [1]. These sheets were 50 cm wide and 0.11 mm thick [1]. The sheets were applied in horizontal strips, are single layer and are unidirectional. Carbon-Fiber-Reinforced-Polymers or Carbon-Fiber-Reinforced-Plastics (also known as CFRP or simply FRP) are composite materials that are becoming increasingly popular and available. Certain key characteristics of CFRP materials are their corrosion resistance, high strength, non-magnetic and light weight properties [2]. Other sources report the advantages of CFRP to be their “durability, ability to tailor material properties, ease of installation, and high strength to weight ratio” [3]. Although CFRP is also increasingly being used for new construction, the current use for the masonry walls at USF is as a strengthening and rehabilitation of an existing wall.

FRP systems consist of two parts, fibers and a resin matrix in which the fibers are contained. CFRP is only one type of a variety of FRP systems. There are several kinds of fiber materials that can be used and even more resins that can be selected. As ACI Committee 440 points out, “glass, aramid, and carbon fibers are common reinforcements used with FRP systems” [4].

## 1.6 Infrared Thermography Overview

Infrared thermography, also known as thermal imaging is a technology that can detect surface temperatures of objects in plain sight. Although there are certain conditions and guidelines that will allow one to obtain optimal results, it is remarkably easy to use. It mostly consists of pointing and shooting a given object that needs to be imaged with a thermal imaging

camera. The basic idea of using this technology was to try to find if there were hot spots on the surface of the CFRP sheets, which would indicate that the bond was not good in those locations.

There are advantages and disadvantages to testing a specimen such as these walls. One good thing is that they are well aged and the effect of bond over time can be studied. A disadvantage is that the walls never received IR evaluation directly after they were built, so workmanship defects will be present alongside bond deterioration defects. Whereas it would have been easy to tell which defects were related to workmanship if an IR test would have been performed after construction, it is now difficult or impossible to distinguish what the cause of a defect may have been. A more thorough discussion of this topic, including the strengths and limitations of this technology is presented in Chapter 2. Results of the thermal imaging are in Chapter 6.

## **1.7 Scope**

This study is to determine if weathering has had a significant effect on the epoxy adhesive that bonds the Composite materials (CFRP) to the masonry walls. Regardless of whether it is found that the bond has detached, weakened, or has been unaffected as time has progressed, it is beyond the scope of this research to determine the effect that this weathering or creep has had on the structural integrity of the wall. The longevity and durability of the bond itself is the focus of this research. The additional knowledge on bond durability will be of interest to those in the engineering community trying to maximize the life of their CFRP repairs on masonry or other concrete elements. This portion of the research is limited only to the non-destructive testing required to identify potential weaknesses in the bond. Destructive testing is recommended in chapter 8 for future work based on the results of this study.

## 1.8 Organization of Thesis

Chapter 2 details the various tests used in this research along with a brief snapshot of the testing equipment and an expanded review of IR technology. Additional data and information on material properties is presented in Chapter 3. Chapter 4 unfolds the weathering received by the masonry walls. Chapters 5, 6, and 7 present the data from each of the three tests performed. Chapter 8 takes a look at where this research stops and opportunities for future research. Chapter 9 provides the conclusions of this research. Images too numerous to include in the main body of the paper are included in the appendices.

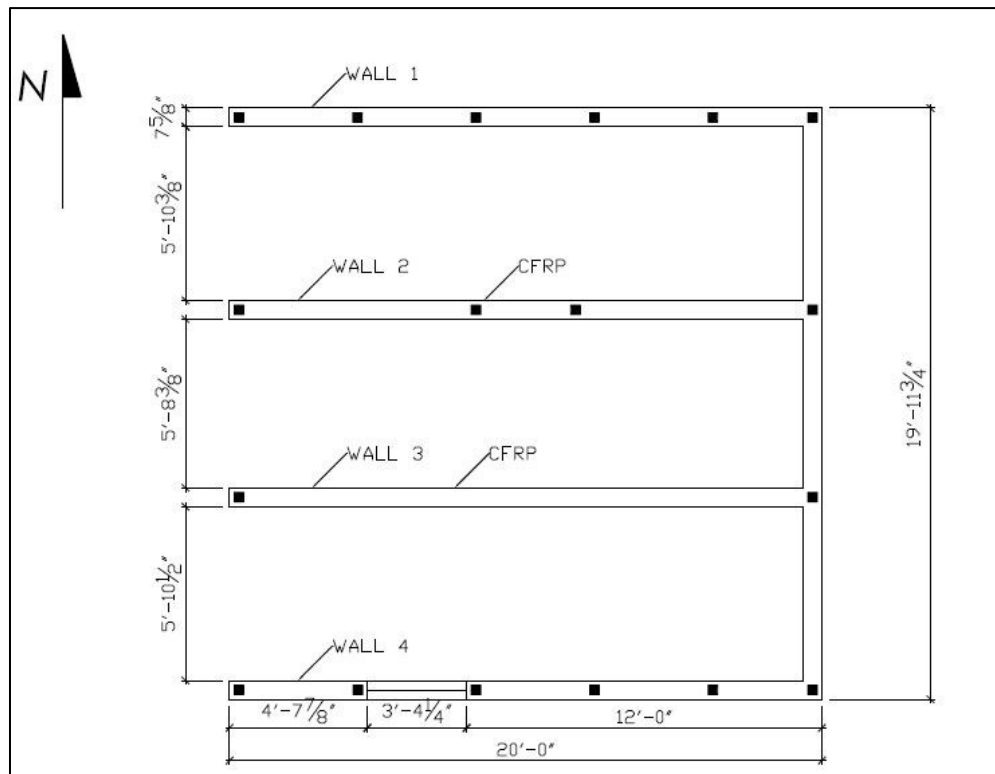


**Figure 1: Plan View of Masonry Walls at USF**



**Figure 2: Photograph of Masonry Walls at USF**

## 2. TESTING AND EQUIPMENT USED

### 2.1 Thermocouple Temperature Measurements

Thermocouples were attached to the masonry walls to observe the temperature response during a prolonged period of time. The crowning test of this research is the infrared thermography, but as that only captures a snapshot of the walls at the moment the thermography is done, this method was used to give some insight as to how the walls respond to temperature during an average day and during an average week. Another goal was to see how the localized wall temperatures at various positions compared with the ambient temperature. Some things that may affect the temperature readings are cloud cover, precipitation, the position of the sun, and humidity.

A Campbell Scientific AM25T Multiplexer was used to run the thermocouple test. The datalogger recorded temperatures for days at a time. The electronic instrumentation was housed in a casing in order to protect it from the elements. The hardware was loaded with a program instructing it to capture data readings every 15 minutes. The thermocouple wires were installed in two different arrangements. The first arrangement consisted of 24 wires attached to one wall on one side only. The second arrangement put 9 wires on each side of the wall to see whether there were temperature differentials occurring along the thickness of the walls. Details of the test results will be presented in Chapter 5. Each thermocouple wire was attached to the surface of the wall with epoxy putty.

## 2.2 Infrared Camera

A Tau 320 thermal imaging camera with a 19mm lens manufactured by FLIR was used to take thermal snapshots of the wall. This camera is capable of detecting wavelengths in the range of 8 to 14 microns. The camera is lightweight and has up to a 921600 Baud rate which allows quicker interaction with a computer or laptop [5]. Other researchers have also used FLIR cameras in structural research. Lai and Tashan both successfully used FLIR cameras to address needs specific to structural engineering in their testing of FRP bond [6, 7].

The camera had to be hooked up to a laptop in order to see a preview of the image as the camera had no preview screen of its own. The ideal time for infrared thermography with a thermal imaging camera is when there are transient thermal conditions. The goal is to see if there are any “hot spots”. Localized temperature differentials become most pronounced at times of thermal transition. Once steady state has been achieved and surface temperature becomes more uniform, it is not as useful to do thermal imaging in these conditions. Temperature is almost always in transition outside of an insulated structure, so this is not a huge concern for this application; although between sunrise and sunset remain the ideal time even in this situation.

When there is a discontinuity directly beneath a surface (such as de-bonding), heat that is transferring through a material gets backed up at the point of discontinuity as it cannot continue to travel if there is no more material to travel through. When this happens the heat has to go around the discontinuity in order to transfer through the material. This creates a concentration of heat at that spot and the “hot spot” that is being sought after.

### 2.3 Thermal Scanner

The structural research group at the University of South Florida put together a series of infrared sensors and built a thermal scanner. The infrared scanners were Omega OS137 infrared sensors. These have the capability of detecting wavelengths in the 0.6 to 0.7 micron range as reported by the manufacturer.

The advantage of this over the thermal camera is that it can create a digital scan of a surface with temperature data associated to every inch of a surface. Each successive scan is correctly scaled and can easily be added to the previous scan. In the end all scans are combined with the final image being a combination of multiple scans. Below the infrared sensors is a heating element. This heating element was not expected to raise temperatures above the glass transition temperature of the epoxy, although in the end some of the sensors picked up values of up to 175°F (nearing the upper range of glass transition temperatures of most epoxies). The values the sensors detected are expected to be relative and not absolute, but suffice it to say that some areas may have gotten quite hot, regardless of whether the value is absolute or relative. However, no damage was noted after the scans were complete. In principle, this scanner works on the same premise as the camera. The only difference is that it provides its own heat and does not require the sun as a heat source. The scanner is started in the high position and is mechanically pulled with a motor to the low position. The heater allows the scanner to create its own transient heat condition. Figure 3b shows an image of the thermal scanner that was used. Results from the scanner in this study must be considered in context as active thermography usually works best in the lab and in highly controlled experiments; the use of this instrumentation was closer to that of a field application as environmental and transient conditions may also show up in the results [8]. Thus anomalies found using this method should be carefully



considered as they may not always be the result of direct heat supplied by the scanner, especially if the scan is in an exterior environment, during the day.

## **2.4 Infrared Thermography**

### *2.4.1 Background*

Infrared thermography is used extensively in this research and some more background information on the technology is warranted. The most common measures to judge the quality of an IR system are the wavelength, temperature range for the intended application, and whether transient conditions are present. In conjunction with this, considering the material properties of the object to be tested is crucial, as certain wavelengths are best suited for different materials [9].

This study is not testing whether thermography works—for instance active thermography has been successfully used in Civil Engineering since the 1990s to detect delaminations [10]. Passive thermography has been around at least since the 1980s as an ASTM standard for using passive thermography dates to that time period [10]. Tashan also notes that IR thermography works well in detecting delamination in CFRP to concrete, but the effectiveness depends on how many layers of CFRP are present [7]. Usually delaminations are marked by areas with the greatest thermal contrast [6]. Lai points out that delaminations resulting from workmanship are typically easier to identify than other forms of delamination [6]. Lai also notes that adhesive properties can be assessed using IR technology [6]. There are ways of estimating defect depth using IR thermography, which can be found in the literature—for instance Taillade demonstrated that depth for multi-layered systems can be determined with the correct instrumentation, setup, and post processing [7, 10, 11].

There are advantages and disadvantages to the technology. IR thermography can pick up anomalies that would be undetectable in some instances with methods such as acoustic sounding [7]. A disadvantage is that some materials can be very sensitive to emissivity and false readings can occur [7, 9]. Flaws may also go unnoticed as the technology is not perfect as will be discussed [6].

#### 2.4.2 *Light*

Infrared cameras and sensors are designed to detect light in the infrared spectrum. Light waves that can be classed as infrared range from 0.7 microns to 1000 microns [9]. The wavelengths of the IR equipment used in this study were long wave (8 to 14 microns) and shortwave (less than 1.7 microns). Generally wavelengths in the 8 to 14 micron range are best for measurement of non-metal surfaces such as concrete, masonry and CFRP [9]. Ghosh also makes this same observation in an evaluation which was especially geared toward use of IR technology in concrete and FRP materials [8]. However, other wavelengths will still work. Objects emit infrared radiation in various wavelengths; it is just that they generally emit more in a particular wavelength, making it easier for the device to detect the radiation of the object [9]. Another consideration may be to use a wavelength that will not be sensitive to surrounding heat sources, but that can detect the wavelength of the desired object [9].

#### 2.4.3 *Active and Passive Thermography*

As was mentioned, heat flow needs to be present in order for anomalies to be detected. This heat can be applied artificially (active thermography) or naturally (passive thermography) [12]. Although very advanced, the technology is not perfect and Tashan notes that consistency and reliability are constantly being reviewed in ongoing research [7]. Lai is more specific and

indicates that there is 88% accuracy in detecting delaminations with IR technology [6]. Ghosh observes that “larger defects at shallow depths are easier to detect”—this means smaller defects at deeper depths may not be picked up by thermography, depending on the limitations of the device and method [8]. Both active and passive methods of IR thermography were used in this study. Passive thermography is the more economical approach as the user does not have to supply the heat [12].

If a decision has to be made to either use active thermography or passive thermography there are some things to consider. Active thermography is best suited for a controlled environment and passive thermography is ideal for an environment that is thermally transient [10]. Ghosh recommends passive thermography as the best option for exterior applications [8]. However, active thermography can work in transient environments. Some anomalies may be the product of other heat sources and other influences—this needs to be considered when interpreting the results of active thermography in a transient environment [10]. If qualitative results are desired, passive thermography is enough, however if quantitative results are needed, active thermography is better [8]. One reason for this is because you can easily discover the amount of heat supplied in active thermography with the correct setup [8]. Identification of exact flaw boundaries is possible with certain types of active thermography and with analysis such as that done by Lai [6]. Another important consideration is whether the applied heat from active thermography will damage the material being tested [10].

In order for active thermography to work, a heat source will typically need to apply heat for around 15 seconds, but this will vary depending on the heat source [10]. Tashan et al note that a quartz lamp worked well as a heat source in studying delamination of CFRP to concrete, although halogen lamps are also used (for 60 seconds) [7]. Whatever the source, it should be

able to provide a uniform level of heating [8, 7]. Another consideration is how well materials conduct heat. CFRP does not conduct heat very well which is both an advantage and a disadvantage—the material will take longer to heat up, however once heated, there is more time to make observations with IR thermography [8].

Most active methods are quite different to the setup in this study. Most still use infrared cameras (not sensors) and the heat source is mounted on a tripod while heat is pulsed. This is seen in multiple places in the literature. An example of this is lock-in thermography, a pulse thermography technique which Ghosh indicates is the most common method used to detect delaminations in FRP [8].

#### *2.4.4 Ideal Conditions and Potential Sources of Error*

There are certain things that can affect the readings of IR instrumentation. ACI 228.2R-98 explains the operation of thermal cameras as follows, “The physical parameters determining the emitted infrared radiation measured during a thermographic survey are: concrete surface emissivity, surface temperature, concrete thermal conductivity, concrete volumetric-heat capacity, thickness of the heated layer, and intensity of the incident solar radiation” [12]. Ghosh indicates that emissivity is especially important in reflective surfaces [8].

There are certain guidelines that should be followed for optimal results. ACI 228.2R-98 suggests removing debris from the surface, allowing for the surface to be dry for 24 hours before testing, avoiding testing in winds above 25 kph, ensuring ground temperature is above 0°C, and testing at night only under clear skies [12, 8]. Deviations from this should be noted as potential sources of error.

Ghosh and the report from ACI also recommends testing when transient conditions are present (for passive thermography) and ACI recommends sunrise as a good time, however it may take around 4 hours of sunshine for anomalies to become obvious [12, 8]. As a result, the use of passive thermography in this study was started in the morning in all cases, with some time to allow for the anomalies to become visible and usually concluded in the early afternoon. Active thermography was not held to this standard, as the main heat source was not the sun. Additionally, these are general guidelines and this study observed solar patterns (by use of thermocouples) on the walls that give additional insight to when these walls in particular are in a transient condition.

For this study, there was no visible debris on the walls. Dust, however may have been present. This is expected on an exterior surface and the effect should be negligible. Ground temperature would not be below 0° C in Florida in the months of April, September, and mid-October when the testing was done. Specific environmental conditions for each day of testing are presented in chapters 6 and 7.

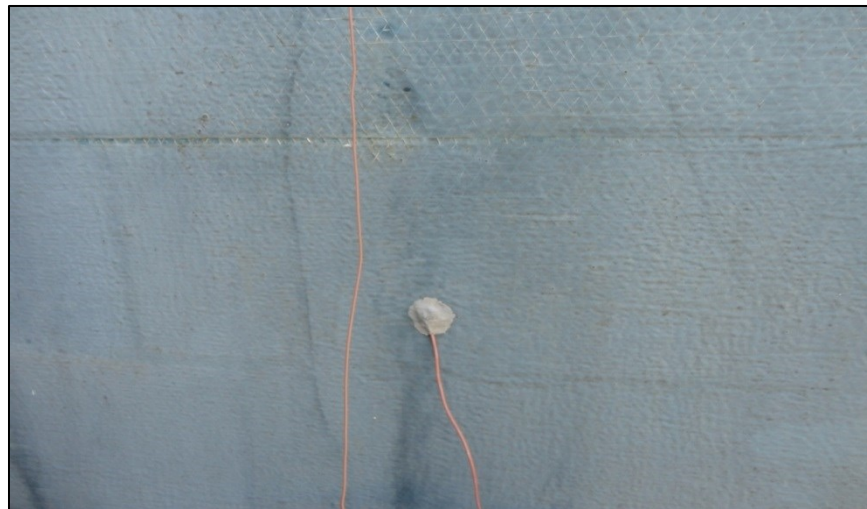


**Figure 3a: Photograph of Thermocouple on Masonry Wall**



**Figure 3b: Photograph of Thermal Scanner**

### 3. MATERIAL PROPERTIES

#### 3.1 Carbon-Fiber Reinforced Polymers

FRP systems are composed of many fibers (generally carbon, glass, or aramid) encased in a matrix of epoxy or some other hardened polymer. Sheets of this can then be adhered to concrete surfaces for structural repair and rehabilitation. The binder used to attach FRP sheets to concrete (or masonry) is generally an epoxy. Other resins are available and may be preferred depending on the application. Wet layup systems are also available where the fiber is saturated with epoxy resin on site [4].

FRP is a very lightweight material. In general, the density is 90 to 100 lb./ft<sup>3</sup> for CFRP [4]. This can be a great advantage, especially in labor costs, as an element with the same degree of structural strength made from steel would take several workers to handle. With FRP having a lower density and generally being paper-thin, one worker can handle much more on his own (and with greater ease) when compared to steel.

The performance of FRP systems is extremely sensitive to temperature and environmental factors. For example, ACI 440.2R declares that in a fire “the strength of externally bonded FRP systems is assumed to be completely lost” [4]. Performance may be compromised even at temperatures well below the level that would be found in a fire. The maximum temperature for this material is assumed to be the transition glass temperature, which generally ranges from 140°F to 180°F [4]. The transition glass temperature is defined as, “the

midpoint of the temperature range over which an amorphous material (such as glass or a high polymer) changes from (or to) a brittle, vitreous state to (or from) a plastic state” [4].

Some other properties of interest are the coefficient of thermal expansion ( $-0.6 \times 10^{-6}/^{\circ}\text{F}$  to 0 along the longitudinal direction and 12 to  $27 \times 10^{-6}/^{\circ}\text{F}$  in the transverse direction), sensitivity to ultraviolet light, and good corrosion resistance [4]. The coefficients of thermal expansion of concrete and epoxy for comparison are  $6 \times 10^{-6}/^{\circ}\text{F}$  and  $30 \times 10^{-6}/^{\circ}\text{F}$  respectively [4]. FRP systems typically have a good reputation for being corrosion resistant materials and this is often the deciding factor between FRP and steel. Lastly, FRP systems can be sensitive to creep, and if this is a consideration, special attention must be paid.

In all cases, FRP properties can vary depending on the manufacturer, and all definitive material properties should be confirmed by them.

The manufacturers of the epoxy systems used in the original study are no longer producing the epoxy products used, so some material properties (such as transition glass temperature) are not readily available; however the bond strength as reported for the original construction of these walls is 8.1 ksi tensile strength for the Henkel epoxy used on wall 2 and 6.8 ksi tensile strength for the Tonen epoxy used on wall 3 [1]. For some perspective on this material property, various manufacturers typically produce epoxies with bond strengths between 5 ksi and 10.5 ksi. The amount of epoxy applied to the walls was to be between 0.6 to 0.8 kg/m<sup>2</sup> [1].

Design life is an important factor when considering a repair with CFRP. CFRP systems are still fairly new, but a common expectation is that a system last at least 30 years after rehabilitation [13]. When it comes to delaminations in FRP, workmanship is an important factor [6] and Lai indicates that bond defects due to this are quite common [6]. Requirements for



workmanship in FRP composites can be found in NCHRP reports [14, 15]. Lai also cites other potential situations contributing to delaminations including when “CFRP-concrete composites...[are] exposed to aggressive environments such as elevated temperatures, ultraviolet radiation, infiltration of moisture and extreme temperatures caused by fire” which serve to weaken and deteriorate the bond [6]. Dolan adds that sustained load is also a factor [16].

The effect of high temperature and time of wetness is also a factor in delaminations and bond strength. Lai tested samples of CFRP bonded to concrete in baths of hot water—these were subjected to water temperatures of 40°C and 60°C for 50 weeks [6]. Lai notes that this caused deterioration “probably because at above a certain critical temperature, water molecules started to act as a resin plasticizer, and the bonds in the polymer (epoxy) chains were disrupted” [6]. He further explains that “the induced swelling stresses may cause permanent polymer matrix cracking, hydrolysis and some degree of fiber-matrix de-bonding thus forming delaminations” [6]. He concluded that bond strength is also affected [6]. The delamination in the walls may follow a similar process. Although not submersed in water, wet and humid conditions persist frequently during the hot months in Florida and this combination may lead to a similar, albeit smaller scale deterioration.

## 4. TEMPERATURE DATA

### 4.1 Introduction

The data used to analyze the thermodynamic oscillations the wall specimens have experienced since 1995 was originally recorded at a weather station located at Tampa International Airport (TIA). The exact location of where the readings were taken is 27° 57' 41.04" N 82° 32' 25.08" W and is at an elevation of 19 ft. The station's name is Tampa WSCMO AP. This information was obtained from a website maintained by the Utah Climate Center at Utah State University [17]. Also available from this database was historical precipitation and rainfall data. This data is not published and is simply a database of free data available upon request. Historical weather data is available from multiple weather stations nationwide with historical coverage varying from station to station. The data is requested in the form of an excel spreadsheet which makes it convenient for analysis. Simple statistical analyses were performed on the data such as arithmetic mean, range, mode, and standard deviation which will be covered in more detail in section 4.3. The location of the masonry walls according to Google Earth is approximately 28° 3'58.72"N 82°24'59.25"W on the USF Tampa Campus. Both places are in Tampa, FL, however, there is a distance of about 10.5 miles between these two locations.

## 4.2 Validity of the Data

Although there is a degree of separation between the station and the site, this is the only data available for use as there are no historical temperature readings available for precisely this site and readings for other sites are not nearly as extensive as the ones that are available from the station at TIA. Not only are the readings from TIA the most extensive readings, it is also the closest active station with up to date records, ensuring that the readings are as accurate and as complete as possible. It is assumed that temperatures will not vary drastically within a general region, in this case, the Tampa Bay Area. To quantify this assumption to some extent thermocouple data was collected at the site on two separate weeks during 2012. With this data comparisons between the site and TIA can be drawn. For instance, on a specific day such as 4/3/12 the difference between the high temperatures at two sites is at a maximum, a difference of 6.1°F. This is shown in Table 1.

On 4/1/12, however, the difference between the high temperatures at the two sites is at a minimum, showing a difference of only a 0.1°F. Looking at isolated events does not give an accurate portrayal of trends between the two sites. Table 1 and Table 2 contain the temperature readings for two weeks of the year 2012. By looking at the data for these weeks as a whole, a better picture can be drawn. Taking the ranges of maximum temperatures and minimum temperatures and calculating the standard deviation of these ranges reveals that the highest standard deviation for this data set is 1.9°F. This means that given a temperature at TIA one would be correct in assuming the same temperature at the site within a tolerance of approximately  $\pm 2^{\circ}\text{F}$  ( $\pm 1^{\circ}\text{C}$ ). This level of accuracy is more than adequate in contrast to having no data at all. Furthermore, as these two sites are within the same region, the trends in temperature should be remarkably similar.

### 4.3 Historical Temperature Data

The temperature oscillations experienced by the CFRP strengthened wall are plotted and shown in Figure 4. The blue lines are the maximum temperatures and the red lines are the minimum temperatures. The maximum high temperature is 98°F and occurs 3 times—on 6/21/98, 6/6/08, and 6/12/10. The minimum low temperature is 25°F and occurs twice—on 2/5/96 and on 1/11/10. This gives an absolute temperature range of 73°F within this recorded period. The most frequently occurring high temperature is 90°F and the most frequently occurring low temperature is 76°F. The average high temperature is 82°F and the average low temperature is 65°F. This means that many high temperatures in Tampa will be around 82°F for a given year and many low temperatures will be around 65°F for a given year. As the life of this structure spans many years, it gives a different perspective to zoom out from the instantaneous maximums and minimums that only occur a few times and see big picture maximum and minimum temperatures. The instantaneous maximum and minimums do not accurately portray what is typically experienced as they are isolated events.

The masonry walls were originally built in February and March of 1995. The CFRP was installed later on 8/14/95. This day reportedly had a high temperature of 93°F and a low temperature of 79°F. These walls were originally built as part of an older Master's Thesis researching the effectiveness of strengthening concrete masonry walls with CFRP materials [1]. In the years following the completion of the research done in 1995, these walls have remained at USF largely untouched and nearly forgotten until this research began. Due to the just mentioned timeline of events, temperature data was collected beginning with 1/1/95 and continues on until 5/9/13. Plots were only taken to 5/10/11, when this research was first getting started. Some time

has passed to the date of this publication, but there is already an ample amount of data in this data set for the purposes of this study.

The maximum and minimum temperatures are not nearly as useful as is the difference between these two values. The daily difference in temperatures shows the thermodynamic reversals the wall experienced on a day to day basis. This cyclic thermodynamic loading experienced by the wall may be comparable to a structural fatigue type situation where extreme stress reversals over time can cause structural materials to fail if this condition is not properly accounted for in the design. This is usually caused by numerous cycles initiating small cracks which then propagate with ongoing cycles until material failure. This is discussed more in section 4.4. Figure 5 shows these reversals. The wall experienced daily reversals as well as annual reversals in temperature. This data was fitted with a trend line using a 15 period moving average. The maximum daily difference in temperatures is 33°F and the corresponding minimum is 3°F. The maximum occurs on 12/11/95 and 3/6/07. The minimum occurs on 6/10/05, 1/30/06, and 3/12/10. The most frequent temperature difference is 16°F. There is an average temperature difference of 17°F for the entire 16 year period. There is a standard deviation of approximately 5°F for these temperature differentials. The bell curve in Figure 6 illustrates the average and standard deviation of these differentials graphically.

#### **4.4 Other Historical Factors**

There are a few other factors that affect what the temperature data means such as how much heat an absorptive surface will absorb compared to a reflective surface (emissivity), the coefficient of thermal expansion, and the glass transition temperature. Exposure to direct sunlight is also a factor. This research is only concerned with the historical temperature variations as the equipment and testing used in this study only report temperature.

Although temperature and related parameters are the focus of this research, some context is warranted on other environmental factors. The most significant of these are rainfall and humidity. Tampa has an average rainfall of about 34 inches every wet season [17]. Annual average high humidity is around 87% [18]. These things can make for a particularly aggressive environment when combined with the temperature ranges noted in this chapter. Figure 7 and Figure 8 show an extensive historical record of these parameters in Tampa, FL for the life of the walls. Windblown sea salt may also be a factor due to the proximity to the coast. UV exposure is another potential factor affecting deterioration, especially if the angle of exposure is direct.

A rough idea of the stress variations may be assessed based on the temperature differentials and the coefficients of thermal expansion mentioned previously. For the largest temperature differential experienced by the wall in comparison to the installation temperature, 61°F, we can find the difference in elongation between two adjacent materials and see how much strain (and stress) would be induced on the epoxy. A typical modulus of elasticity of masonry is 1,710,000 psi. For CFRP 9,000,000 psi is a common value. A good value for an epoxy is around 500,000 psi. With these values and using engineering fundamentals, the masonry would impose around 732 psi of stress and the CFRP would impose around 933 psi of stress. More details on this calculation are available in the appendices.

This is the highest temperature differential for the entire 18 years and the daily ones are nowhere near this value. These results indicate a very low level of stress when compared to the bond strengths quoted in chapter 3, so stress levels should not cause major problems. As noted in ACI 440.2R, differences in the coefficients of thermal expansion do not cause major problems for “small ranges of temperature change” [4]. Thermal cycling may still play a role as it is noted as a possible cause of deterioration in a statement by NCHRP but they do not say this with

certainty and they do not make any general statements as to when this becomes a problem [16]. What may be more of a concern is the combination of high temperature and moisture as noted in the previously mentioned study by Lai [6]. This occurs on an annual basis and poses a greater threat. In summary, the literature indicates that temperature differentials together with weathering could cause deterioration in the bond, although there is more research to be done on the temperature fatigue process and its effect on bond as indicated in the gap analysis done by Karbhari [19].

**Table 1: Week 1 Comparison of Temperature Data. TIA Source Data from Public USU Database [17].**

Date	Site Readings (°F)		TIA Readings (°F)	
	Max	Min	Max	Min
3/31/2012	84.9	69.4	82.9	70.0
4/1/2012	84.8	65.6	84.9	68.0
4/2/2012	88.5	64.5	84.9	66.9
4/3/2012	92.1	65.6	86.0	68.0
4/4/2012	90.8	66.7	86.0	68.0
4/5/2012	86.4	67.5	84.0	69.1
4/6/2012	83.4	69.1	82.9	66.9
4/7/2012	81.4	60.0	82.9	61.0

**Table 2: Week 2 Comparison of Temperature Data. TIA Source Data from Public USU Database [17].**

Date	Site Readings (°F)		TIA Readings (°F)	
	Max	Min	Max	Min
8/11/2012	86.5	74.5	88.0	77.0
8/12/2012	87.5	74.6	90.0	77.0
8/13/2012	85.8	74.7	89.1	78.1
8/14/2012	87.7	75.7	93.0	78.1
8/15/2012	91.3	73.9	91.9	77.0
8/16/2012	89.5	76.3	91.9	80.1
8/17/2012	84.4	75.9	88.0	77.0
8/18/2012	78.7	72.3	82.9	73.0

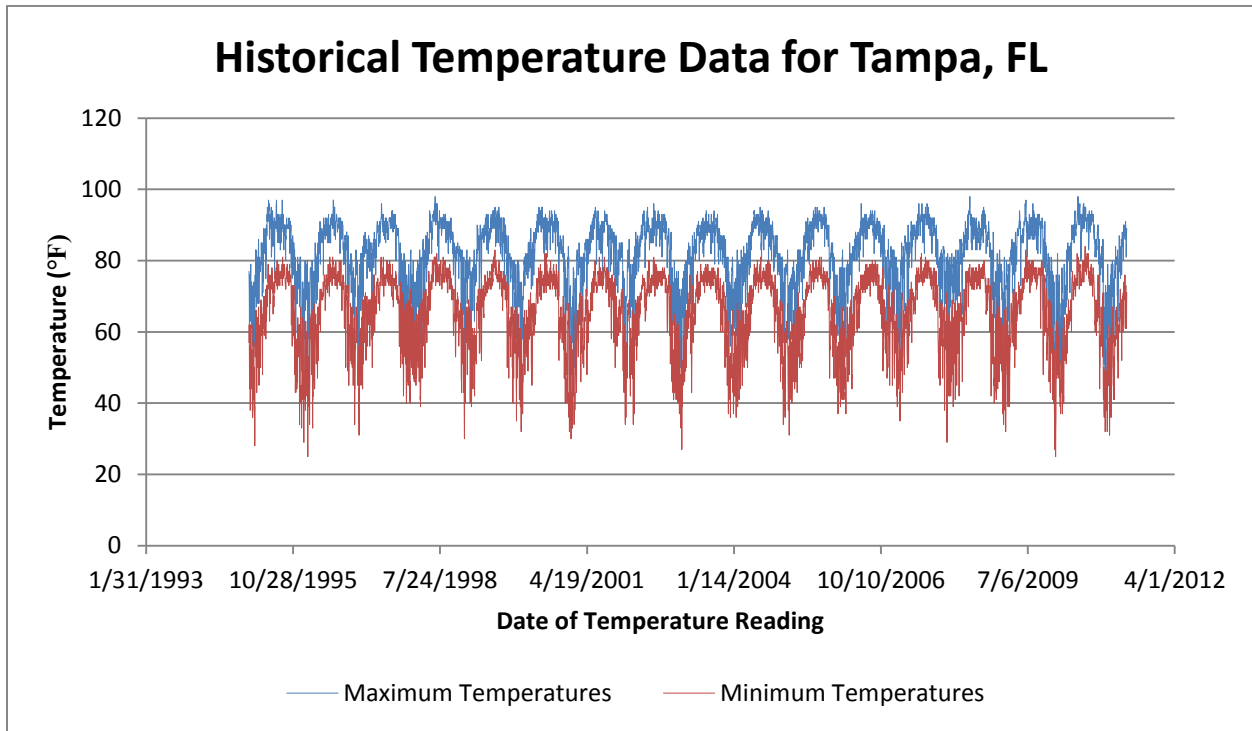


**Figure 4: Historical Maximum and Minimum Temperatures for Tampa, FL. TIA Source Data from Public USU Database [17].**



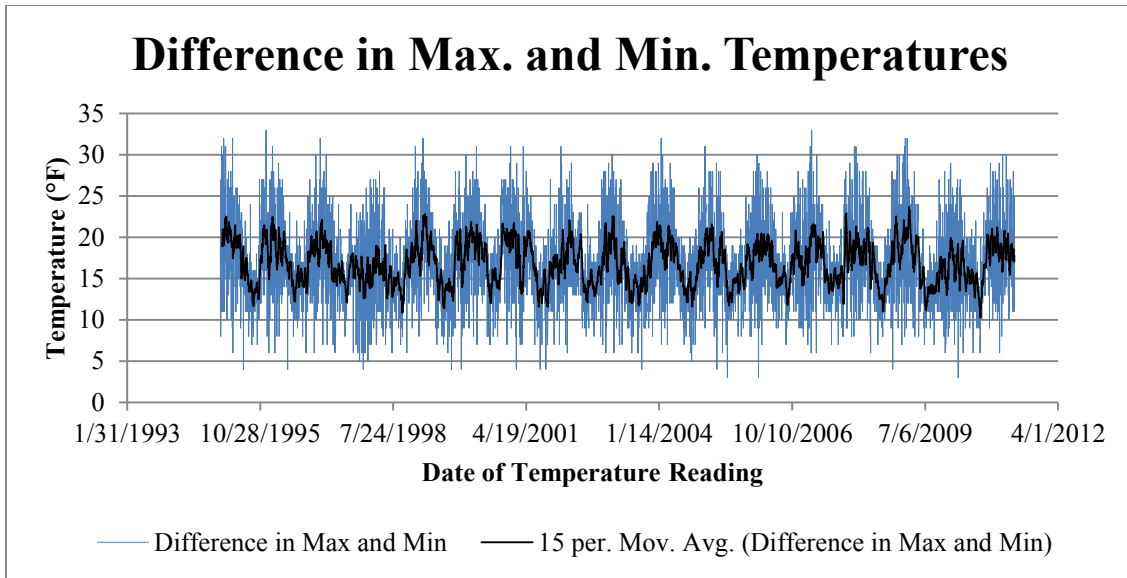


**Figure 5: Historical Daily Reversals in Temperature. TIA Source Data from Public USU Database [17].**

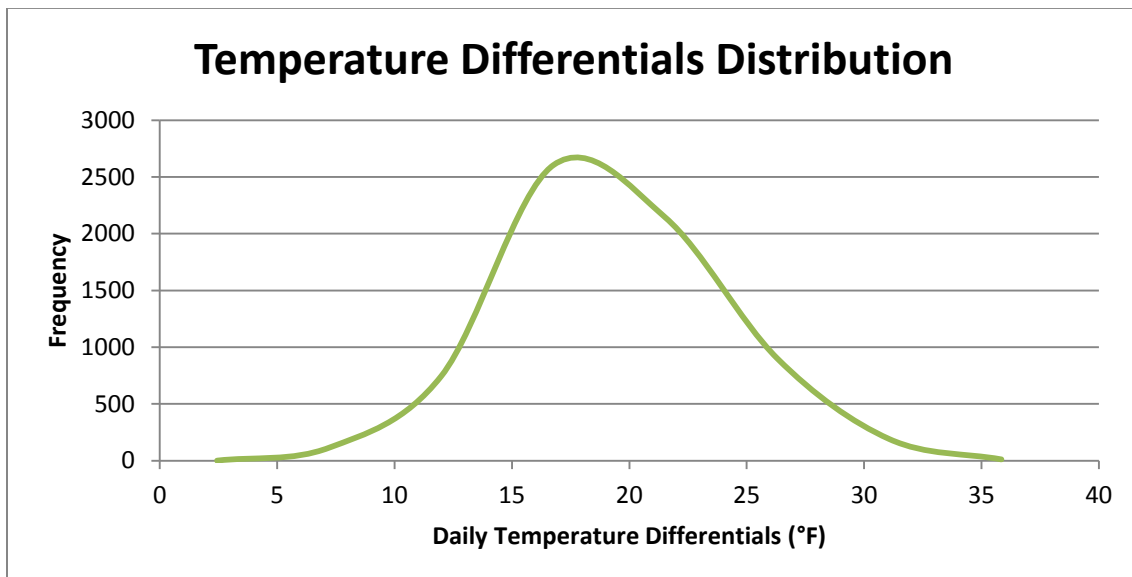


**Figure 6: Bell Curve of Historical Temperature Differentials. TIA Source Data from Public USU Database [17].**

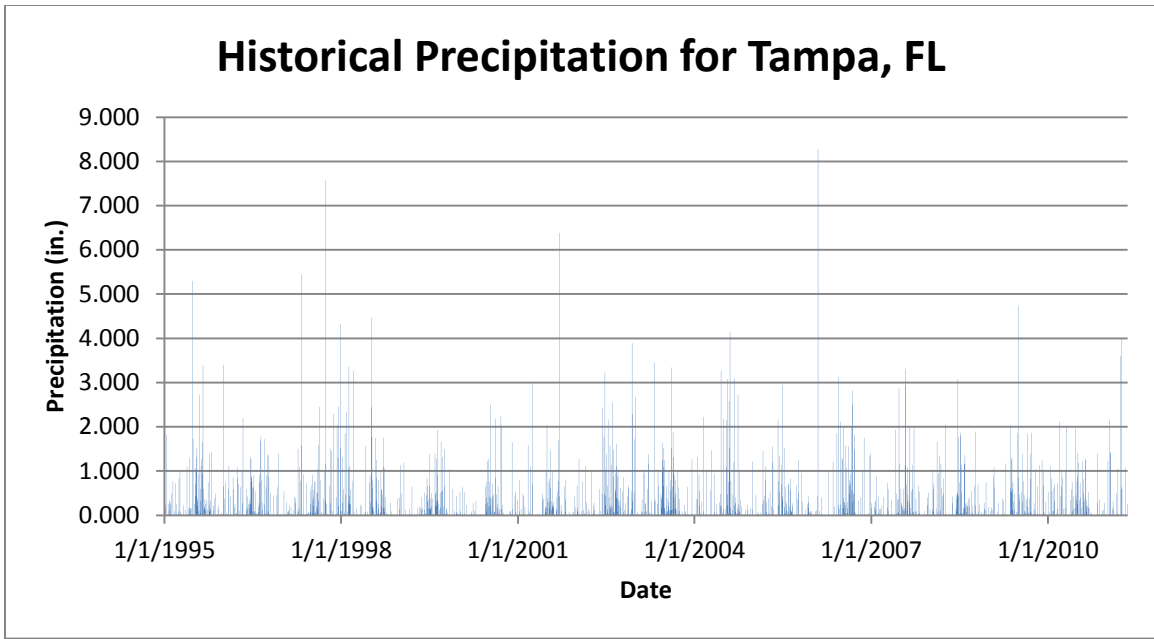


**Figure 7: Historical Rainfall in Tampa, FL. TIA Source Data from Public USU Database [17].**

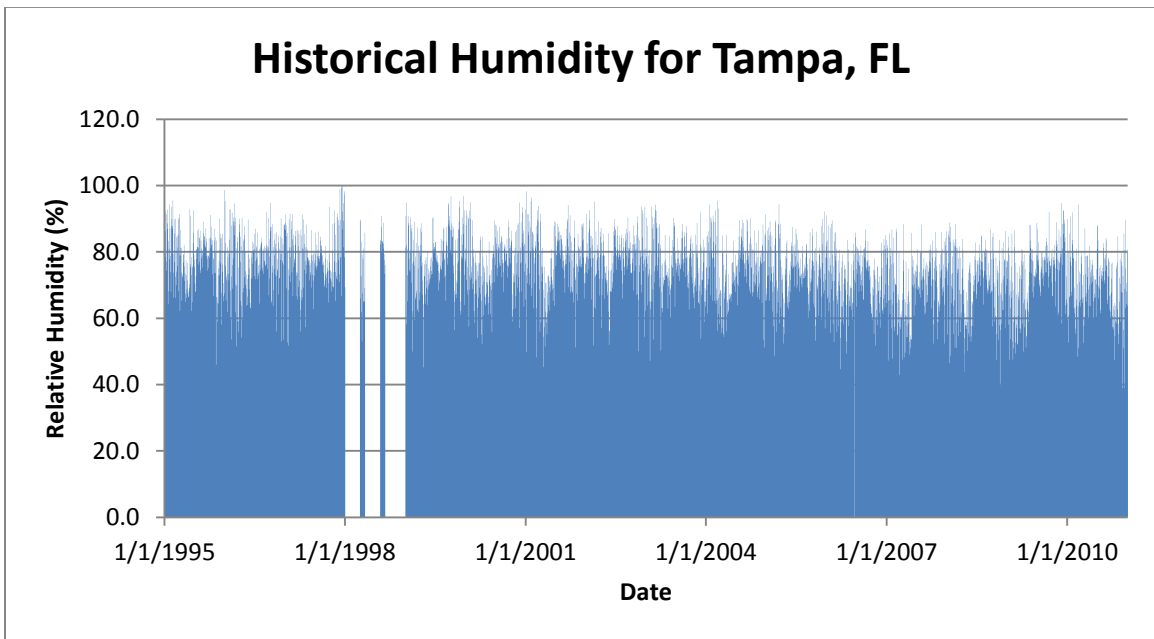


**Figure 8: Historical Relative Humidity in Tampa, FL. TIA Source Data from Public USU Database [17].**

## 5. THERMOCOUPLE RESULTS

### 5.1 Thermocouple Arrangement

Thermocouples were placed on the walls in the arrangement shown on Figure 9. The 2'-3" spacing was typical in the horizontal direction. The nominal spacing in the vertical direction was approximately 2'-0", but that spacing was offset by a few inches (as shown) in order to avoid placing thermocouples directly on the mortar joints. The desired temperature data was for the wall itself since the joint temperature may have some local variations unique to the mortar joint. This may have provided false hot spots or cold spots. A second arrangement consisted of thermocouples being placed opposite the nine rightmost thermocouples, on the other side of the wall.

Figure 10 shows the walls after the thermocouples were installed. Initially epoxy adhesive with a consistency close to that of peanut butter was used in an attempt to attach the thermocouples to the wall. However, many of the wires pulled away from the bond holding it to the wall overnight as this binder took considerable time to cure. Epoxy putty manufactured by PC-Products was then used and this offered the best results. Particularly when attaching to the CFRP, which has a much smoother surface than masonry, the putty worked surprisingly well. This epoxy putty was a basic plumbing putty available at home improvement stores. It consisted of two parts which were molded together by hand immediately before attachment of the thermocouple. This putty was able to carry the weight of the wire within about a minute or two.

Full cure was achieved after 60 minutes, as opposed to the much longer cure times of the traditional epoxy initially used.

Wall 3 did not get thermocouples installed. Wall 2 is taken as a control wall and it is assumed that other walls at this site will experience similar temperatures conditions as this. The basis of this assumption is that the sun has the same relative position to each wall during the course of the day (angle of exposure is similar) and both walls have the same overhanging construction.

## 5.2 Testing Results for Arrangement 1

Results are summarized in Figure 11, Figure 14, and Figure 18 using a statistical approach. All of these figures show wall 2 in elevation. Position 25 shows the ambient temperature results. Figure 11 and Figure 14 show the North side of the walls. The north side is the one with CFRP. The top two rows of thermocouples on the north side were mounted directly on the CFRP. The bottom row was mounted directly on masonry. The walls were monitored on two separate weeks. Figure 8 shows the result for the first week of monitoring performed from 3/31/12 to 4/7/12. This was only conducted on the CFRP side of wall 2 for this week. Figure 18 and Figure 19 show the results obtained during the second week of 8/11/12 to 8/18/12. This week was used to monitor the temperatures on both sides of the wall in order to see if the positions chosen reveal consistent or varying rates of heat transfer. This second arrangement will be the focus of section 5.3.

From Figure 11 a few trends can be detected. The top two rows are generally hotter than the bottom row. The difference is not overwhelming, but the slight variation may be due to material differences, such as thermal conductivity. This is possible since the top two rows are on a different material (CFRP) than the bottom row (masonry). It may also be that the black color

of the CFRP absorbs more light than the masonry and keeps it slightly warmer on average. Probably the largest single contributing factor is that the bottom row received the least direct sunlight and therefore did not get as hot. Additionally, the temperature range resulting from sunlight is outside of the general glass transition temperature for an epoxy, which is usually between 140°F to 180° F [4]. Care must be taken with this observation as it's recommended to keep maximum temperatures at least 30°F below the glass transition temperature when wet [19]. The values here are still outside of that range, however these readings are from March and April. In Florida June and July are typically the hottest months, so temperatures on the wall could get considerably hotter. The ambient temperature is generally cooler than any of the wall surface temperatures. It is also noteworthy to point out that the west and the middle sections of the wall are generally hottest. Overall, these variations do not seem to be of a local nature, but of a global one.

Figure 12 shows wall temperatures at position 4 on 4/1/12. On this day the sun rose at 7:20 AM and set at 7:47 PM [20]. This curve is typical of the general trend of all the positions on the wall during a given day. All days showed the same trend, so the first full day of data was selected. A thermocouple near the top of the wall was chosen since the top of the wall heats up more than the bottom. From the figure, it appears that the maximum temperature occurs at about 5:00 PM. The wall warms up continuously until late afternoon, when temperatures begin to decline. So in addition to the annual cyclic temperature loading shown on Figure 4, there is a daily cycle the wall goes through. 1:00 PM seems to be approximately a midpoint of the transition period from minimum to maximum temperature. One thing to note is that there is no real plateau and transient conditions seem to be the norm on this wall. This makes it so almost any time of the day is good for passive infrared thermography. This of course, assumes

favorable environmental conditions. A snapshot of what the wall is experiencing at this midpoint in time can be seen in Figure 14. Whereas the summary shown in Figure 11 gave a general envelope of wall temperatures for the week, this allows us to see a specific condition the wall has experienced.

All thermocouples 1 through 24 are shown in Figure 13. Ambient conditions are also plotted in this figure. In this figure it is interesting to note that the temperature range of the low temperatures is around 5°F whereas the temperature range for the high temperatures is around 10°F. This indicates that difference in maximums is double the difference in minimums. All wall locations essentially cool down to close to the same temperature, but during the day the temperature difference between positions on the wall increases and grows further and further apart. The highest temperatures are found at locations on the upper west region of wall 2. Since most thermocouples cool down to close to the same temperature, but some heat up a lot more than others, thermal oscillations are greatest in the top west region of the wall.

In general, Figure 14 reveals that at this inflection point where wall temperatures are in full flux, there are still no real local anomalies. In general this snapshot shows the bottom left corner to be the coolest and temperatures gradually get warmer diagonally toward the top right. This is due to uneven sunlight exposure. This is partially due to the fact that the wall running north-south blocks sunlight as the sun rises in the east. This makes the east side cooler and the west side warmer.

In addition to sunlight, another factor that is likely to be a major contributor to these temperature patterns on the wall is the way in which it was constructed. The west end of the wall overhangs on a steel beam above the ground whereas the east side of the wall is on a foundation that rests directly on the soil. This overhanging end is shown in Figure 15 and Figure 17. The

end that overhangs dissipates heat differently than the end that is in contact with the ground. The overhanging portion cannot dissipate heat as readily and therefore is hotter, whereas the grounded end can transfer heat to the ground and can cool down more efficiently. The thermal image in Figure 16 also illustrates this same thermal pattern.

Overall, a lot of good data and interesting trends were obtained from this arrangement, such as the data enabling a comparison between site temperatures and temperatures at TIA. The main purpose to compare wall temperatures to ambient temperatures was also successful. Additionally, as a result of this test, the solar patterns on the wall are now better understood. These readings also served a role in the tests performed with the thermal camera as will be discussed in chapter 6.

### **5.3 Testing Results for Arrangement 2**

On the week of 8/11/12 to 8/18/12 more readings were taken on wall 2. Thermocouples were set up on both sides of the wall in order to provide a way of seeing how heat was flowing through the masonry. This arrangement also serves to see if one side is heated differently than the other. The thermocouples on the south side were mounted directly on masonry. The positions of thermocouples 6 to 7, 14 to 16, and 22 to 24 remained the same on the north side of the wall. New thermocouples (1 to 9) on the south of the wall were added exactly opposite the ones shown in Figure 18 with the arrangement shown in Figure 19. Figure 18 and Figure 19 provide a statistical summary for each thermocouple position on the wall for the week readings were taken. As in the previous arrangement, position 25 reports on ambient conditions.

Figure 18 and Figure 19 reveal that temperature on both sides is pretty consistent without even a full degree of variation in the mean temperatures measured. Both sides give the same global trend noticed with the previous arrangement—that temperatures are coolest at the bottom

left and progressively get warmer toward the top right (or bottom right to top left when looking at the south side toward the north as in Figure 19). It seems that the bottom row is still the cool row even when all the thermocouples are mounted directly on masonry. This confirms that the most likely cause for the difference in temperature from bottom to top is difference in exposure to direct sunlight. As a result of this, the material (whether the thermocouple is mounted on masonry or CFRP) is observed to have a negligible contribution to the surface temperature.

In terms of layout, Figure 20 gives another perspective on the arrangement of these thermocouples. In this figure, the designation N-6, for example is thermocouple 6 on the north side of the wall. S-3 corresponds and is opposite to N-6 and so on. S-3 is thermocouple 3 on the south side of the wall.

Figure 25 plots the temperature of both sides of the wall for locations 16 and 4 which are exactly opposite each other. The plot contains data for the entire week of monitoring. This plot in fact is typical of all positions on the wall considered in this arrangement and its corresponding thermocouple on the other side of the wall. The figure shows that both sides have essentially the same temperature and exhibit exactly the same trends at exactly the same time. The two data sets are so similar that they are essentially superimposed on top of each other. This does not necessarily mean that heat flow does not vary at any of those locations; however it does mean that the temperature at the start and end points is always the same. This makes sense because both exterior surfaces are equally exposed to the elements and are being heated by the same source (the sun) at the same time. Perhaps if thermocouples were located at the center of the walls, differences in heat flow might have been detected. However, they may not even exist. Another thing that might have worked would have been to use a different heat source on only one side, perhaps at night, and then take readings of heat flow through the thickness of the wall.



It should be noted that there are inherent differences in heat flow along the thickness of the wall when there are hollow masonry units. In this case heat flow would get disrupted by air in a hollow masonry cell.

Figure 21 and Figure 22 show the double sided arrangement at a specific time to illustrate an actual condition the wall experienced. The same trend as noted previously.

The contours in Figure 23 and Figure 24 clearly show the diagonal warming trend on both sides of the walls. Additional contours are available for both thermocouple arrangements in the appendices.

The ambient results obtained were once again useful for comparison with temperature readings at TIA, so this test served multiple purposes. The ambient results are also useful for comparison to wall temperatures. In general the ambient temperature was one of the coolest temperatures if not the coolest. This test has only established overall heating trends in the walls, but the IR tests will be able to detect local anomalies which will locate de-bonded regions.

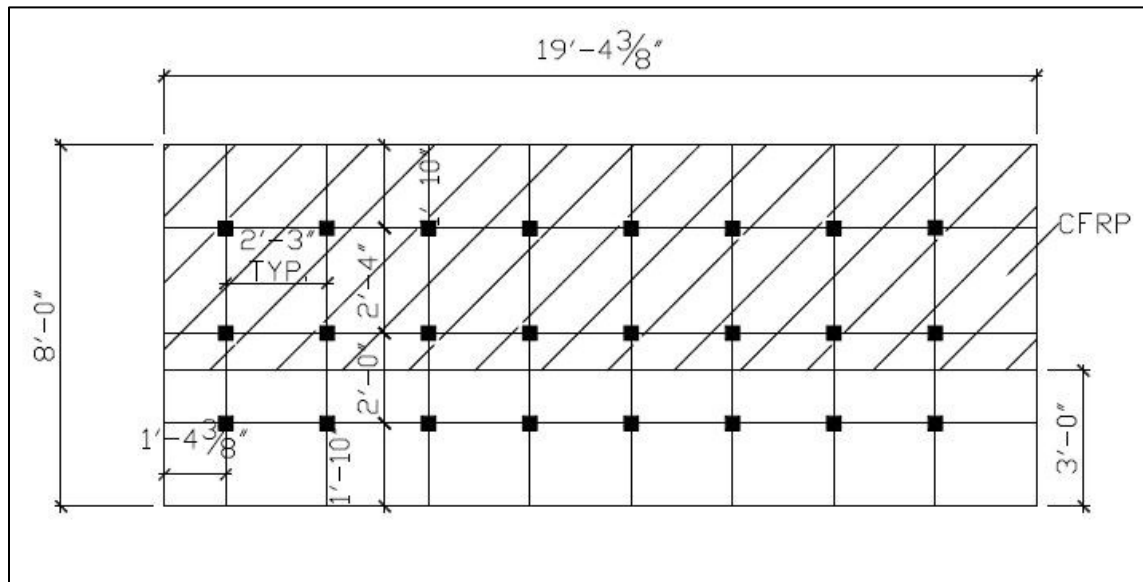


**Figure 9: Thermocouple Arrangement #1 on Wall 2 Elevation (Looking South)**



**Figure 10: Thermocouples Installed on Wall 2**

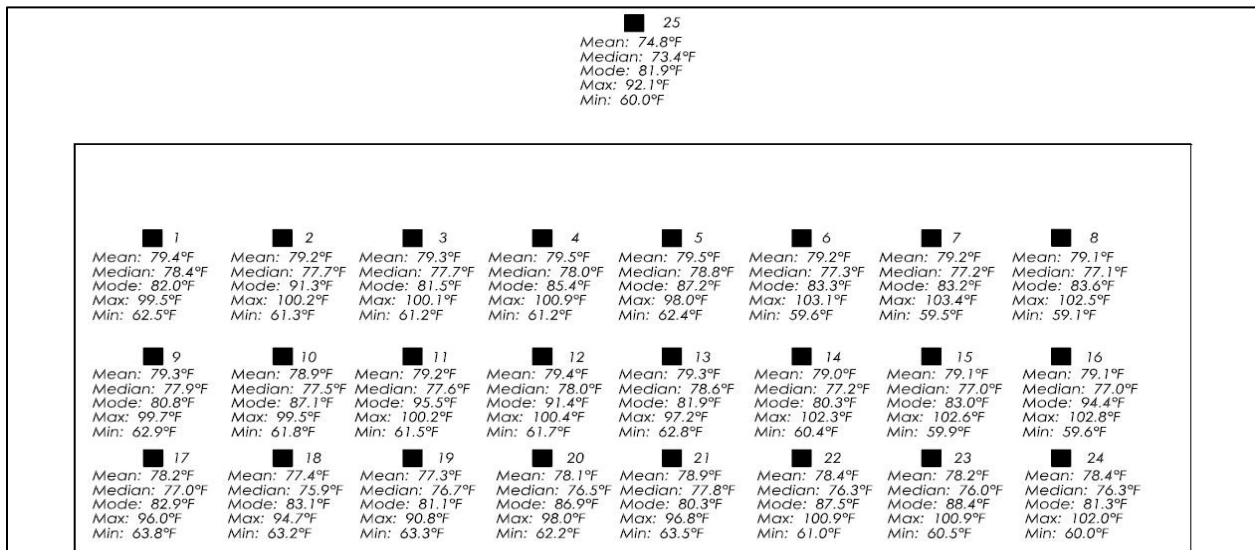


**Figure 11: Wall 2 North Side Data Summary 3/31/12 to 4/7/12 (Looking South). Thermocouples 17 to 24 are on Bare Masonry.**

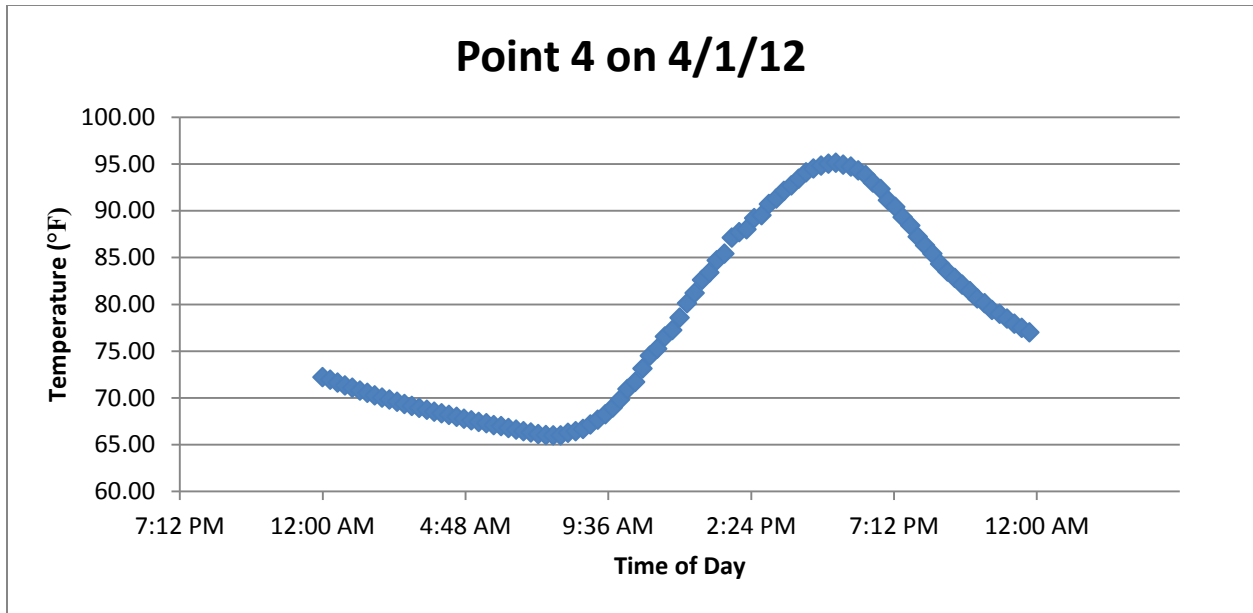


**Figure 12: Daily Behavior of Thermocouple Position 4 on North Side of Wall 2**

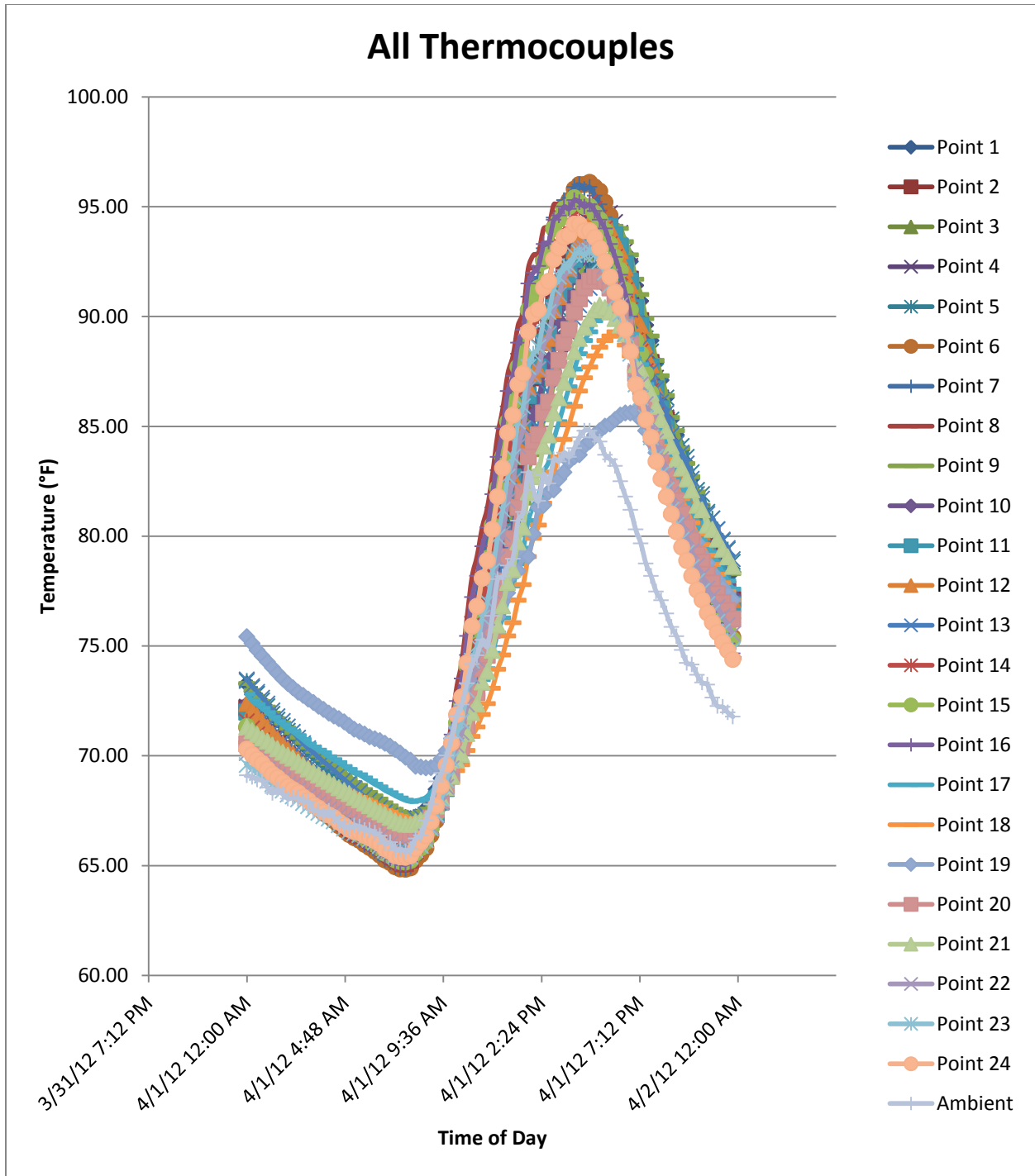
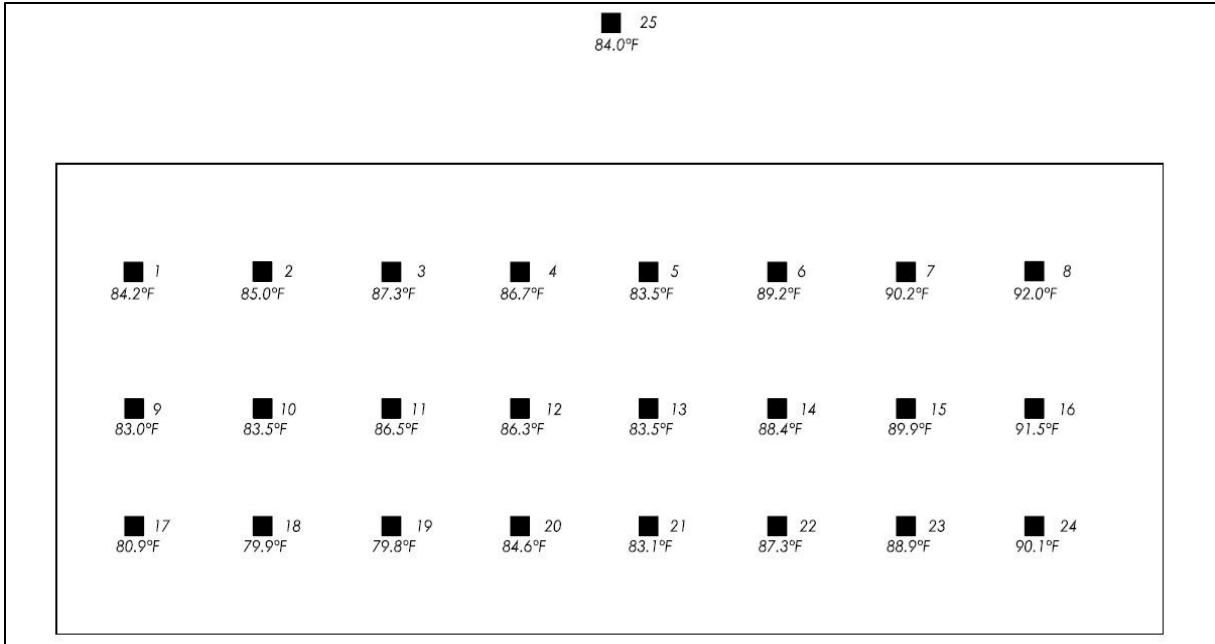
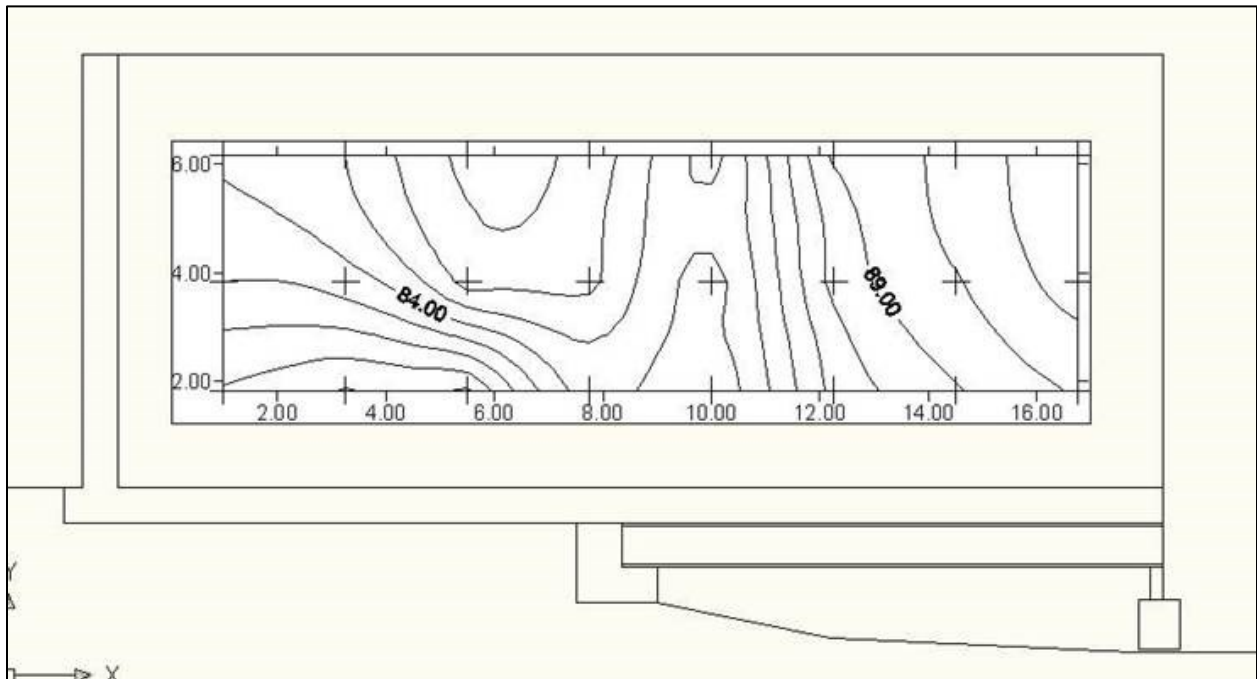


Figure 13: All Thermocouples Data on North Side of Wall 2



**Figure 14: North Side of Wall 2 Temperature Data on 4/4/12 1:00 PM**



**Figure 15: Thermal Contours on North Side of Wall 2 at 1:00 PM 4/4/12**



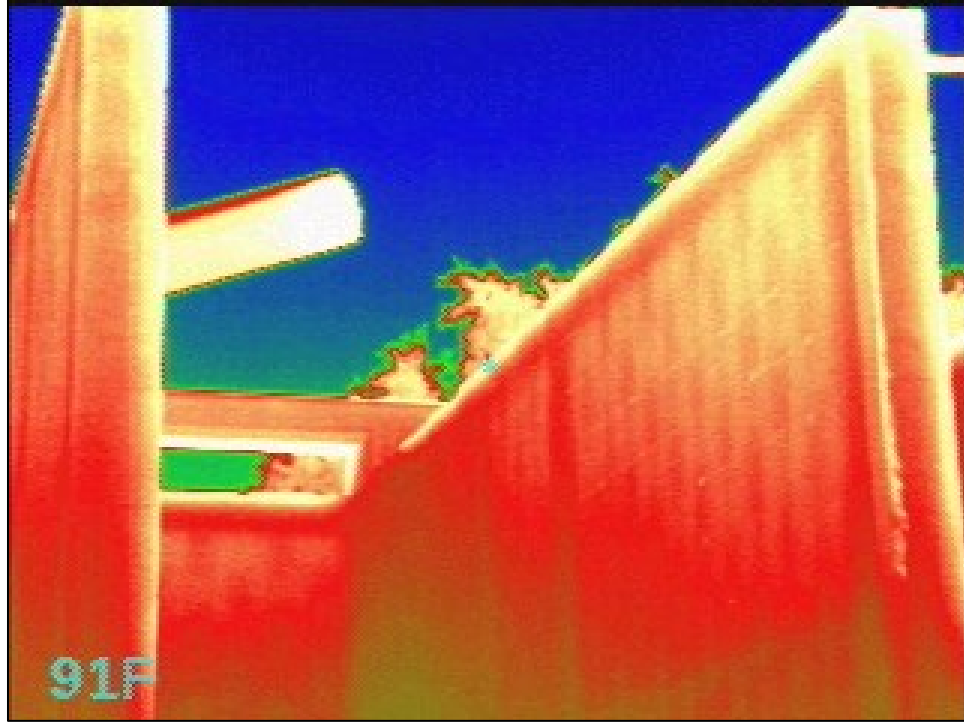


**Figure 16: Passive Heat Variation on North Side of Wall 2 on 10/17/13 at 10:31 AM**



**Figure 17: Overhanging End of Walls**

**Table 3: Sunrise and Sunsets for 8/11/12 to 8/18/12. Source Data from Public Database [20].**

Date	Sunrise	Sunset
8/11/12	6:58 AM	8:12 PM
8/12/12	6:59 AM	8:11 PM
8/13/12	6:59 AM	8:11 PM
8/14/12	7:00 AM	8:10 PM
8/15/12	7:00 AM	8:09 PM
8/16/12	7:01 AM	8:08 PM
8/17/12	7:01 AM	8:07 PM
8/18/12	7:02 AM	8:06 PM

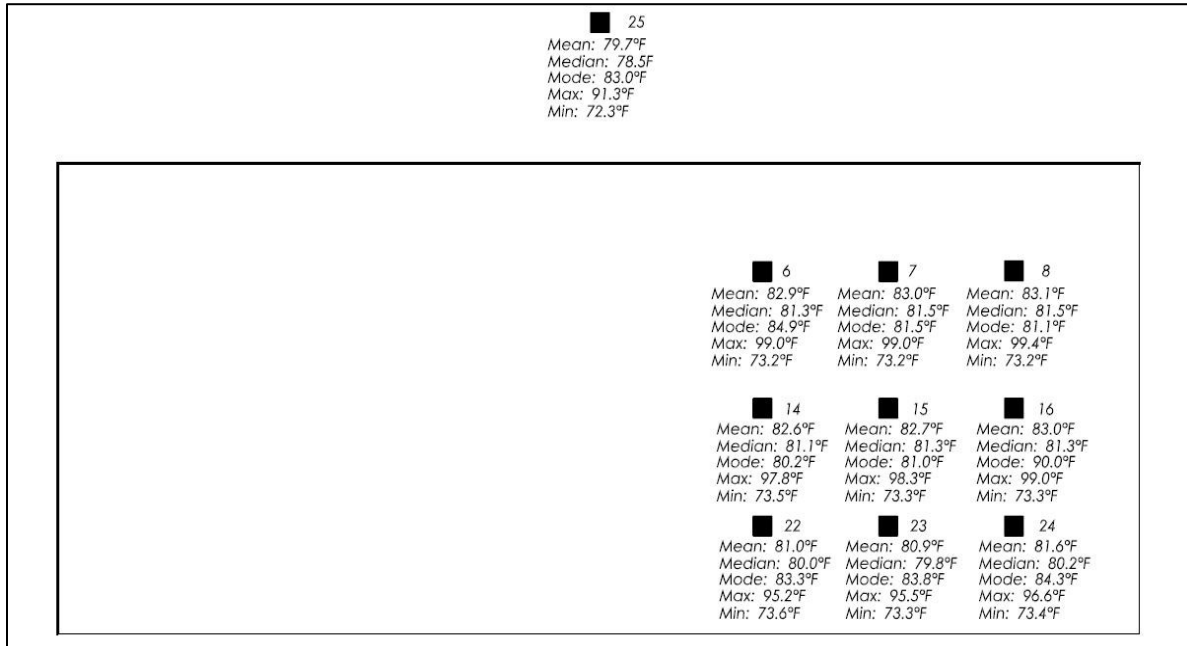


**Figure 18: North Side of Wall 2 Thermocouple Summary 8/11/12 to 8/18/12**

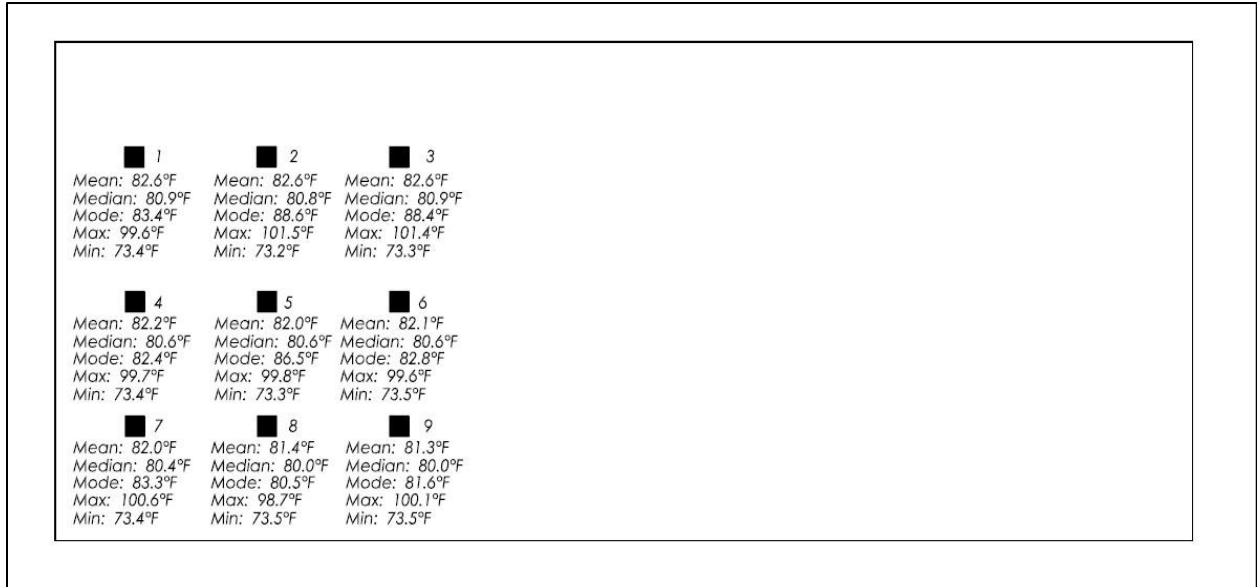


**Figure 19: South Side of Wall 2 Thermocouple Summary 8/11/12 to 8/18/12**

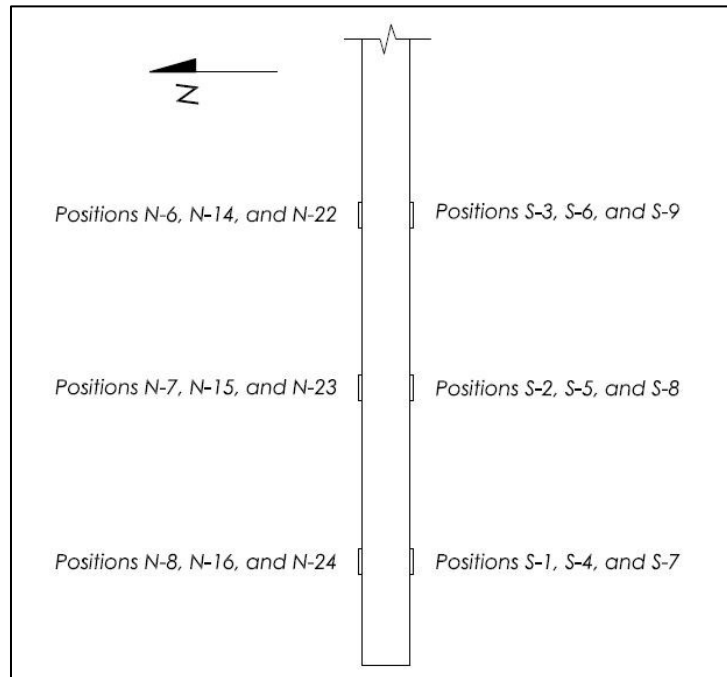


**Figure 20: Plan View of Double-Sided Thermocouple Arrangement on Wall 2**



**Table 4: Corresponding Opposite Thermocouples on Wall 2 Double-Sided Arrangement**

North Side	South Side
N-6	S-3
N-7	S-2
N-8	S-1
N-14	S-6
N-15	S-5
N-16	S-4
N-22	S-9
N-23	S-8
N-24	S-7

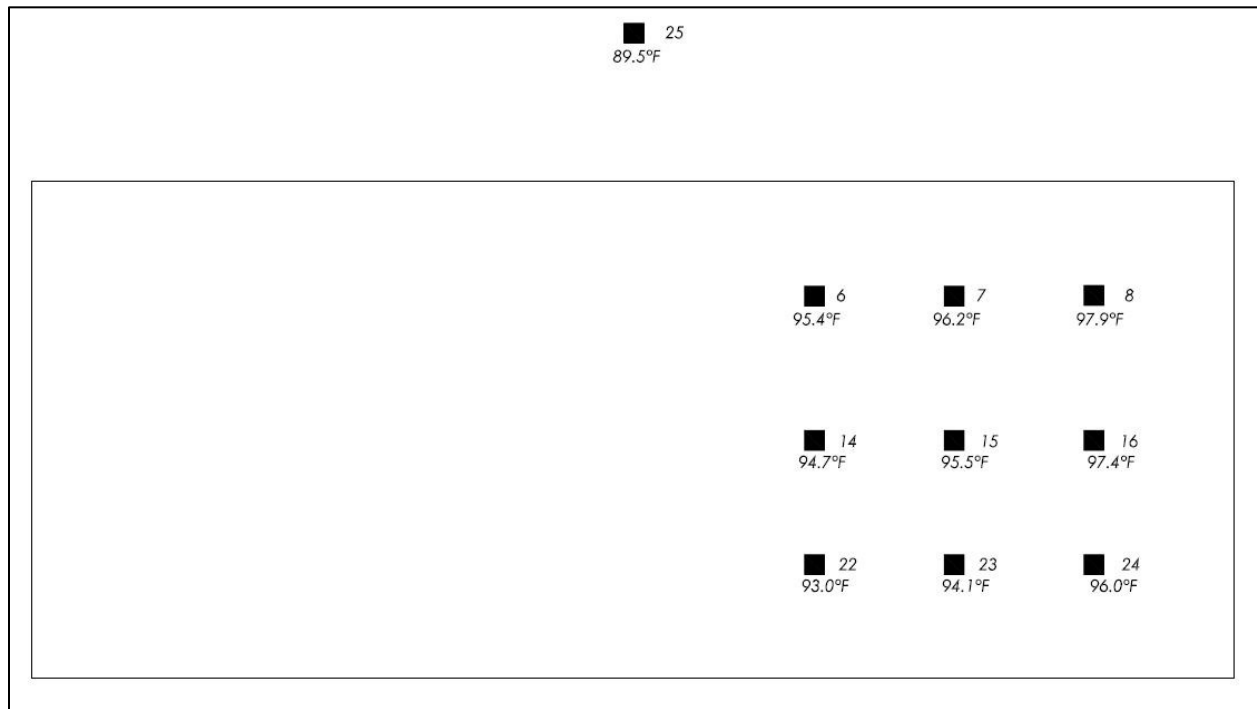


**Figure 21: North Side of Wall 2 8/16/12 at 1:00 PM**

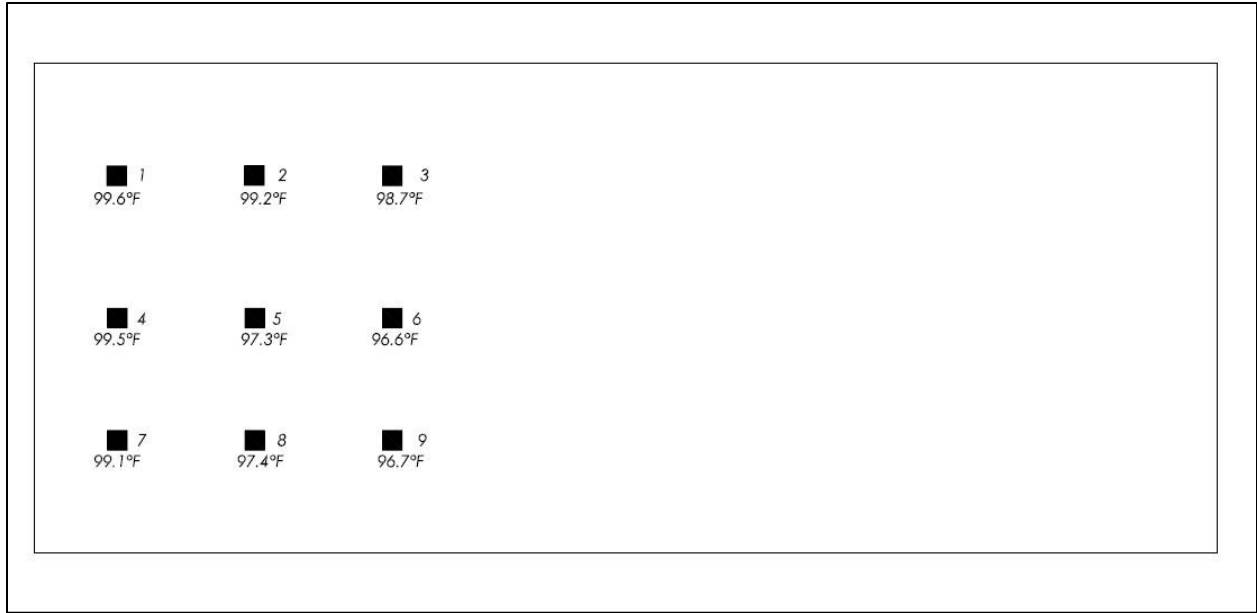


**Figure 22: South Side of Wall 2 8/16/12 at 1:00 PM**

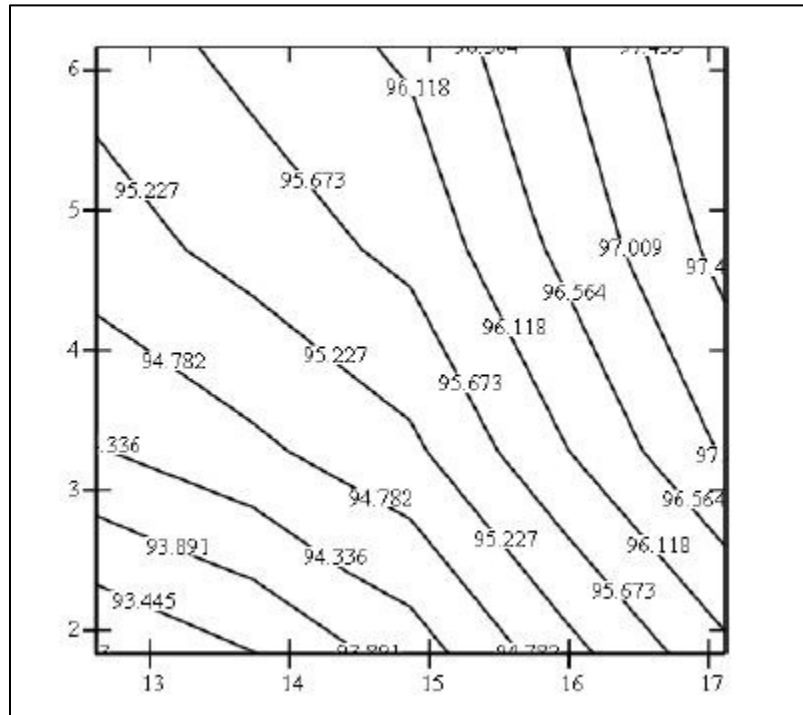


**Figure 23: Contour North Side of Wall 2 8/16/12 1:00 PM (Looking South)**

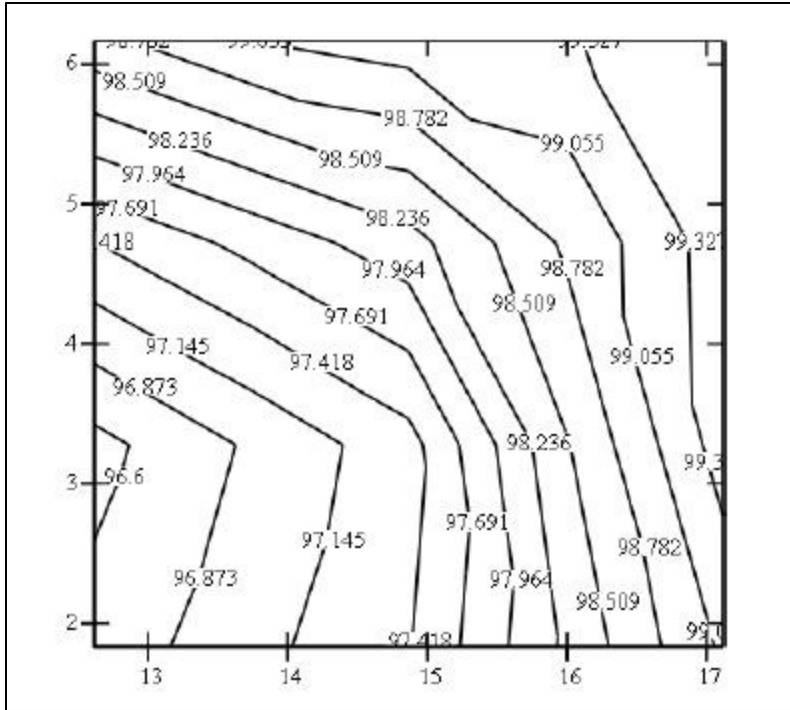


Figure 24: Contour South Side of Wall 2 8/16/12 1:00PM (Looking South)

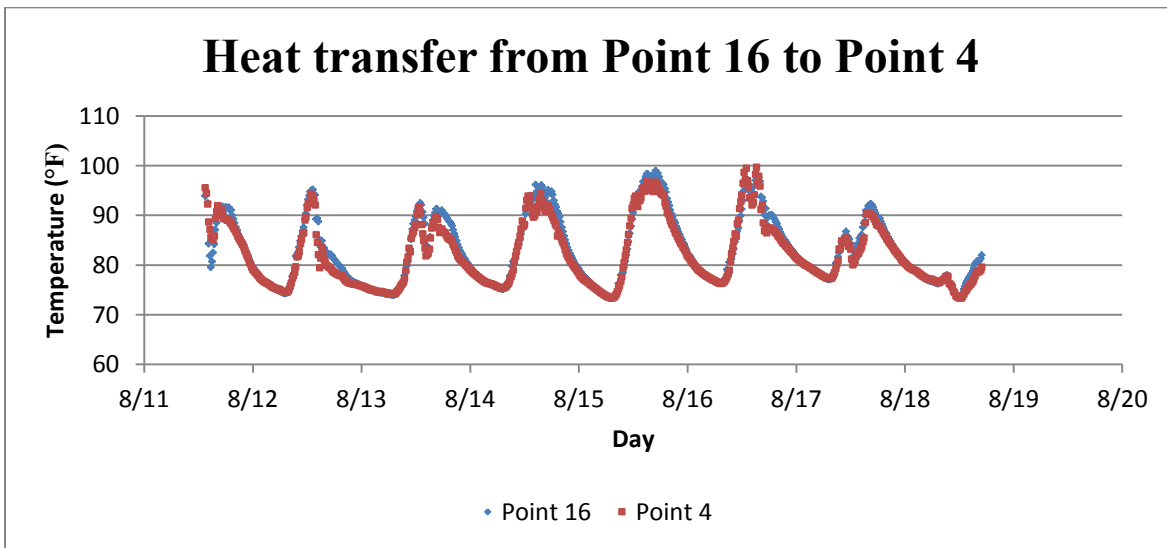


Figure 25: Double-Sided Temperatures on Wall 2

## 6. THERMAL IMAGING RESULTS

### 6.1 Method of Thermography

The thermocouples were taking measurements as the thermal imaging was being performed with the thermal camera on 4/7/12. This day was more of a blind test of predefined positions on the wall. By blind, it is understood that the locations were chosen not because of any likelihood that they would contain hot spots or cold spots. Having the thermocouples running simultaneously to the thermography makes it possible to tell whether the infrared thermography is giving absolute or relative temperatures. A thermal image was taken at each of the 24 thermocouple locations, which also included the immediate surroundings of that location. Wall 3 was not considered on day 1. Only wall 2 was considered as it is the only one installed with thermocouples. This is important, as one main purpose of this test on day one is just to see whether the camera detects absolute or relative temperatures.

A second day of thermography was undertaken on 4/28/12 which was preceded by sounding (or tapping) the FRP lightly with a hammer to try and locate de-bonded areas. Tapping was used to know where to perform thermography.

Tapping is a qualitative way to perform sounding. There is instrumentation that would allow for quantitative assessment. However, the literature indicates that much more common is the qualitative approach. For example, Taillade et al and Lai note that hammer tapping is common [11, 6]. Mirmiran recommends only a “hard object” and that tap testing be done with “at least one strike per [square foot]” [14]. A quantitative approach may add value and should be

considered especially when tapping will not be followed up by more advanced methods such as thermography. Sounding is an important method as it is another non-destructive method that can often detect de-bonds. The method is not perfect; otherwise other non-destructive methods such as thermography would not be necessary. In a study done by Tashan, he found that 20% to 30% of defects found through IR thermography were undetectable by sounding alone [7]. This was likely done by qualitative hammer tapping. A quantitative sounding may provide better results, but thermography will likely still detect things that quantitative sounding cannot. All said, sounding is just another tool that can help in detecting delaminations.

The areas chosen for thermography by sounding would be chosen because there was a suspicion of de-bonding. The sound and feel of de-bonded material is distinct and this method works quite well. The idea was to find de-bonded areas (if there were any) and then see if the infrared camera would detect them. Both walls were tested in this manner.

The thermal imaging camera not only detects temperature; it detects radiation and other thermal properties and tries to translate all of it into temperature (these properties were discussed in chapter 2). The translation, however, gets skewed if some of the other thermal properties such as emissivity are present in abundance. Although the images shown in this chapter display some gradation, an actual temperature reading at these locations is unlikely to report as much sensitivity and variation as the camera. In contrast, the thermocouples only detect temperature.

As mentioned in section 2.4.4 one of the parameters detected by IR cameras is the intensity of solar radiation, which varies throughout the day and throughout the year. This could mean that at different times of the day or at different times of the year the camera will give different results even if the temperature is the same. This being the case, however, does not invalidate the results. What is needed from the thermal camera is for it to detect that one spot is

warmer than another, and the actual temperature reading obtained is not the data being sought after. The relative temperature for an object and its surroundings is what is helpful in detecting a hot spot, not actual temperature readings, so the results are valid for their intended use. The effect of the other factors aside from temperature is typically to make the temperature reading higher than what it really is. This assumes that all temperatures get equally skewed, which should be a good assumption, considering all of the thermography is of the same material (CFRP).

## **6.2 Day 1**

Thermography was started at around 10:15 AM and completed at around 2:30 PM on 4/7/12. There was no rain this day or the entire previous day. This allowed for the recommended 24 hours of dry conditions recommended by ACI 228.2R-98 and mentioned in section 0. The average expected winds for the day were 23 kph [21]. The day was clear in the morning and got cloudier in the afternoon. Based on these conditions this day was average for thermography since the wind was borderline.

The thermal imaging camera was hooked up to a Hewlett Packard G60-630US Notebook laptop computer. The camera has no display screen, so the laptop was used to observe a live feed of the thermal image and snapshots were taken using the FLIR Camera Controller GUI when the correct locations were found. The live feed has a dot or crosshair at the center of the display and the temperature of any object within the crosshair is previewed as shown in Figure 26. The image obtained can be saved as a picture file or it can be converted to an excel file of temperature data. Videos can also be produced. Roxio Easy VHS to DVD software was used to record the video. The snapshots taken from the camera are black and white, the videos are in color. Temperature data can also be obtained in excel format and can be plotted to produce a

color image of the snapshots taken. These images have also been included, however, in general the granularity and detail available in the original black and white snapshots is superior. One difficulty that arose during this day of thermography was that the laptop screen was difficult to see once the sun came out. As no local anomaly was found, Figure 27 to Figure 36 have been selected as representative of what was obtained from this day of thermography. The entire batch of thermal images from this day of thermography is included in the appendices.

An overall image of the wall was taken. Figure 27 shows that the wall as a whole looks pretty uniform. Figure 29 shows a regular photograph of the same wall. In the thermograph there are some variations in temperature, but this comes from blockage of sunlight from objects above the wall casting their shadow. Figure 29 shows the overhead obstructions that are casting their shadows in the thermal image.

Figure 30 shows thermocouple 2 and its surroundings. No local anomalies appear at this location. The mortar joints are clearly visible; they have a unique thermal behavior that differs from the masonry block. Figure 32 is a photograph at the same location as Figure 30.

Figure 33 shows thermocouple 6 and its surroundings. The thermocouple wire can be seen. The top of the wall is a lot warmer. This is not a real hot spot as the top of the wall gets direct sunlight from three sides, and is warmer than the rest of the wall. Other portions of the wall only get sunlight from one surface. Away from corners, the temperature of the wall is very uniform.

Figure 36 is a snapshot of location 16 and the vicinity. Again, no real local anomalies that can be attributed to localized de-bonding. The thermocouple wire in this image has a piece of duct tape wrapped around it that seems to have a different thermal reflection due to its unique material properties. This can also be seen in Figure 38.

To demonstrate some of the variation found in detecting temperatures with the thermal camera, thermocouple data for the exact time and locations where thermography was used is available. For locations 2, 6, and 16 the thermocouple readings at the time of thermography were 66.7°F, 83.5°F, and 89.5°F respectively. The corresponding camera readings were approximately 40°F, 77°F, and 93°F. This confirms that the precision of the thermal camera is not reliable in terms of absolute temperature and can vary to some degree. The difference in temperatures is because the camera does not detect temperature directly, but instead measures radiation reflected from a surface. Because of this, any temperature data obtained with the thermal camera is to be taken as a relative temperature and not as an absolute temperature. Quantitative temperature data from the thermal camera is not used in this study, only qualitative data is used (images) because temperatures are relative.

Overall on this day of thermography, no anomalies were found that could easily be identified as hot spots indicative of CFRP de-bonding.

### **6.3 Day 2**

Thermography began on 4/28/12 at 11:30 AM. This day saw no rain. The previous day was also completely dry. The wind speed was an average of 3 kph [21]. The day was clear with clouds in the afternoon. These environmental conditions made this day near optimal for thermography.

This day of data collection involved less thermography, as sounding of the FRP material was performed in order to locate de-bonded areas. A specific section of the walls was chosen to be the focus of this day of sounding and thermography. This was done for simplicity and because the west side of the wall generally gets the hottest as demonstrated in chapter 5. The hottest area of the wall was desirable because it goes through the highest degree of thermal



fatigue. From the west end of the wall and 5'-0" eastward was the strip of the wall that was chosen. This created a 5'-0" x 5'-0" area of CFRP to work with. Sounding with a hammer was done at approximately every square foot of the marked off area. Striking was random and included both masonry blocks and mortar joints. Once a de-bonded area was found from sounding, the location was noted and thermography was used to see if it could confirm a suspected or known delamination. This was all done on wall 2. Wall 3 was also investigated with the same methods, but nothing was found after sounding. A global thermal image was still taken for wall 3 which showed nothing out of the ordinary.

As day 1 had not found any de-bonded areas, the expectation was that there would not be any on day 2. However, two were found by sounding and confirmed with thermography. Prior to this it seemed that if there were hot spots, they were the type that would go undetected as can happen in some instances as noted in chapter 2. As none were detected on day 1, at this stage it was uncertain whether that meant that there actually were no de-bonded areas or if there were some, but that for some reason the camera was ineffective in detecting them.

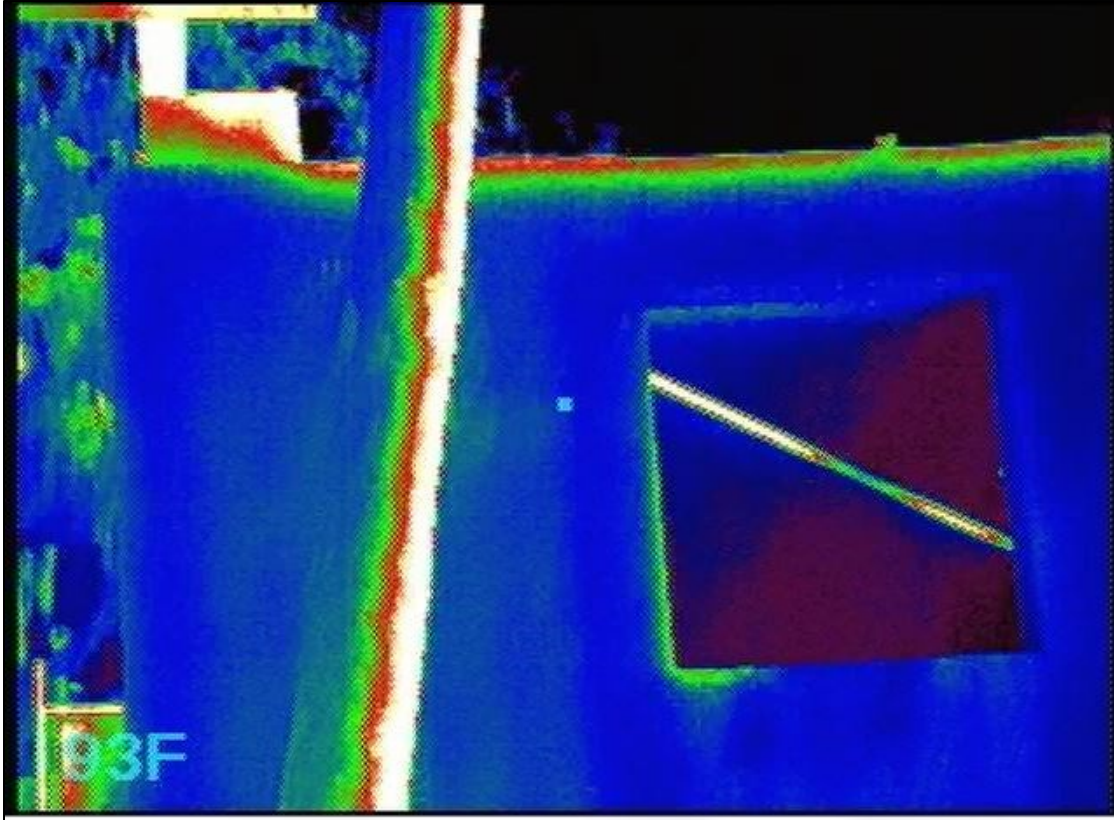
One conclusion that can be drawn from this is that it can be very difficult to detect a hot spot with a thermal camera unless you already know it is there. Knowing the spot is already there allows for more attention and focus to be paid to a very localized area. The camera is quite temperamental and if the area is not straight ahead, directly in view, and conditions just right, anomalies will likely go unnoticed and will blend in to the thermal environment that surrounds them. Various angles and distances were attempted during thermography.

Figure 39 shows a hot spot that was picked up from sounding the FRP. It was visible with the thermal camera after focusing in on this area. The amount of attention given to this one particular area is more than would typically be given to a spot on a long section of wall. It was

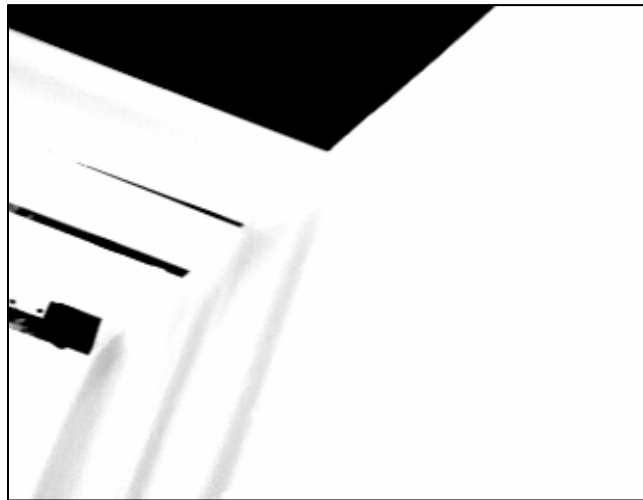
detected because its location was already known. The hot spot was approximately 1” in diameter and was located about 1” to the left and 1” below thermocouple location 15 as shown in Figure 44.

Figure 41 also shows a hot spot not far from the first. This de-bonded area was found by sounding the FRP and confirmed with infrared thermography. This area was also approximately 1” in diameter. It was located 6” above thermocouple location 15 and 2” to the left of this position. Figure 43 shows a photograph of location 15 and its surroundings. The de-bonded areas are visible and appear as the puffy areas of CFRP.

No hot spots were detected on the 25 square foot section of wall on wall 3 after sounding. A thermal image was still taken of the 5’-0” x 5’-0” area as shown in Figure 23. There are no obvious anomalies. One thing that was noticed on wall 3 from a simple visual inspection was that there was a tear in the FRP as shown in Figure 48. This tear is located 31.5” from the west end of the wall and 42.5” from the base of the wall. The cause of this is unknown.



**Figure 26: Thermal Camera Display during Operation on 7/30/11 at 11:49 AM**



**Figure 27: Global Thermal Image of Wall 2 at 2:07 PM (North Side)**



**Figure 28: Color Thermal Image of Wall 2**



**Figure 29: Wall 2 Global Photo**



**Figure 30: Thermal Image Location 2 10:32 AM (Wall 2 on the North Side)**

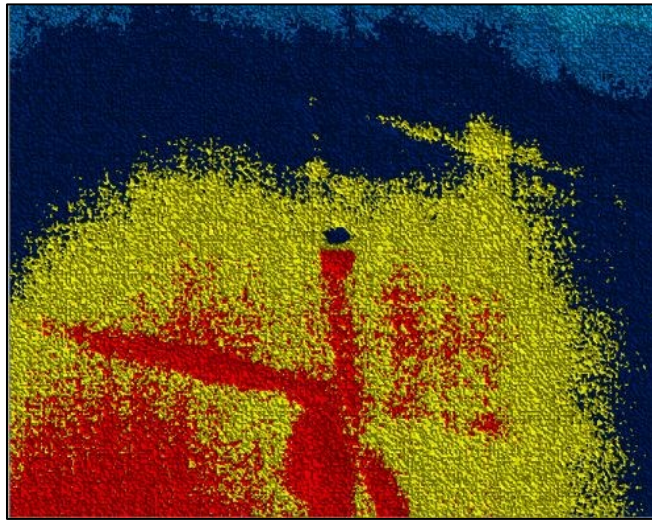


**Figure 31: Color Thermal Image at Location 2**





**Figure 32: Wall 2 Location 2 Photo (North Side)**

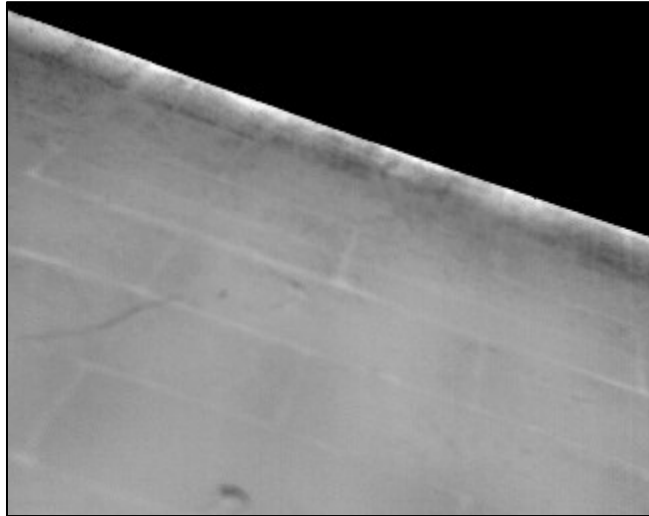


**Figure 33: Thermal Image Location 6 1:19 PM (North Side of Wall 2)**

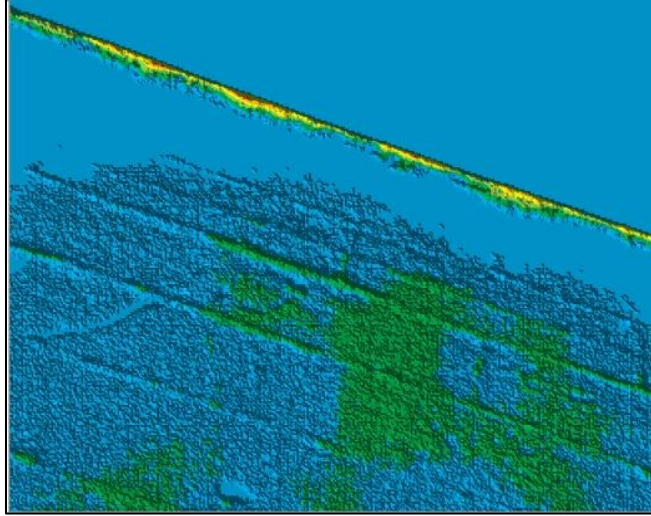


**Figure 34: Color Thermal Image at Location 6**

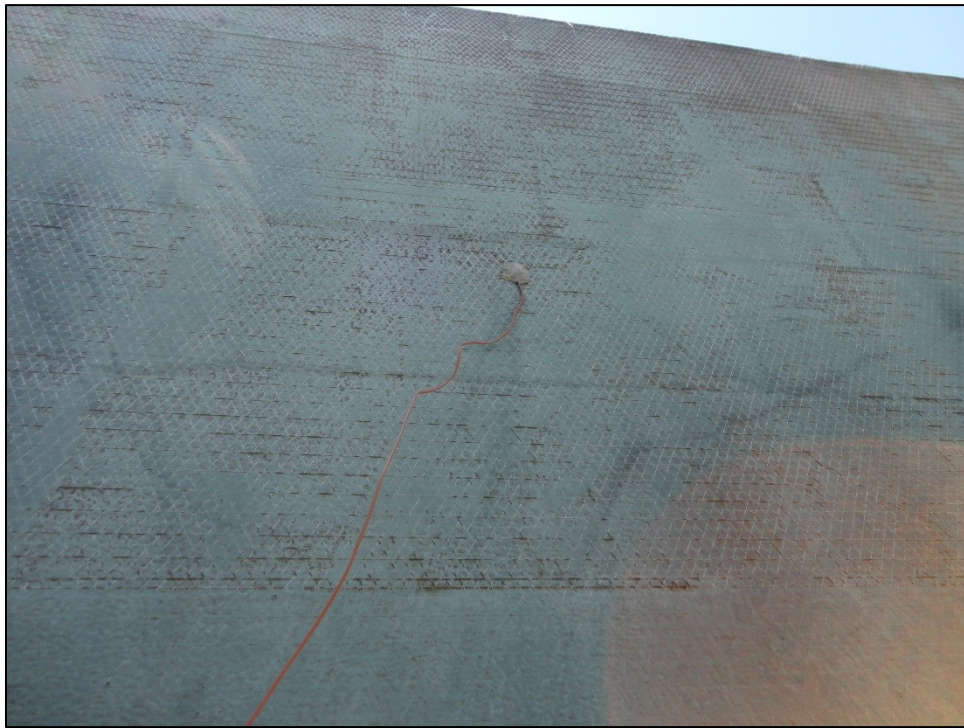


**Figure 35: Location 6 Photo (North Side of Wall 2)**

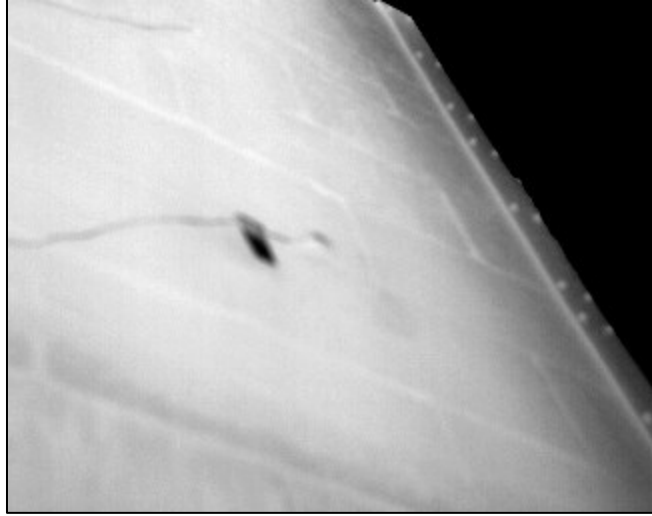


**Figure 36: Thermal Image Location 16 1:54 PM (North Side of Wall 2)**

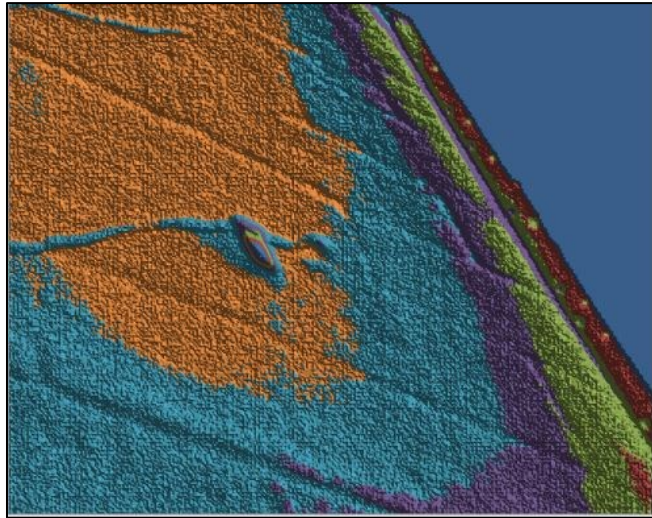


**Figure 37: Color Thermal Image at Location 16**



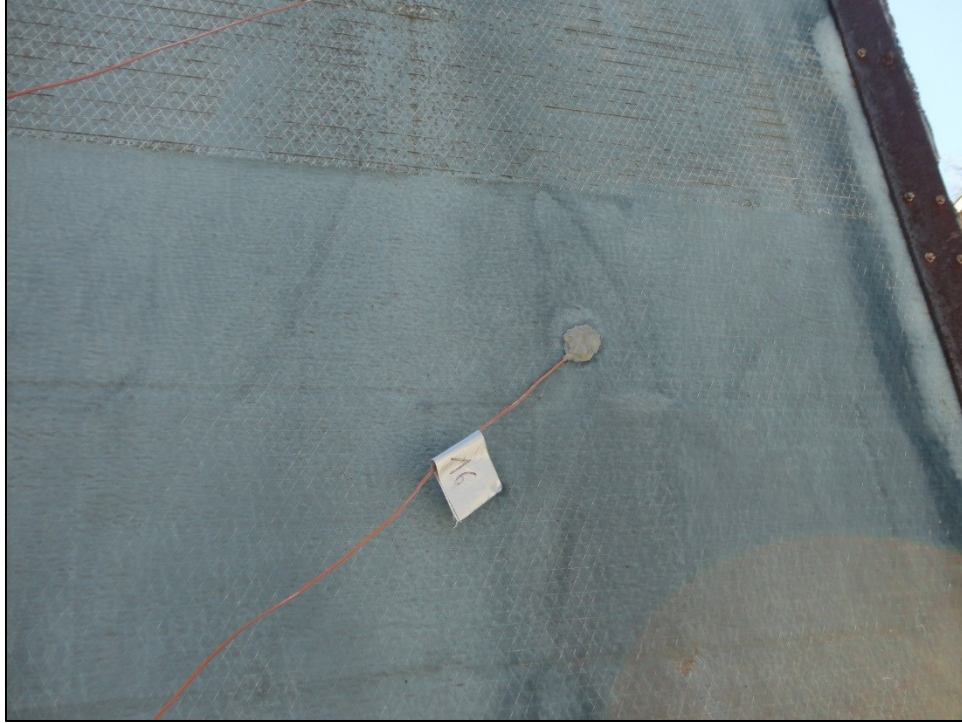


**Figure 38: Location 16 Photo (North Side of Wall 2)**

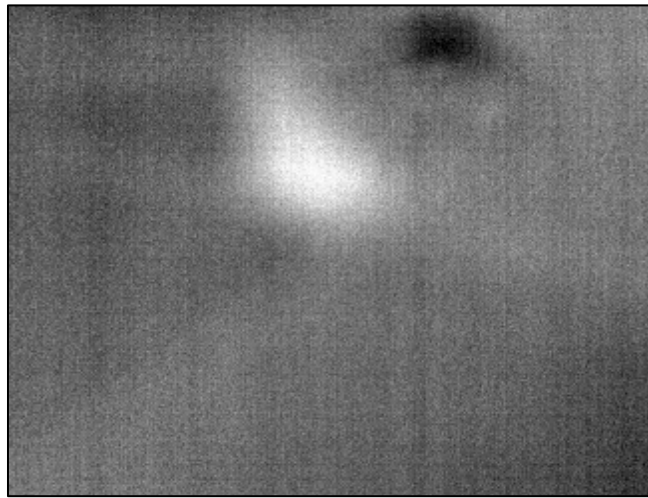


**Figure 39: Hot Spot 1 on 4/28/12 at 12:39 PM (North Side of Wall 2)**

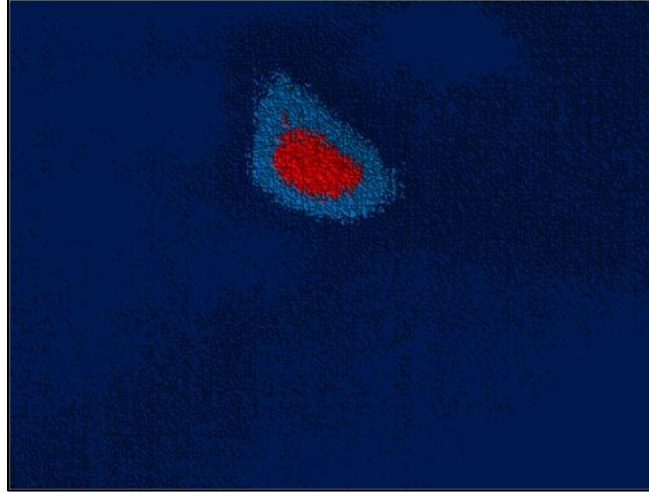


**Figure 40: Color Thermal Image of Hot Spot 1**



**Figure 41: Hot Spot 2 on 4/28/12 at 1:00 PM (North Side of Wall 2)**

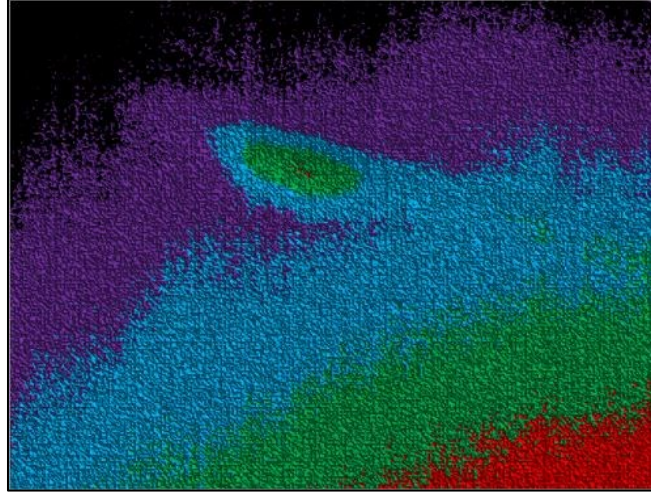


**Figure 42: Color Thermal Image of Hot Spot 2**

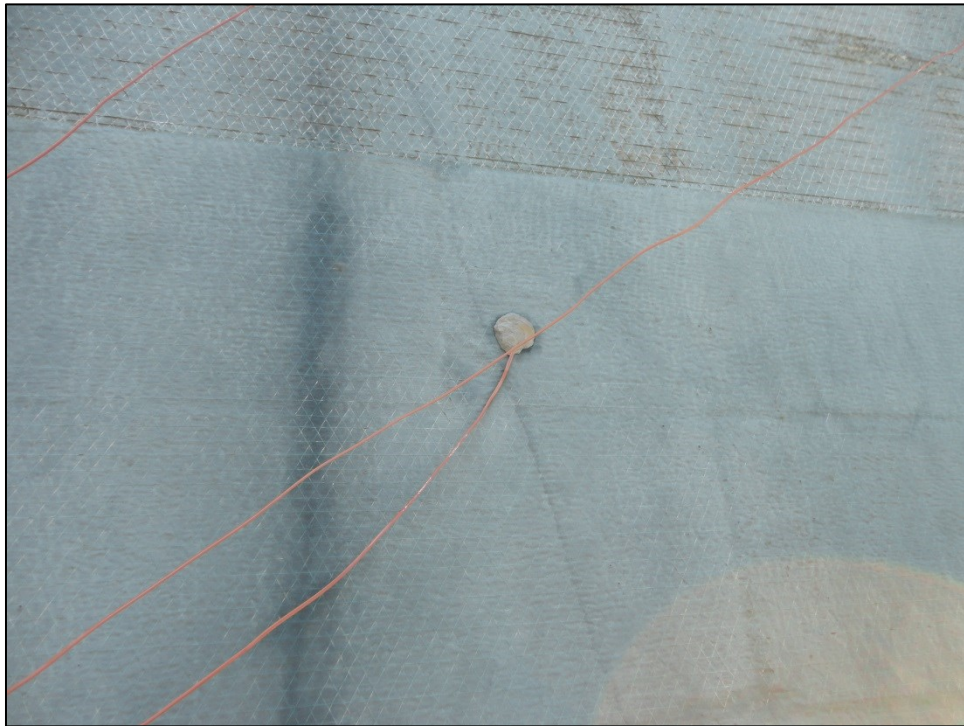


**Figure 43: Wall 2 at Location 15 near Where Hot Spots 1 and 2 were Found**

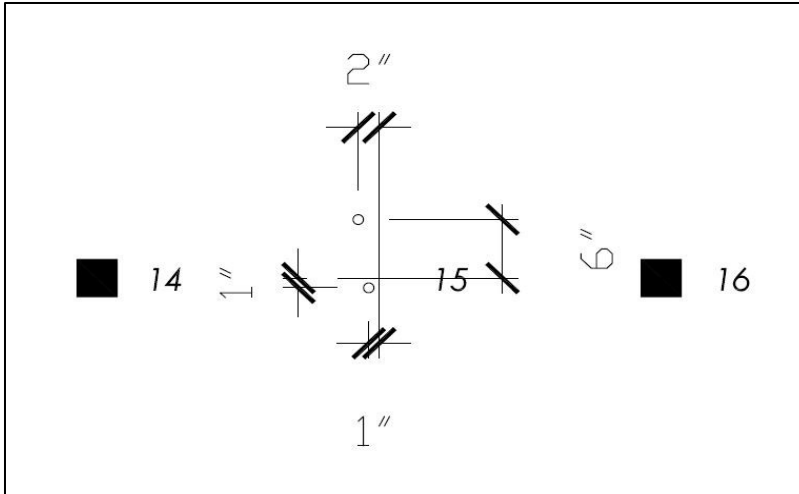


**Figure 44: Location of Hot Spots Found on Wall 2 with Thermal Camera**

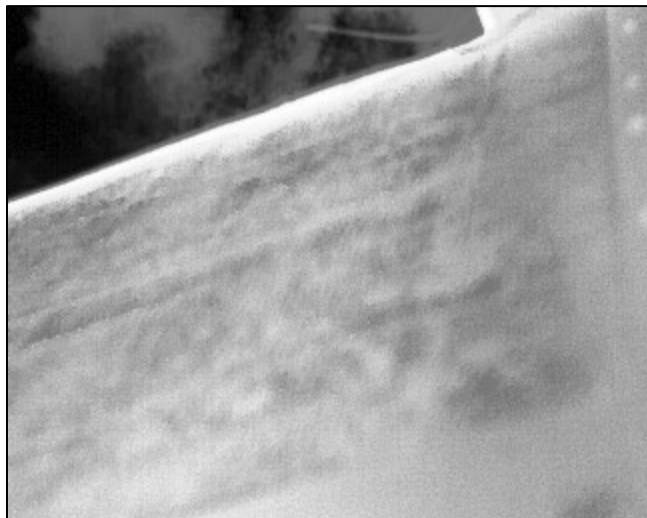


**Figure 45: Global Image of North Side of Wall 3 on 4/28/12 at 1:08 PM**



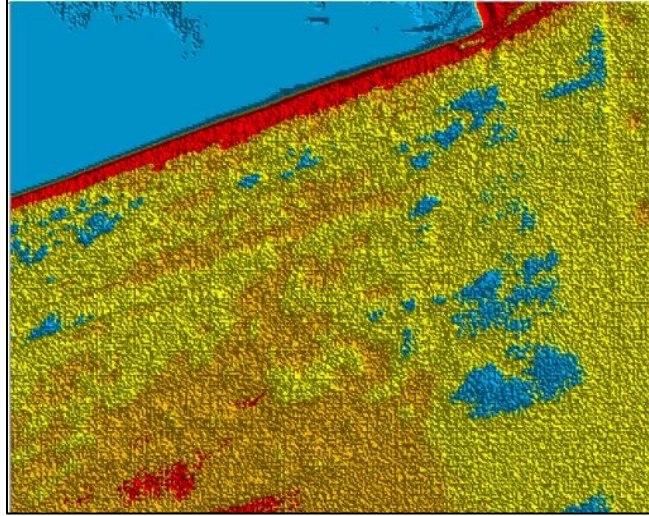


**Figure 46: Color Thermal Image of Wall 3**



**Figure 47: Global Photo of Wall 3**

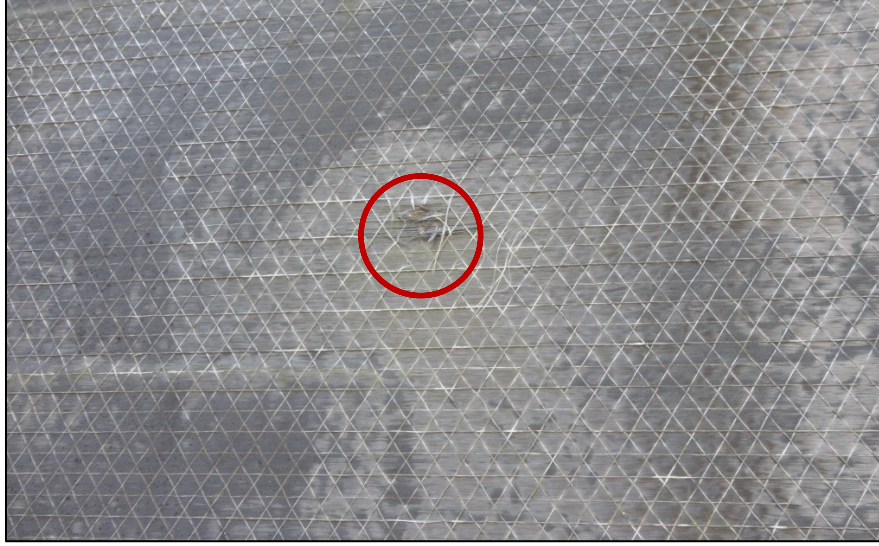


**Figure 48: Tear in Fabric on North Side of Wall 3**

## 7. THERMAL SCANNER RESULTS

### 7.1 Scanning Setup

Wall 2 and wall 3 were tested using the thermal scanner. Both of these walls had CFRP installed. Figure 51 and Figure 55 are a general schematic on the scans made with the device. The scanning was performed in a staggered pattern. One scanner width was skipped after every scan and then the widths that were skipped were picked up during a second pass. This was done in order to avoid residual heat from a neighboring scan from interfering with the next scan. Some overlap was allowed to ensure a continuous section of wall was being scanned.

The scanner used was extremely heavy. The setup of the test takes a significant amount of time and effort, more than performing the test itself. This was mostly due to the elevations that needed to get scanned. The setup required getting the thermal scanner at the correct elevation to access the FRP portions of the walls. This was done by placing a steel channel on scaffolding or tables. The scanner could then be wheeled along the channel as if it were on a track. A clamp was used to ensure the scanner was at a consistent distance away from the wall. Miscellaneous masonry blocks were used to adjust to the precise elevation needed. The test required an assistant to run. One person would operate the software as the other moved the scanner along the track. Start and end elevations were noted as the testing progressed, as was the distance of the scanner from the eastmost wall. Figure 49 shows the setup for the thermal scanner.

## 7.2 Scan of Wall 2

On 9/27/12 wall 2 was scanned. The scanning was done in the evening. There was no rain on this day or the day before. Other environmental conditions such as wind and cloud cover are more pertinent to passive thermography.

The scanner has 10 infrared sensors. This results in a scan width of 1'-1 1/2". As scans were performed every 1'-0", there was some overlap as shown in Figure 50. Twelve scans were performed in the middle section of the wall. The entire wall could not be scanned due to overhead obstructions on the east side and the scaffolding being used for the test on the west side blocked access there. The sensors were denoted IR1 to IR10 from left to right when facing the wall relative to a person who is also facing toward the wall.

The procedure for this day consisted of the following: moving the thermal scanner to the desired location, clamping it to the wall, measuring where the scanner was along the length of the wall, measuring the high position of the scanner, initiating the heating element, starting the mechanical operation that lowers the sensors from the top of the wall to the bottom of the FRP, start recording data, stop the sensors from moving, stopping the recording of data, powering off the heating element, and measuring the low position of the scanner.

One step that was neglected on this day of testing was placing a heat shield in front of the heating element so the heater did not warm up the top portions of the wall while it was not in operation. The shield could not be found, so testing proceeded without it. Theoretically, this could result in hot spots at the top of most scans. These scans would not normally be any hotter than the rest of the wall because of any defect in the bond. In reality, this only shows up on some scans.



On this day of scanning one of the infrared sensors was not operating properly (IR9). A thermal image has been generated in excel based on the temperature data obtained from the scans. The malfunctioning sensor was in the overlap portion of the scans, so its data has been replaced by the overlapping sensor's data. The last scan (on the far right) is the only one that includes just one strip from the malfunctioning sensor. Figure 51 shows a diagram of the scans that were performed. Figure 53 shows the results from those scans. Figure 54 shows the wall after post processing. Images which overlay sensors onto the scan images are found in the appendices.

There were certain factors that had to be accounted for in order to make the data useable. The scanner consisted of 10 separate sensors, each with a slightly different calibration. Also, the speed of the scanner was not perfectly constant and had some noticeable variations in scan rate. The rate was also adjusted on this day due to operator error. This results in certain areas receiving more heat than others, potentially creating false readings (hot spots). Difference in calibration can also create false readings. In post processing of the data, correction factors were determined to account for these potential sources of error.

The correction factor for sensor calibration was found by comparing the reported values of IR1 to every other sensor. All of the scan data for the entire wall was used in determining this factor in order to drown out the occasional anomaly that was expected to result. All of the sensors were then normalized to the calibration of IR1. IR1 was chosen arbitrarily as a convenient sensor to calibrate all other sensors to.

The correction factor for scan rate was found by averaging all temperature values for the 10 sensors. These average temperatures were then averaged again to find the average overall temperature for each pass. The scan rate was also averaged for each pass. A trendline was

drawn between datapoints for each pass plotted on a graph with average scan rate on the x-axis and average temperature on the y-axis. The equation of this trendline was then used to find out what average temperature would result at a central scan rate. The correction factor then results from comparing the average temperature for an individual scan to the theoretical average temperature that would be given at the rate all passes are being normalized to. This resulted in dividing the normalizing temperature by the unique average temperature for each scan. The normalizing scan rate for this day of scanning was 0.1 ft/s. This rate was at a midpoint between the fast scans and the slow scans. More detail on correction factors is contained in the appendices.

The remaining vertical striping that remains after the application of the correction factors cannot be due to wall conditions because the FRP was installed in horizontal strips. Repeating continuous vertical defects spanning multiple horizontal strips are highly unlikely. The cause must therefore be related to the test method, and is most likely attributed to a variation in the heating element intensity from left to right. Also the calibration correction factors helped clear up the images, but they are not perfect and can only smooth them out to a certain point. Also, every effort was made to keep sensors at a consistent distance from the walls by use of a clamp, however, some variation may still have resulted.

A cartesian coordinate system is used in locating anomalies (and recommended pull-off locations in chapter 8) with the origin as shown in Figure 52. Figure 54 is annotated indicating areas of significance in the scan. Refer to Table 5 for a commentary.

After post processing, well defined anomalies have appeared. The thermal scan did reconfirm one of the hot spots that were found previously through sounding the FRP and through

the use of the thermal camera. This hot spot is certainly a de-bonded area as it has now been confirmed with three different tests.

The confirmed hot spot is located as shown in the figures at the end of the chapter. The spots are so close to being at the exact same location that it is safe to say they are the same spot. Especially once the diameter of both the spot and the sensor that detected them are accounted for, an inch of difference does not make it a different hot spot. Note that there is another isolated spot near the confirmed hot spot that may also be de-bonded. There are several other local anomalies that may also be de-bonded areas which are also identified. Areas with high thermal contrast were selected as areas of interest.

The eighth scan from the left seems to have been corrupted in some way and the data for this section should be neglected.

### **7.3 Scan of Wall 3**

On 10/13/12 a second scan was performed. This scan was done on wall 3 and was done during the day. There was no rain on this day or the previous day. This allows for the surfaces to be dry and provides for the best thermography results. Again, other environmental factors such as wind speed and cloud cover are not relevant to active thermography.

The same procedure was followed as for wall 2, except that IR9 was fixed and the heat shield was found. This does not make significant changes, as IR9 data gets deleted on most scans due to the overlap and the heat shield did not seem to have a great effect as noted in section 7.2. Figure 57 shows the scans that were done on the wall, while Figure 58 shows the results. Table 6 explains the annotations in Figure 58. The results from this day of scanning went through the same post processing described for the first scan. The factors were not assumed to be the same for this scan, and were recalculated to tailor them specifically to this set of data.

They were slightly different. IR1 was again used as the normalizing sensor. The normalizing rate chosen for this scan was 0.2 ft./s as this was the approximate midpoint between the sets of data points. As this data is meant to be relative, any arbitrary rate could have been chosen within the range of rates that were plotted.

The scaffolding used on wall 2 was replaced by a table, which served the same purpose (to support the steel channel), but was lighter and easier to put in place. This is what is shown in Figure 49.

Large warm regions on the wall have reduced in size after post processing. As this scan was done during the day, it appears that this active form of thermography also picked up some passive heat supplied by the sun. Similar global heat patterns were seen with the IR camera as shown in Figure 16. There are mostly global anomalies and just a few local anomalies. There is no sagging in the wall that would indicate de-bonding of the size of the hot regions.

Figure 60 shows the scanning results superimposed on a sketch of the wall. This is to scale and visually shows where the thermal variations are occurring on the wall.



**Figure 49: Thermal Scanner Setup on Wall 3**

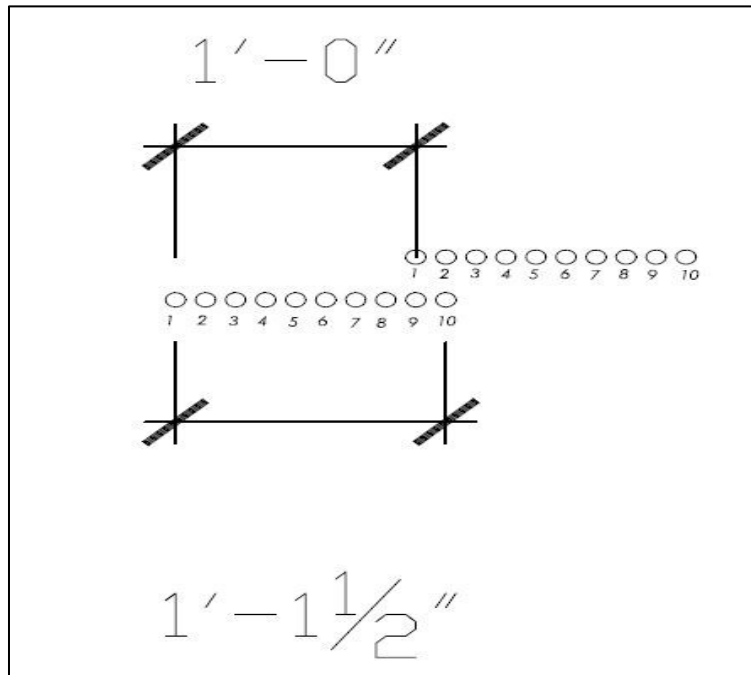


**Figure 50: Relative Position of IR Sensors on Adjacent Scans**

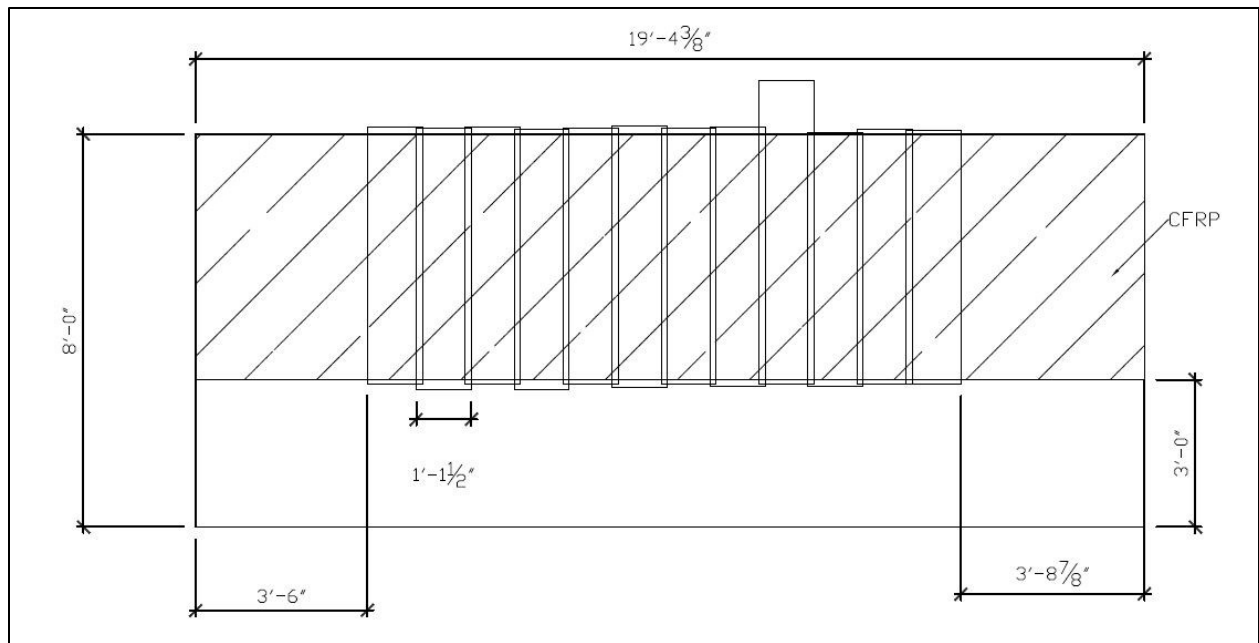


**Figure 51: Wall 2 Thermal Scans (on North Side)**



**Figure 52: Elevation of North Side of Walls Denoting Coordinate System Used in Tables**



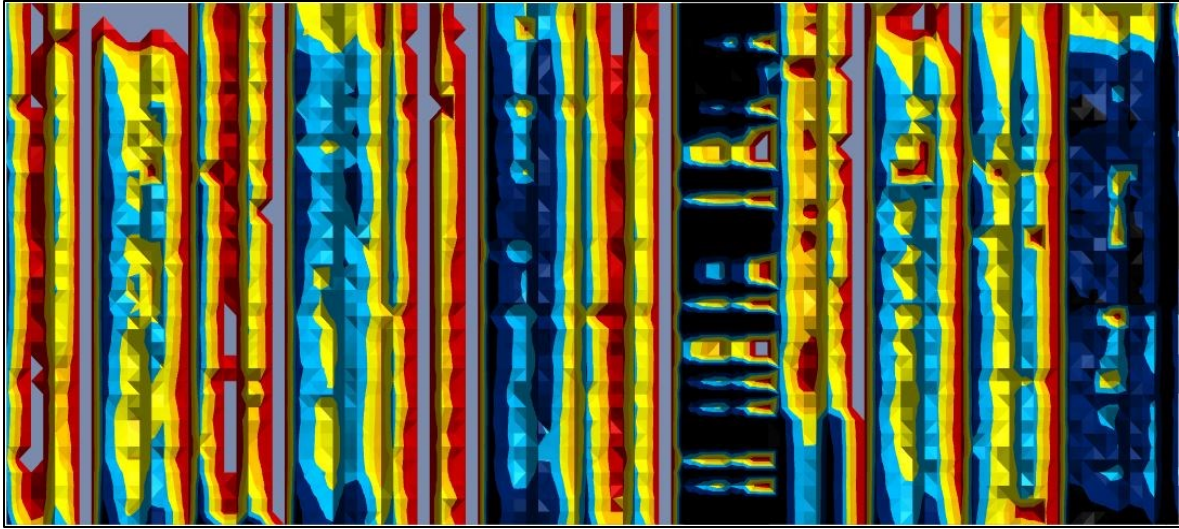


Figure 53: Wall 2 Thermal Scan Results Prior to Post Processing

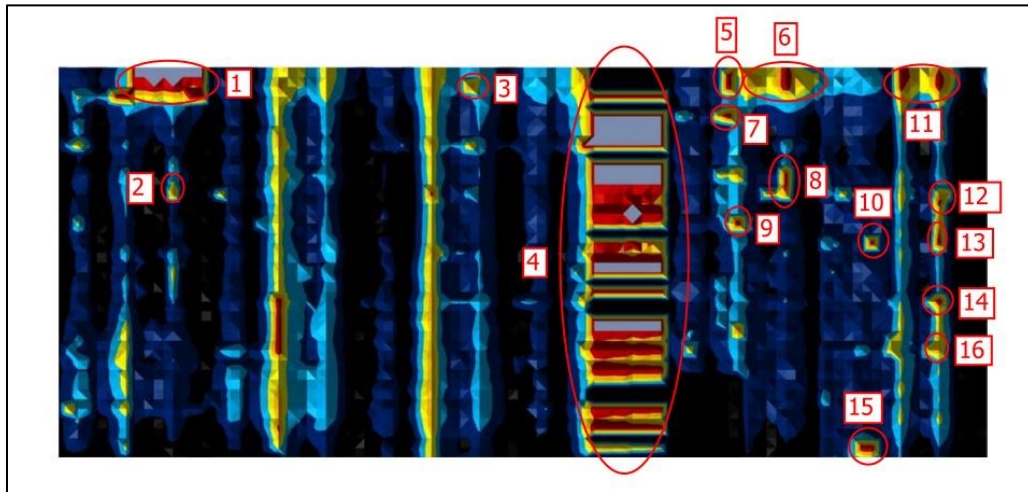


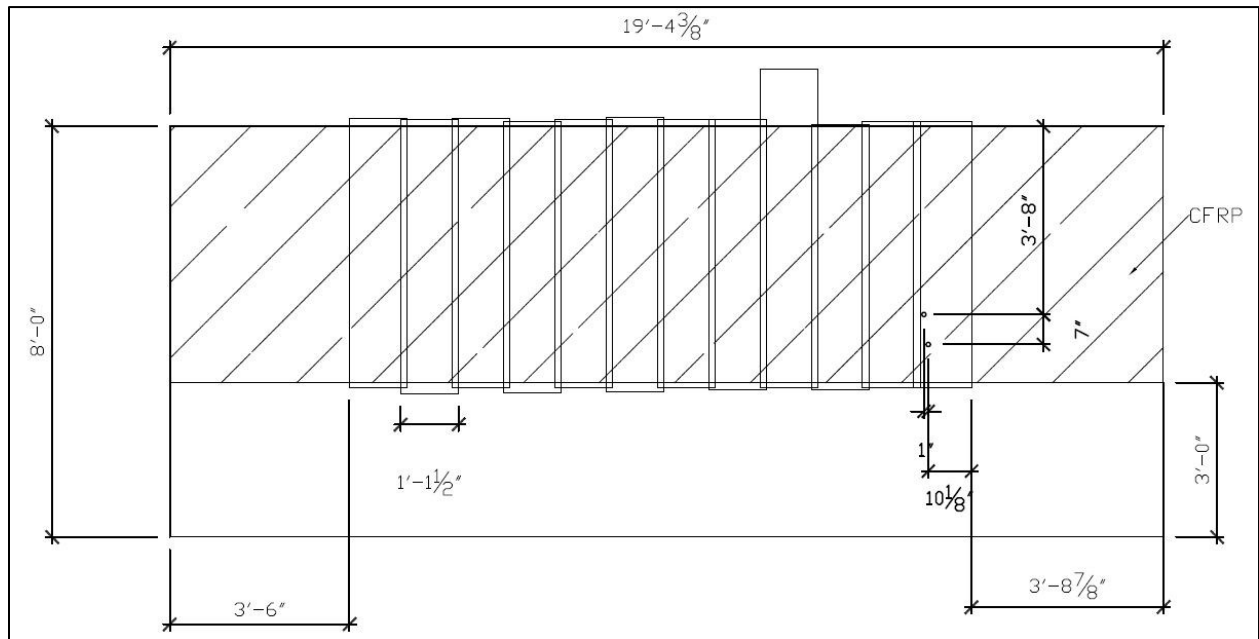
Figure 54: Thermal Scan Results on Wall 2 after Post Processing

Table 5: Explanation of Wall 2 Scan Annotations

Anomaly #	Coordinates (X, Y)	Comments
1	4'-10", 7'-11"	False reading. Scanner stopped
2	5'-0", 6'-5"	Defect
3	8'-10 1/2", 7'-10"	Defect

**Table 5 (Continued)**

Anomaly #	Coordinates (X, Y)	Comments
4	10'-11", ALL	False reading. Corrupted scan.
5	12'-3", 7'-10"	Defect
6	12'-9", 7'-10"	False reading, scanner stopped.
7	12'-3", 7'-5 ½"	Defect
8	13'-0", 6'-7"	Defect
9	12'-4 ½", 6'-1"	Defect
10	14'-1 ½", 5'-9 ½"	Defect
11	14'-9", 7'-11"	False reading, scanner stopped.
12	15'-0", 6'-4"	Defect
13	15'-0", 5'-10"	Defect
14	15'-0", 5'-0 ½"	Defect
15	14'-0 ½", 3'-2"	Defect
16	15'-0", 4'-5"	Defect. Hot spot 2 detected with thermal camera.



**Figure 55: Hot Spots from Thermal Camera on Wall 2 (North Side of Wall)**



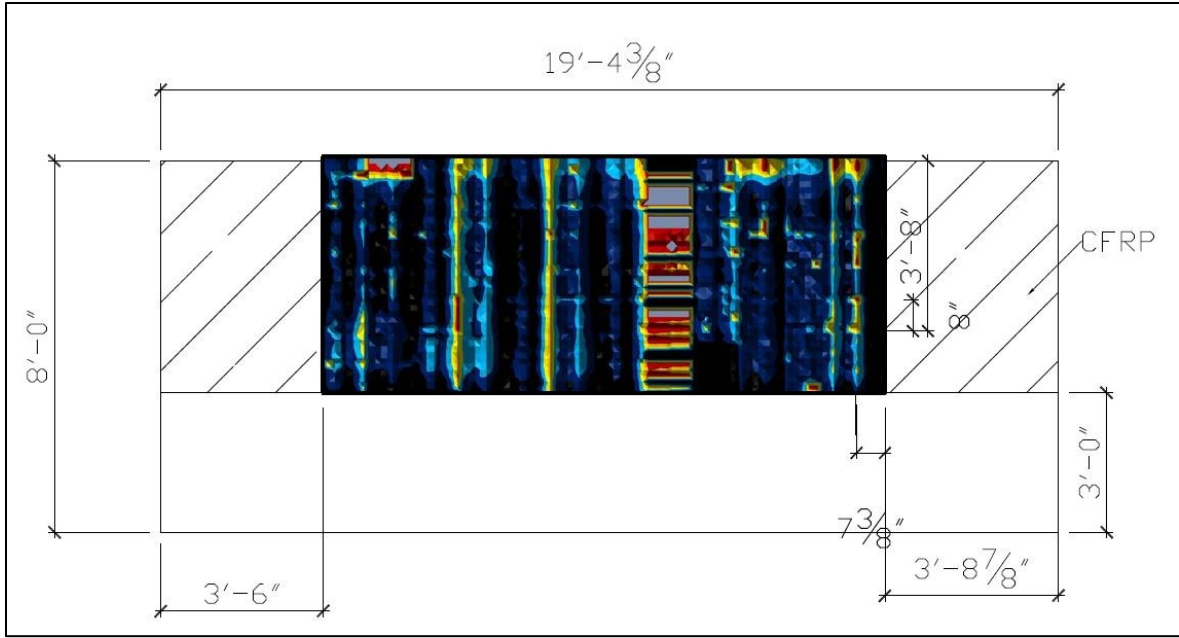


**Figure 56: Scanning Results on Wall 2 (North Side of Wall)**

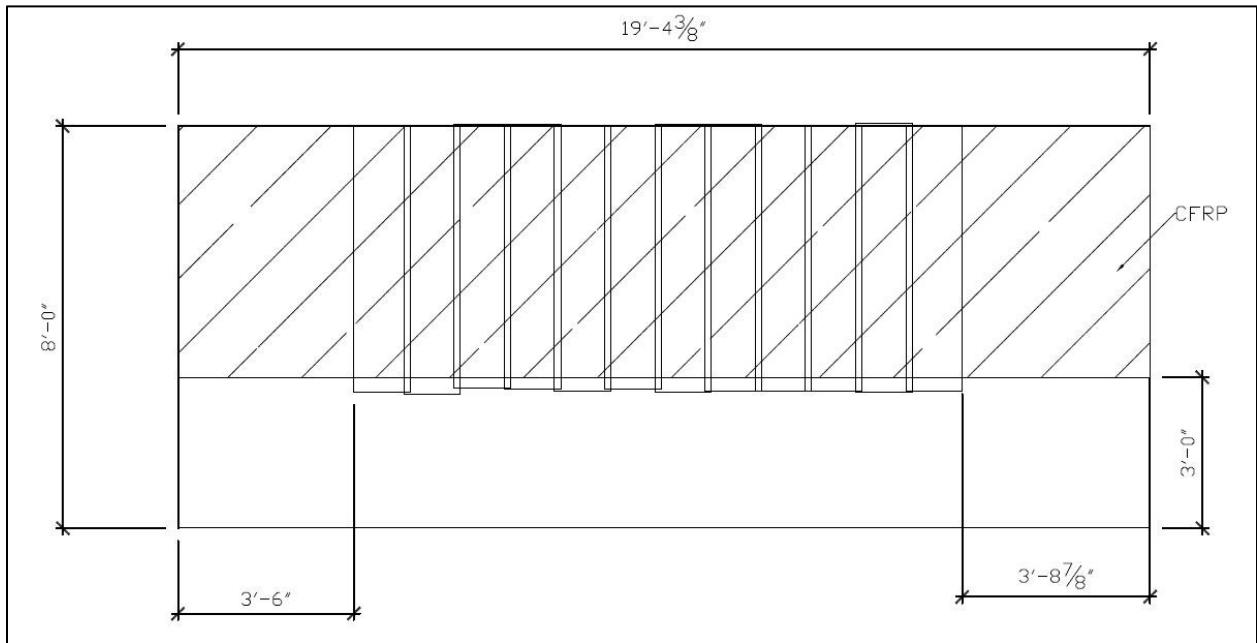


**Figure 57: Wall 3 Thermal Scans (on North Side of Wall)**



Figure 58: Wall 3 Scan Results Prior to Post Processing

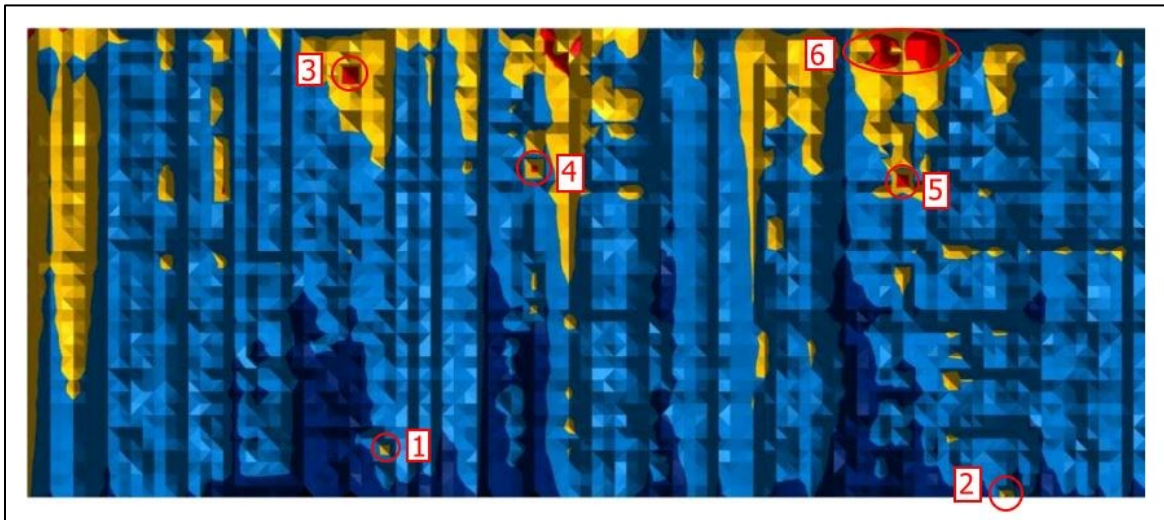


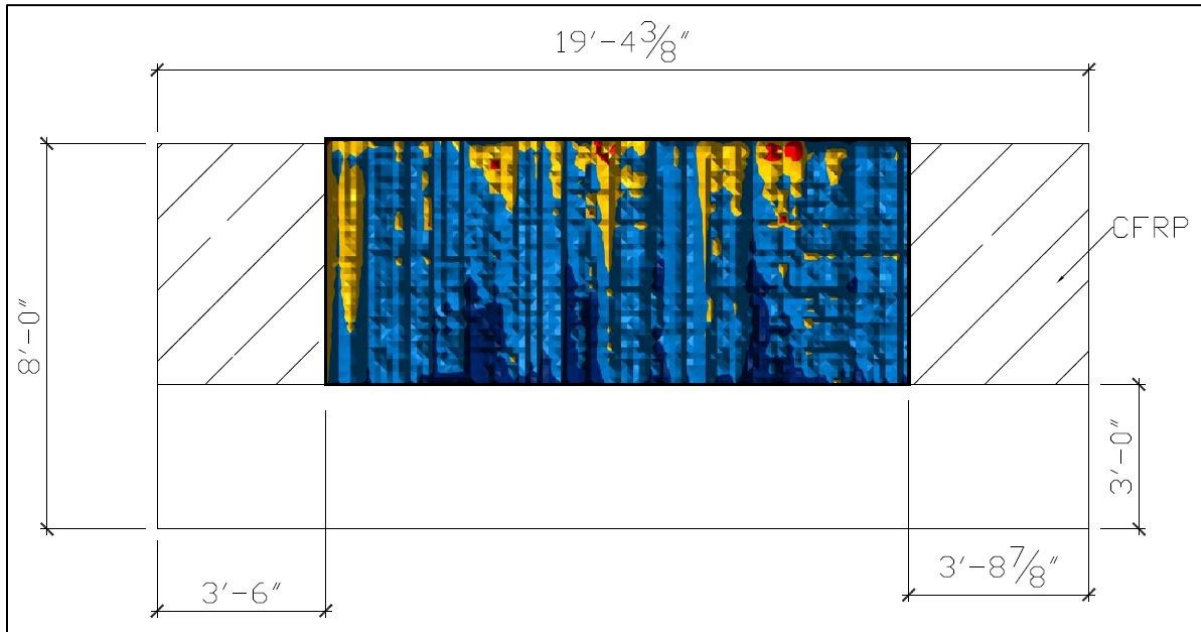
Figure 59: Wall 3 Scan Results after Post Processing

Table 6: Explanation of Wall 3 Scan Annotations

Anomaly #	Coordinates (X, Y)	Comments
1	7'-4 1/2", 3'-6"	Defect
2	14'-1 1/2", 3'-0 1/2"	Defect
3	7'-0", 7'-7"	Defect
4	9'-0", 6'-7"	Defect

**Table 6 (Continued)**

Anomaly #	Coordinates (X, Y)	Comments
5	13'-0", 6'-5"	Defect
6	13'-0", 7'-10"	False Reading, scanner stopped.
-	Global warm regions	Caused by passive heat sources.



**Figure 60: Results on Wall 3**

## 8. RECOMMENDATIONS AND PREDICTIONS

### 8.1 General Predictions

With the results of all the tests a few predictions can be made. From the thermocouple data indicating that the top corner on the west side of the wall is the hottest and temperatures cool gradually diagonally, the west side, and the top west corner in general will have experienced greater temperature variation throughout the years. This means the thermal fatigue is greatest here, and will have caused a weakening of the bond when combined with other environmental factors such as moisture and humidity. Not surprisingly, the hot spots that were found in this study were mostly on the west side of wall 2. Only the west side was tested with thermography in conjunction with sounding, but the majority each wall was tested with the scanner, which confirmed one of the hot spots on the west of wall 2. Pull-off tests will be weaker on the top west side. In the event that the testing equipment did not pick up all of the de-bonded areas, this area has the greatest likelihood of having additional defects. As noted earlier, even advanced IR technology cannot always locate defects 100% of the time. Figure 61 illustrates the prediction regarding de-bonding in general.

### 8.2 Limitations

There are limitations to the predictions that can be made from this study. As noted earlier, even thermal imaging systems can fail to locate de-bond or may produce false readings. Lack of a hot spot at a location does not mean that there is not a delamination at that location.

Some hot spots may be the result of a false reading, although an effort was made to ensure there is no known reason for any of the hot spots found to be the result of a false reading. Known false readings have been noted.

The thermal scanner used was not ideal, as it is an active form of thermography being used in an application best suited for passive thermography. This alone produced false readings, especially during the daytime. Additionally, the wavelength of the scanner's sensors was not ideal, although the wavelength used still works.

Although hot spots seem to be located more in the areas receiving high thermal fatigue, there may be other causes for delaminations. As noted earlier, workmanship may have caused some de-bonding. No scans are available directly after installation; therefore workmanship cannot be ruled out as a potential cause for any individual de-bonds. The loading done as part of the original study may have produced some de-bonding as well, but again, there is no thermography available before or after the loads were removed.

Due to the nature of the location, certain environmental factors such as freeze-thaw are not accounted for. Environmental cycling in environments significantly different from Florida may deteriorate bond at different rates and produce varying results.

The limitations to the findings presented in this study partially involve the equipment used. All of the tests performed only measure one major parameter—temperature. In reality there are many other parameters such as humidity, UV exposure, and chemical reactions.

Finally, although individual de-bonds cannot be assigned a specific cause of failure with certainty, there can be more certainty for a group of defects if they are all located in an area known to have high environmental cycling, that at least some of them can be attributed to thermal fatigue. This is the case on wall 2.

### 8.3 Pull-Off Testing

Pull-off testing is recommended to confirm that the hot spots that were detected are indeed de-bonding and should be done in accordance with ASTM D7522. For this testing, a device is attached perpendicular to the surface of the masonry wall. Small disks attached to the surface of the CFRP with epoxy and are then pulled in tension until the disk completely detaches. The surface should be cleaned prior to attaching the disks and allowed to dry [22]. The exact type of epoxy is not important as long as it has greater bond strength than what is expected from the substrate strength [22]. A typical compressive strength for concrete masonry units is 1900 psi. The tensile strength will be much lower. Epoxies typically come in strengths ranging from 5 ksi to 10.5 ksi (as noted earlier). Therefore a lower bound epoxy with a tensile strength of 5 ksi should be used and will be more than adequate. Curing should be carried out in strict adherence to the manufacturer's recommendations to achieve the desired bond strength. The curing will vary depending on the manufacturer, but generally takes seven days. The disks should be kept perpendicular to the wall surface for the entire length of the cure. Tape sometimes works, but a more secure method of fastening these disks would be better. The amount of force it takes to pull the disk off is then measured [22]. This procedure is done in order to test how the strength of the epoxy bonding the CFRP sheet to the masonry wall compares to the strength it is reported to have had originally. As the walls are not enclosed, testing should be performed under favorable weather conditions. It should not have rained for a period of at least 24 hours.

Pull-off tests that are de-bonded should pull off with no force if the delamination is at least the same area as the disks. Otherwise, some force will be required. Pull-off tests with good bond will fail in the substrate region. Pull-off tests with weaker than expected bond may fail in

the bond or in the substrate, depending on if the bond has weakened to the point where it is weaker than the substrate.

Specific locations are recommended for testing as shown in Figure 62: the hot spot that was confirmed by sounding, thermography, and scanning; four other anomalies identified on wall 2; and at least five tests in a good/cold region. This would involve a total of ten pull-off tests on wall 2. Table 7 provides additional details on pull-off recommendations for wall 2. Wall 3 should test all anomalies except for the one that is too close to the FRP edge, one additional test in a region of high thermal fatigue, and five in a region of low thermal fatigue. Anomaly 2 on wall 3 would put the pull-off disk partially on bare masonry and this would skew the results. Recommendations for wall 3 are shown in Figure 63 and are further explained in Table 8. One location is recommended that is not in its corresponding location (weak bond in upper west region and strong bond in lower east region). This is because an anomaly was found here, however, except for this one; the others follow the pattern of either being at the top of the wall, on the west, or both in order to validate the general prediction. These tests should preferably be completed within a year or two in order to ensure that the results of the non-destructive testing are still valid and significant further deterioration does not occur. The locations specified should be close to the coordinates listed, but a tolerance of  $\pm 1$  in. is acceptable as the disks themselves are generally 2 in. in diameter.



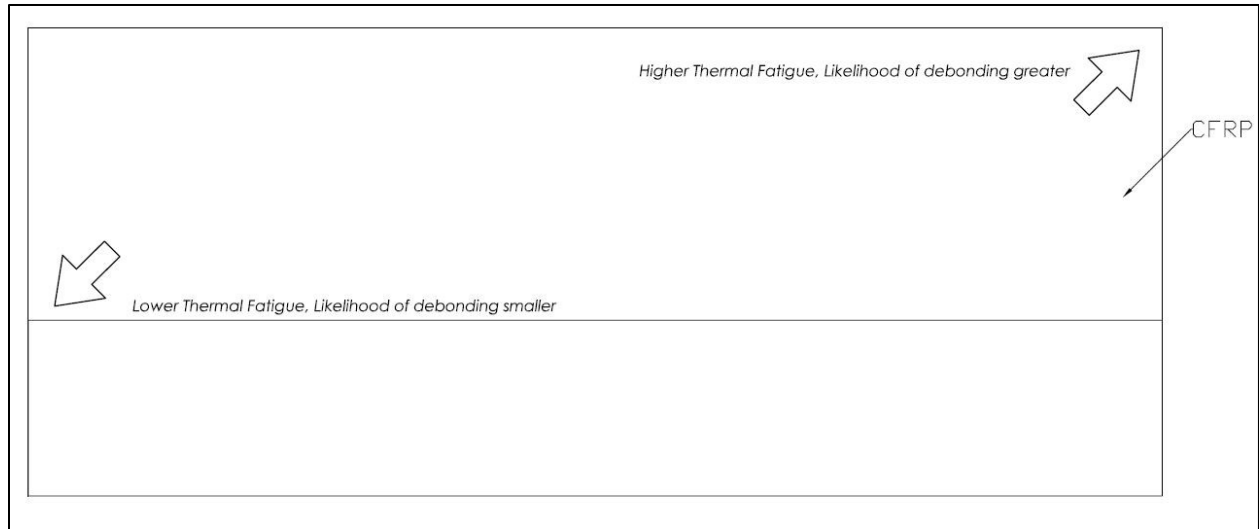


**Figure 61: General Predictions on CFRP Bond on Walls 2 and 3**

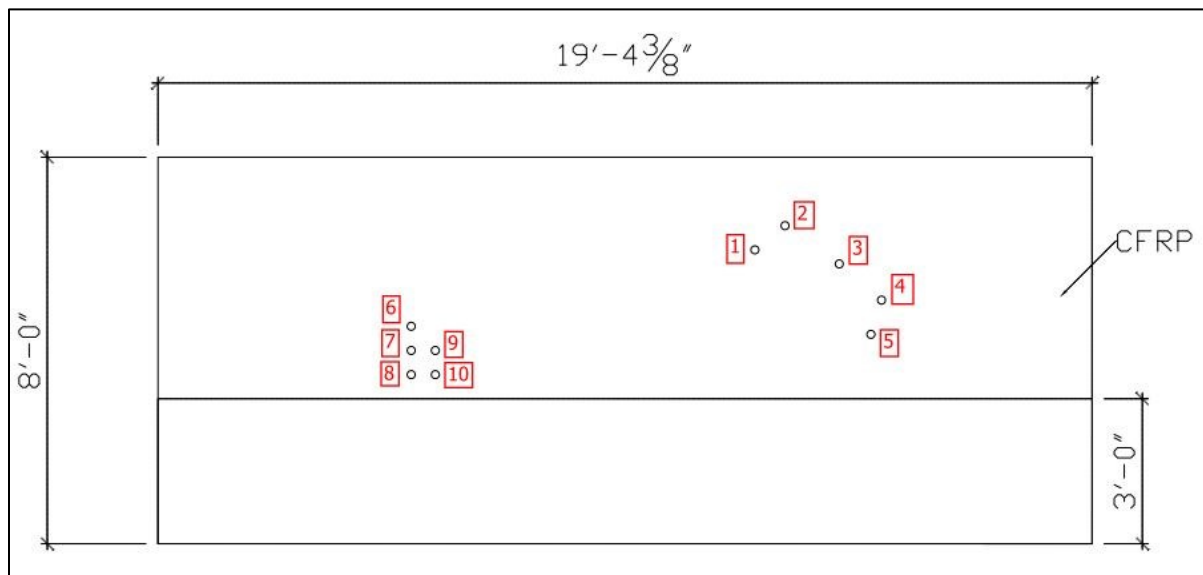


**Figure 62: Wall 2 Pull-Off Recommendations (North Side Elevation Shown)**

**Table 7: Pull-Off Recommendations Wall 2. Origin is as Shown in Figure 52.**

Pull-Off #	Coordinates (X, Y)	Expected Outcome	References
1	12'-4 1/2", 6'-1"	No Bond	Anomaly #9, Figure 54
2	13'-0", 6'-7"	No Bond	Anomaly #8, Figure 54



Table 7 (Continued)

Pull-Off #	Coordinates (X, Y)	Expected Outcome	References
3	14'-1 1/2", 5'-9 1/2"	No Bond	Anomaly #10, Figure 54
4	15'-0", 5'-0 1/2"	No Bond	Anomaly #14, Figure 54
5	14'-9 1/2", 4'-4"	No Bond	Anomaly #16, Figure 54, Hot Spot 2 from Figure 41
6	5'-3", 4'-6"	Substrate Failure	Lower thermal fatigue, Figure 14
7	5'-3", 4'-0"	Substrate Failure	Lower thermal fatigue, Figure 14
8	5'-3", 3'-6"	Substrate Failure	Lower thermal fatigue, Figure 14
9	5'-9", 4'-0"	Substrate Failure	Lower thermal fatigue, Figure 14
10	5'-9", 3'-6"	Substrate Failure	Lower thermal fatigue, Figure 14

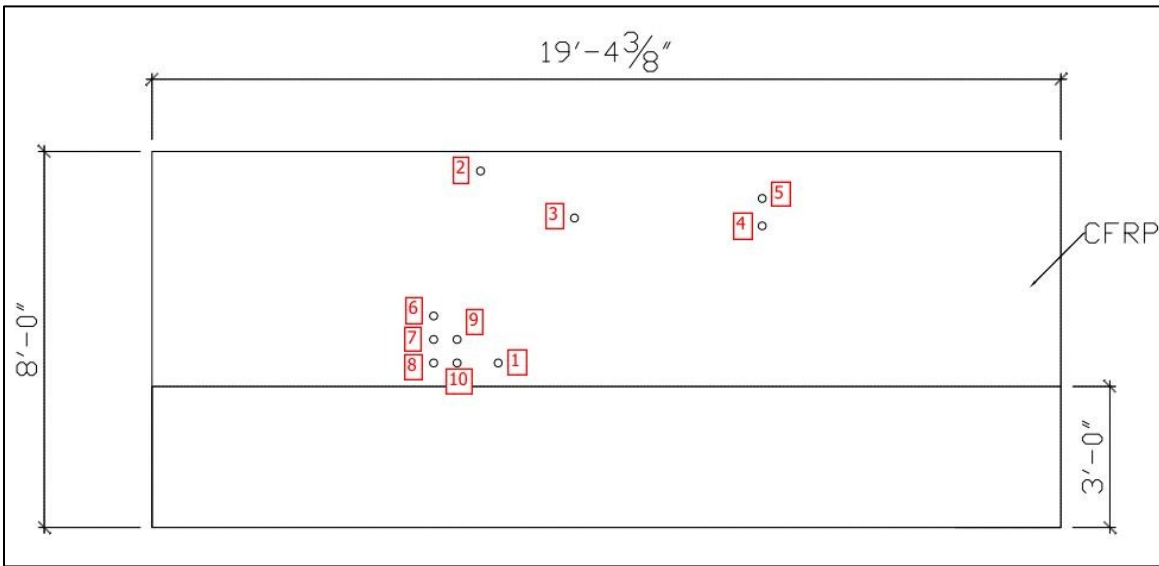


Figure 63: Wall 3 Pull-Off Recommendations (North Side Elevation Shown)

**Table 8: Pull-Off Recommendations Wall 3. Origin is as Shown in Figure 52.**

<b>Pull-Off #</b>	<b>Coordinates (X, Y)</b>	<b>Expected Outcome</b>	<b>References</b>
1	7'-4 1/2", 3'-6"	No Bond	Anomaly #1, Figure 59
2	7'-0", 7'-7"	No Bond	Anomaly #3, Figure 59
3	9'-0", 6'-7"	No Bond	Anomaly #4, Figure 59
4	13'-0", 6'-5"	No Bond	Anomaly #5, Figure 59
5	13'-0", 7'-0"	Bond Failure	Higher thermal fatigue, Figure 14
6	6'-0", 4'-6"	Substrate Failure	Lower thermal fatigue, Figure 14
7	6'-0", 4'-0"	Substrate Failure	Lower thermal fatigue, Figure 14
8	6'-0", 3'-6"	Substrate Failure	Lower thermal fatigue, Figure 14
9	6'-6", 4'-0"	Substrate Failure	Lower thermal fatigue, Figure 14
10	6'-6", 3'-6"	Substrate Failure	Lower thermal fatigue, Figure 14

## 9. CONCLUSION

The question driving this study was whether the durability of the bond had allowed it to survive seventeen years of weathering and thermal fatigue. The data obtained indicates that the bond has failed in certain localized areas of the wall. Overall, however, the bond has remained through the years throughout a large portion of the walls. Whether it has lost strength in areas that did not show up as anomalies will be the subject of future research.

Ten pull-off tests are recommended for each of the two walls investigated (the walls shown in Figure 64). Hot spot locations are identified where bond may have deteriorated. Five of these hot spot locations are identified for wall 2. Due to the limited number of anomalies found on wall 3, only four hot spot locations are recommended and one additional spot is placed in a location of high thermal and environmental fatigue. The remaining five locations on each wall were selected because bond was expected to be good so that pull-off tests there would result in cohesive failure in the masonry substrate.

Specific conclusions are as follows:

- Wall 2 (See Figure 64 at the end of this chapter):
  - Figure 62 shows the recommended positions for pull-off testing on wall 2. Pull-off 5 was selected because this is the spot that was found by sounding and confirmed with the thermal camera as well as with the thermal

scanner. This location should have essentially no pull-off reading as it should be completely de-bonded.

- Locations 1 through 4 are recommended because they showed up in the thermal scan of wall 2. Complete de-bond is predicted.
- Locations 6 through 10 are recommended because they are supposed to be in good/cold regions as indicated in the results shown in Figure 54. These should have higher bond strength. Note that the locations predicted to have high pull-off values are more toward the east and to the bottom whereas the locations predicted to have no pull-off value are more toward the west and to the top of the wall.
- Wall 3 (see Figure 64 at the end of this chapter):
  - Figure 63 shows the recommended pull-off locations on wall 3. It had five confirmed hot spots, only four of which are recommended for testing. It also had large warm and cool regions, although they were due to passive interferences.
  - Additional pull-off testing on wall 3 is recommended at locations 2 through 4 (complete de-bond is predicted), location 5 (weak bond), and at locations 6 through 10 (stronger bond predicted). These recommendations are made based on the results found in Figure 59.
  - The pull-off locations shown are the recommended minimum. Additional tests may be carried out based on the results of the thermography, if desired.

- Comments:
  - Hot spot 1 and hot spot 2 found through sounding and confirmed with thermography are most likely due to workmanship defects due to their ease of detection [6]. These were puffy and felt as if they had a physical bubble in the cured FRP. It is likely that this air was entrapped from the beginning due to workmanship defects. Other hot spots that were more difficult to detect and that required IR technology are likely due to debonding as a result of bond deterioration.
  - Even in measuring temperature, these instruments are not always ideal. For instance, the thermal camera seemed to have trouble picking up local temperature variations if they were not extremely pronounced. The manufacturer states that the camera has an NEdT performance of <50mK at f/1.0 which indicates a high sensitivity, however it struggled in this particular application of detecting CFRP anomalies on exterior masonry walls using a passive thermography approach [5].
  - The thermal scanning device used in this study is recommended to be used at night in exterior applications to reduce passive interferences.
  - Two hot spots were located on wall 2 with the camera and by sounding and none on wall 3 using these methods. Twelve hot spots were located on wall 2 with the thermal scanner and only 5 on wall 3. By all measures, wall 3 which used the Tonen epoxy is performing better in terms of bond after 18 years than wall 2 which used the Henkel epoxy. Even though the

Henkel epoxy had a higher tensile strength, the Tonen epoxy had a better formulation to resist Florida weathering.

- Recommendations for Future Work:
  - Note that it would be ideal to leave enough FRP to allow for follow-up tests to be done, to see what an additional 10 years of weathering and thermal fatigue does to the bond. Perhaps a good time to test would be at 30 years when the usual design life of CFRP is nearing its end. Other parameters may also be researched aside from thermal fatigue, such as humidity, UV and time of wetness. Ideally, a weather station should be set up to monitor the environment.
  - Installing an entirely new strip of FRP on some of these walls and performing thermography on it from the beginning (after it has cured) would be best. This way there would be a scan at 0 years, 10 years, 20 years, and 30 years. Having the initial scan provides the assurance that workmanship defects can be ruled out in all future defects after the initial scan as the bond ages and is subject to environmental cycles. Keeping any new CFRP in the bays of these walls would be ideal as the resulting uneven temperature distribution provides an interesting and desired variable. This allows a comparison of the behavior of sections of the wall that receive differing degrees of thermal swings.



**Figure 64: The Two Walls Investigated**

## REFERENCES

- [1] A. H. Hartley Jr., "Strengthening of Concrete Masonry Walls Using CFRP Material," *Master's Thesis*, 1995.
- [2] A. M. Shalaby, F. H. Fouad and a. R. Albanese, "Strength and deflection behavior of spun concrete poles with CFRP reinforcement," *PCI Journal*, p. 55, 2011.
- [3] K.-K. Choi, G. Urgessa, M. M. R. Taha and A. K. Maji, "Quasi-Balanced Failure Approach for Evaluating Moment Capacity of FRP Underreinforced Concrete Beams," *Journal of Composites for Construction*, p. 236, 2008.
- [4] ACI Committee 440, "Guide for the Design and Construction of Externally Bonded FRP Systems for Strengthening Concrete Structures," American Concrete Institute, Farmington Hills, MI, 2008.
- [5] FLIR, Inc., *Tau Camera User's Manual*, Goleta, CA: FLIR, Inc., 2010.
- [6] W. Lai, "Characterization of the deterioration of externally bonded CFRP-concrete composites using quantitative infrared thermography," *Cement & Concrete Composites*, vol. 32, no. 9, pp. 740-746, 2010.
- [7] J. Tashan, "Investigation of the parameters that influence the accuracy of bond defect detection in CFRP bonded specimens using IR thermography," *Composite Structures*, vol. 94, no. 2, pp. 519-531, 2011.
- [8] K. K. Ghosh, "A critical review of infrared thermography as a method for non-destructive evaluation of FRP rehabilitated structures," *International Journal of Materials and Product Technology*, vol. 25, no. 4, pp. 241-266, 2006.
- [9] LumaSense Technologies GmbH, *Infrared Thermometer Handbook*, Santa Clara, CA: LumaSense Technologies, 2011.
- [10] C. Maierhofer, *Non-destructive evaluation of reinforced concrete structures*, Boca Raton: CRC Press LLC, 2010.
- [11] F. Taillade, "Shearography and pulsed stimulated infrared thermography applied to a nondestructive evaluation of FRP strengthening systems bonded on concrete structures," *Construction and Building Materials*, vol. 25, no. 2, pp. 568-574, 2010.



- [12] ACI Committee 228, "Nondestructive Test Methods for Evaluation of Concrete in Structures," American Concrete Institute, Farmington Hills, MI, 1998.
- [13] V. M. Karbhari, "Design factors, reliability, and durability prediction of wet layup carbon/epoxy used in external strengthening," *Composites Part B: Engineering*, vol. 38, no. 1, pp. 10-23, 2007.
- [14] A. Mirmiran, "NCHRP Report 514: Bonded Repair and Retrofit of Concrete Structures Using FRP Composites," Transportation Research Board, Washington, D.C., 2004.
- [15] A. Mirmiran, "NCHRP Report 609: Recommended Construction Specifications and Process Control Manual for Repair and Retrofit of Concrete Structures Using Bonded FRP Composites," Transportation Research Board, Washington, D.C., 2008.
- [16] C. W. Dolan, "NCHRP Web only Document 155: Design Guidelines for Durability of Bonded CFRP Repair/Strengthening of Concrete Beams," Transportation Research Board, Washington, D.C., 2008.
- [17] Utah State University, "GIS Climate Search," 2008. [Online]. Available: <http://climate.usurf.usu.edu/products/data.php>. [Accessed 19 May 2011].
- [18] C. Results, "Current Results," Current Results Nexus, 2013. [Online]. Available: <http://www.currentresults.com/Weather/Florida/humidity-annual.php>. [Accessed 8 October 2013].
- [19] V. Karbhari, "Durability Gap Analysis for Fiber-Reinforced Polymer Composites in Civil Infrastructure," *Journal of Composites for Construction*, vol. 7, no. 3, pp. 238-247, 2003.
- [20] S. Edwards, "SunriseSunset.com," Steve Edwards, [Online]. Available: <http://www.sunrisesunset.com/>. [Accessed 5 November 2013].
- [21] Weather Underground, Inc., "wunderground.com," Weather Underground, Inc., [Online]. Available: <http://www.wunderground.com>. [Accessed 5 October 2013].
- [22] ASTM Committee D30, "Standard Test Method for Pull-Off Strength for FRP Bonded to Concrete Substrate," ASTM International, West Conshohocken, PA, 2009.

## APPENDICES

## Appendix A: Wall 2 Thermal Imaging



**Figure A1: Global View of Wall 2 at 2:07 PM**

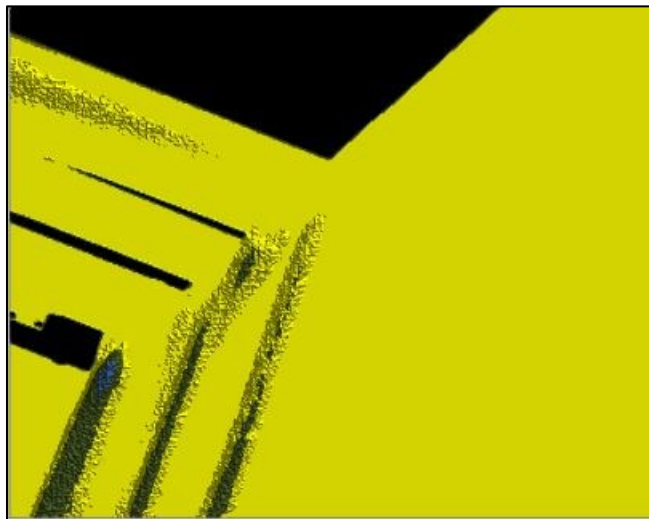


**Figure A2: Color Thermal Image of Wall 2**

**Appendix A (Continued)**



**Figure A3: Wall 2**



**Figure A4: Thermal Image at Location 1 at 10:17 AM (North Side of Wall 2)**

**Appendix A (Continued)**

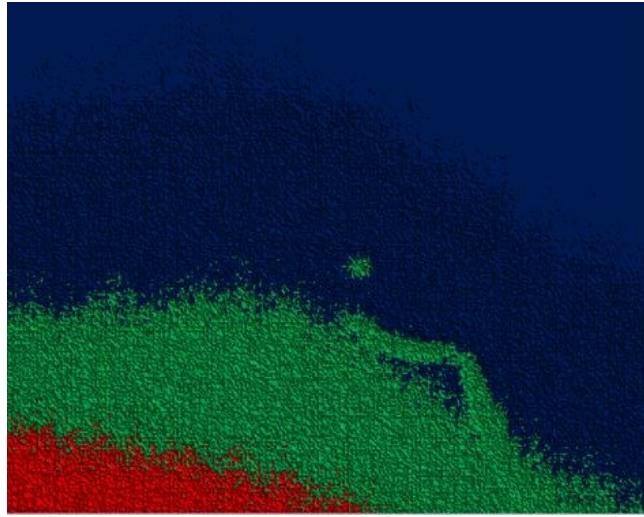


**Figure A5: Color Thermal Image at Location 1**



**Figure A6: Photo at Location 1 (North Side of Wall 2)**



**Appendix A (Continued)**



**Figure A7: Thermal Image at Location 2 at 10:32 AM (North Side of Wall 2)**

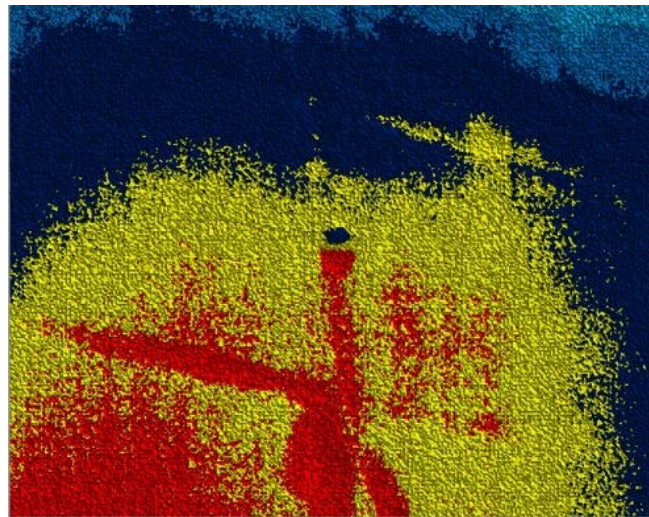


**Figure A8: Color Thermal Image at Location 2**

**Appendix A (Continued)**



**Figure A9: Photo at Location 2 (North Side of Wall 2)**



**Figure A10: Thermal Image at Location 3 at 10:43 AM (North Side of Wall 2)**

**Appendix A (Continued)**

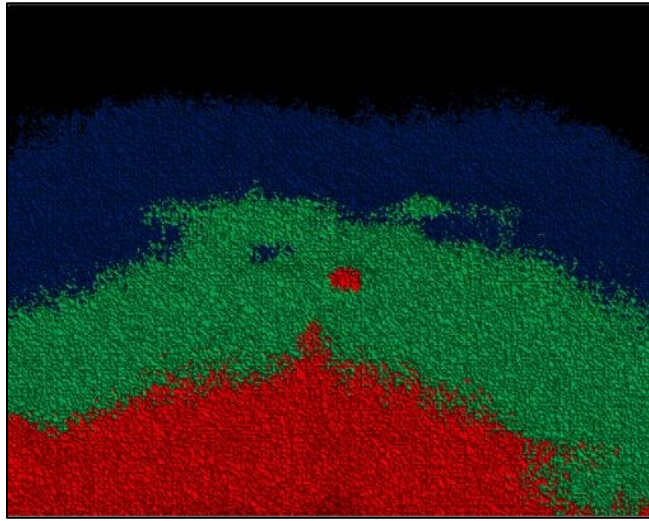


**Figure A11: Color Thermal Image at Location 3**

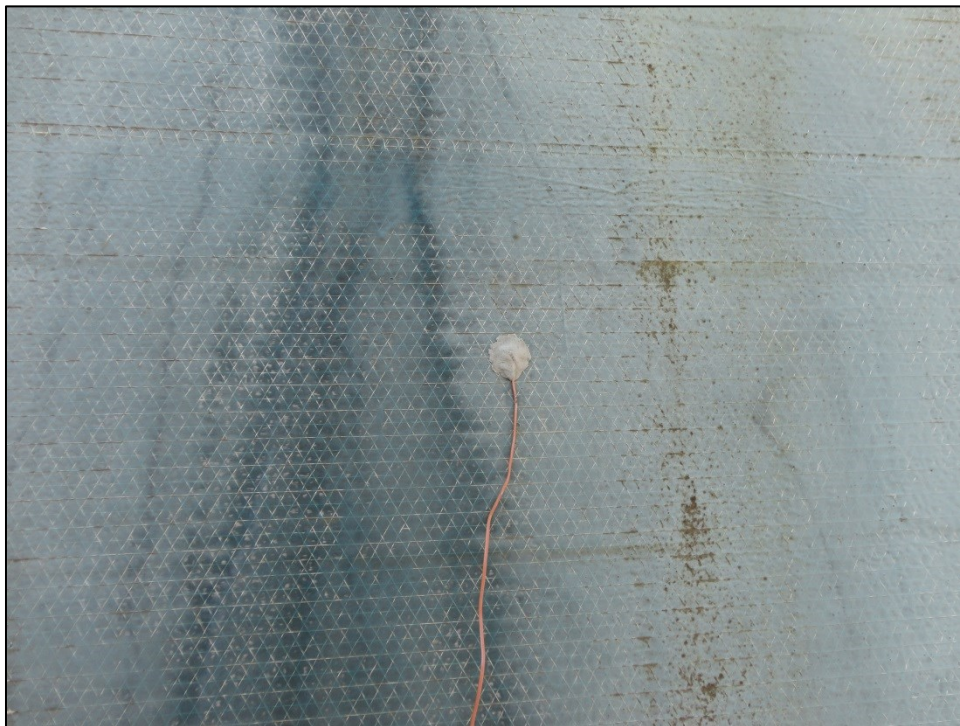


**Figure A12: Photo at Location 3 (North Side of Wall 2)**



**Appendix A (Continued)**

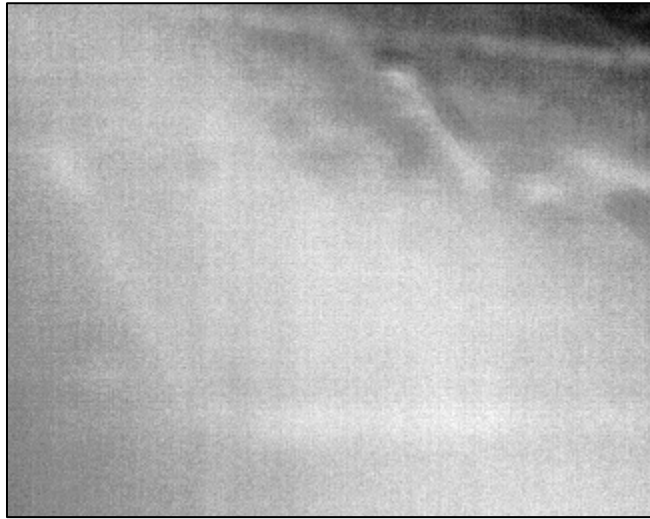


**Figure A13: Thermal Image at Location 4 at 11:00 AM (North Side of Wall 2)**

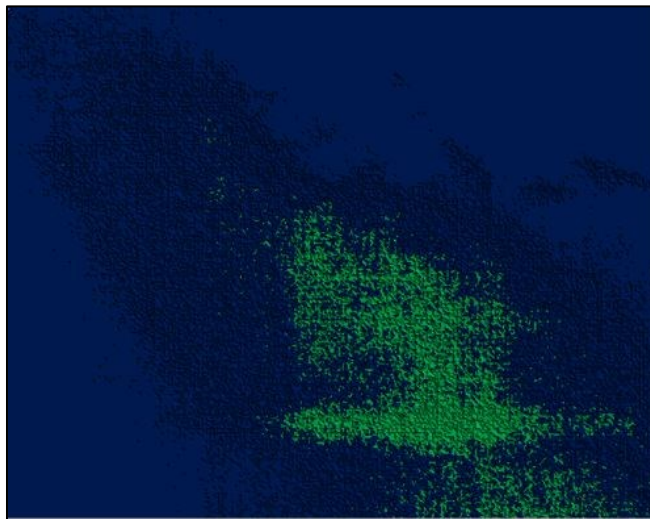


**Figure A14: Color Thermal Image at Location 4**

**Appendix A (Continued)**

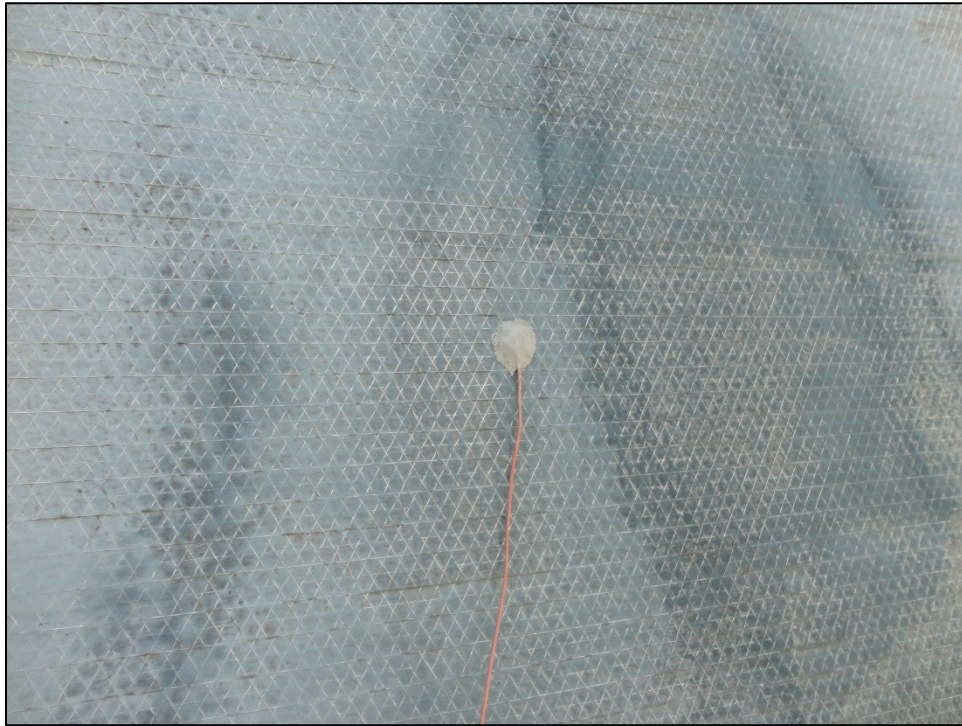


**Figure A15: Photo at Location 4 (North Side of Wall 2)**

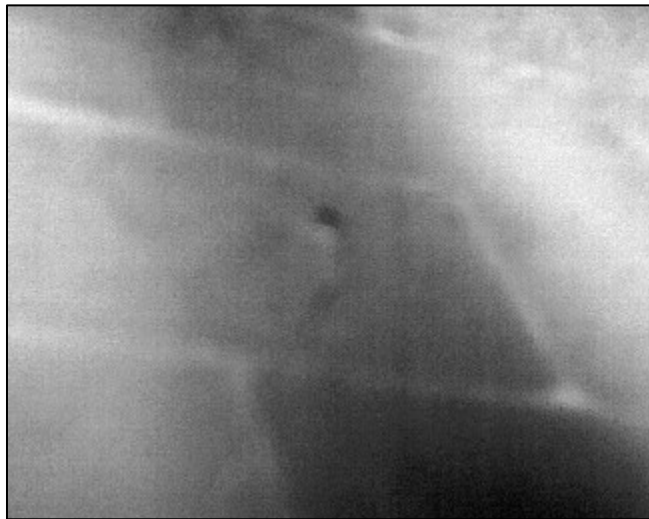


**Figure A16: Thermal Image at Location 5 at 12:57 PM (North Side of Wall 2)**

**Appendix A (Continued)**

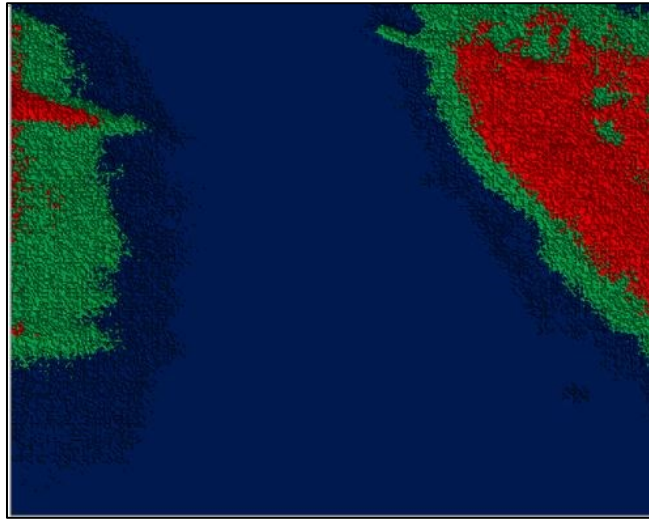


**Figure A17: Color Thermal Image at Location 5**



**Figure A18: Photo at Location 5 (North Side of Wall 2)**



Appendix A (Continued)

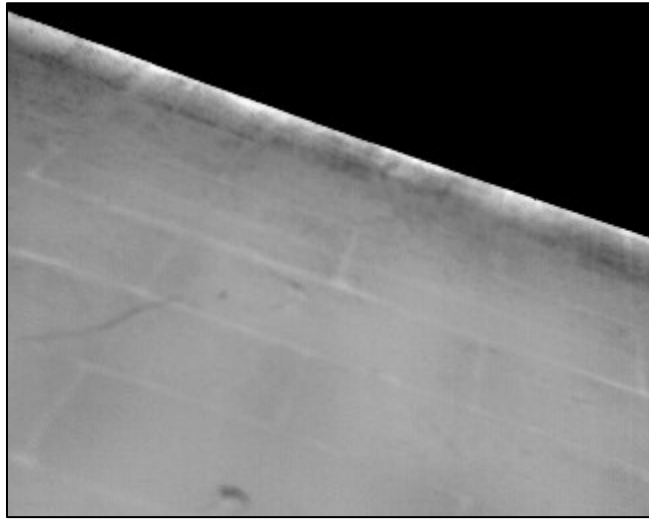


Figure A19: Thermal Image at Location 6 at 1:19 PM (North Side of Wall 2)

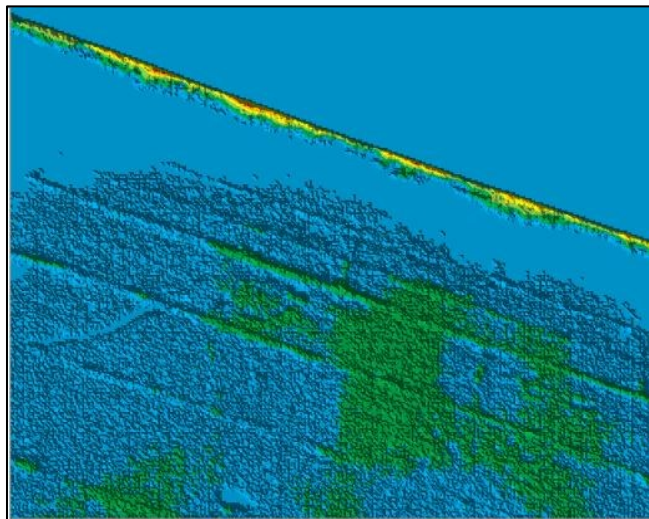
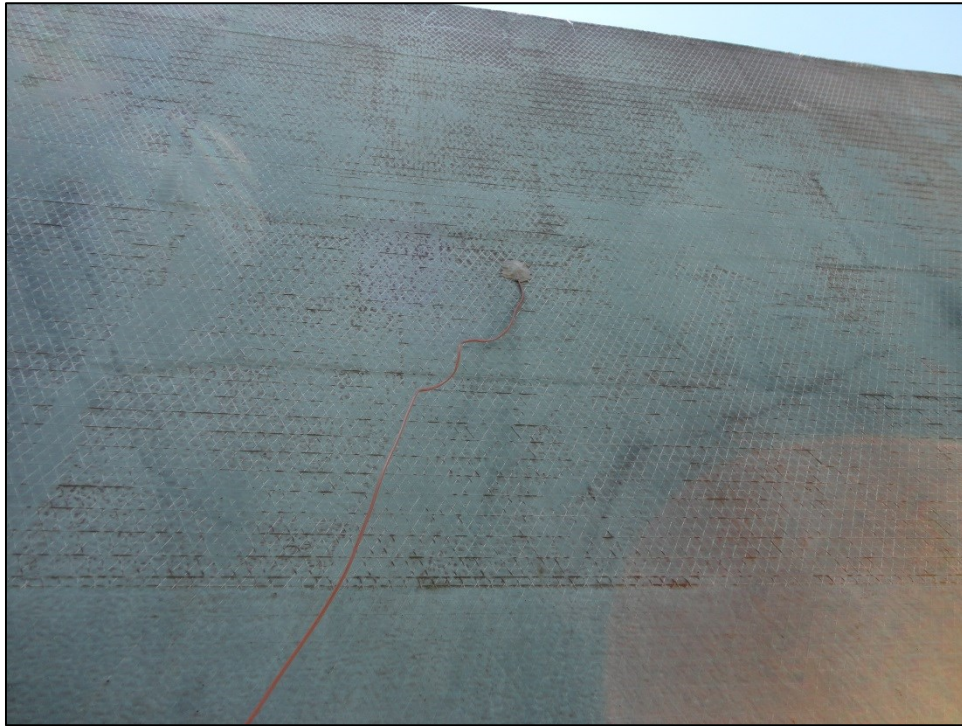
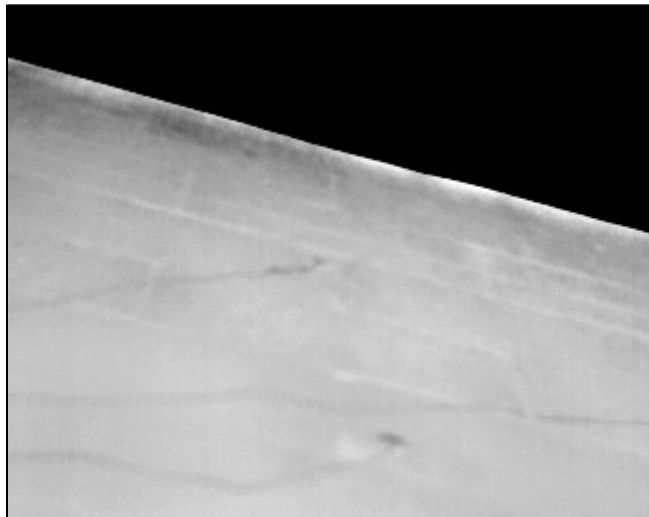


Figure A20: Color Thermal Image at Location 6

**Appendix A (Continued)**



**Figure A21: Photo at Location 6 (North Side of Wall 2)**



**Figure A22: Thermal Image at Location 7 at 1:41 PM (North Side of Wall 2)**

**Appendix A (Continued)**

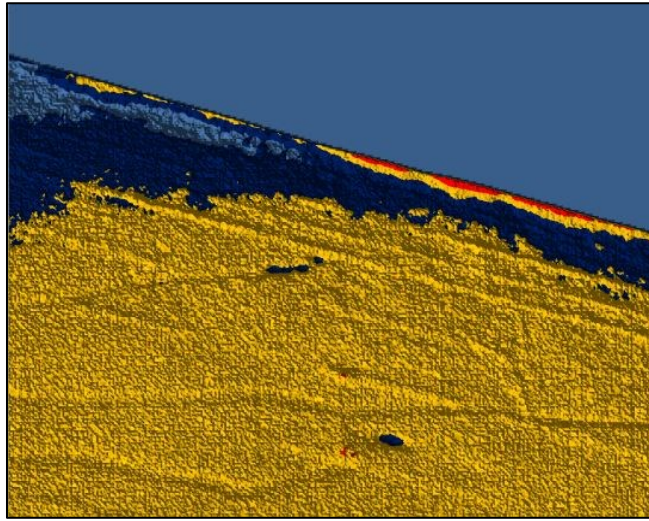


**Figure A23: Color Thermal Image at Location 7**



**Figure A24: Photo at Location 7 (North Side of Wall 2)**



Appendix A (Continued)

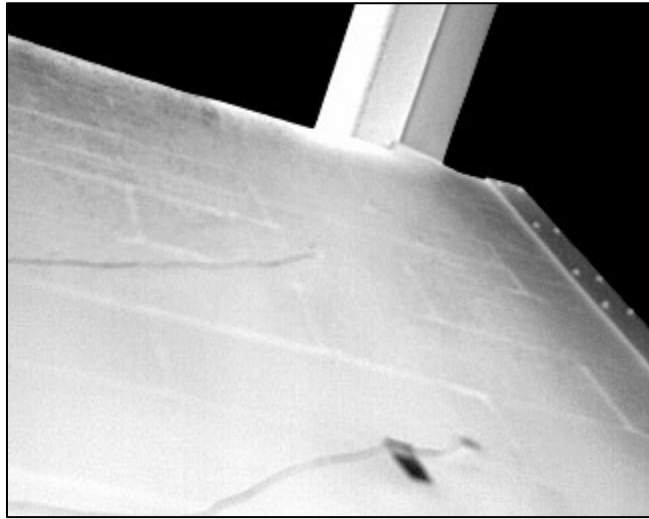


Figure A25: Thermal Image at Location 8 at 1:51 PM (North Side of Wall 2)

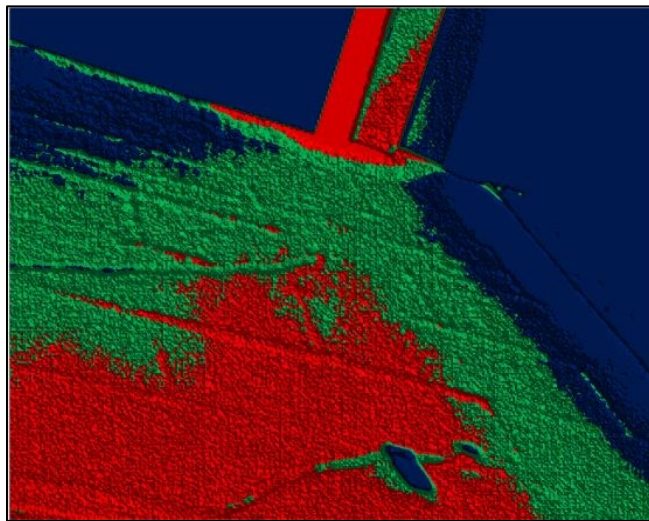
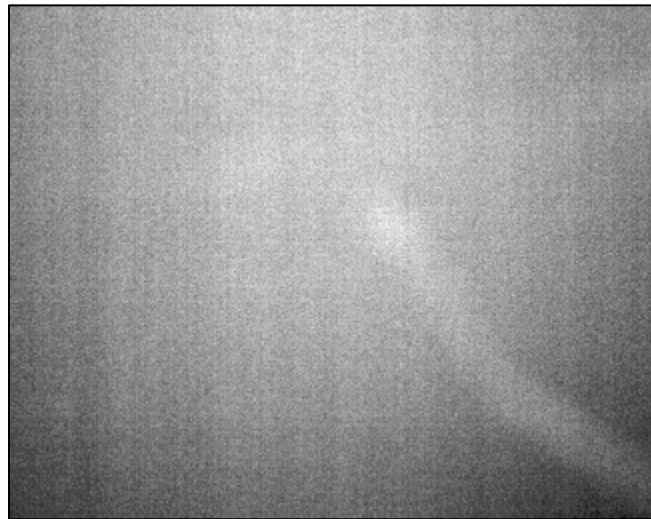


Figure A26: Color Thermal Image at Location 8

**Appendix A (Continued)**



**Figure A27: Photo at Location 8 (North Side of Wall 2)**



**Figure A28: Thermal Image at Location 9 at 10:24 AM (North Side of Wall 2)**



**Appendix A (Continued)**

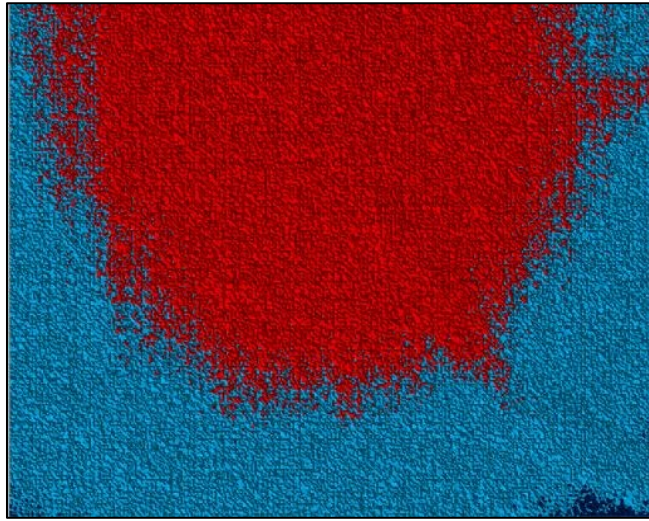


**Figure A29: Color Thermal Image at Location 9**

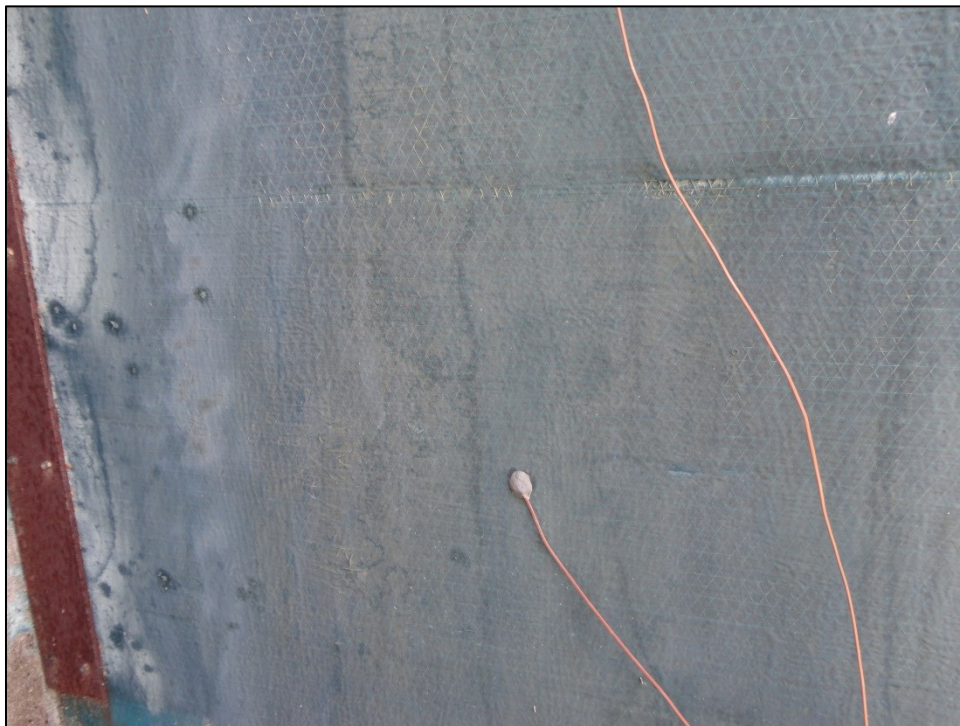


**Figure A30: Photo at Location 9 (North Side of Wall 2)**

**Appendix A (Continued)**



**Figure A31: Thermal Image at Location 10 at 10:34 AM (North Side of Wall 2)**

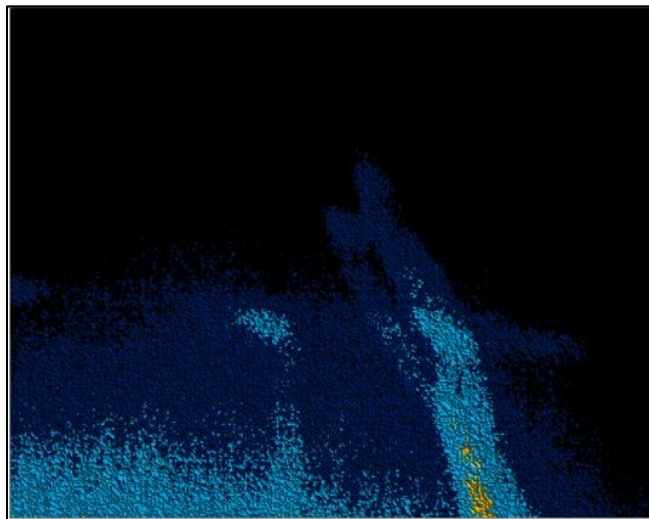


**Figure A32: Color Thermal Image at Location 10**

**Appendix A (Continued)**

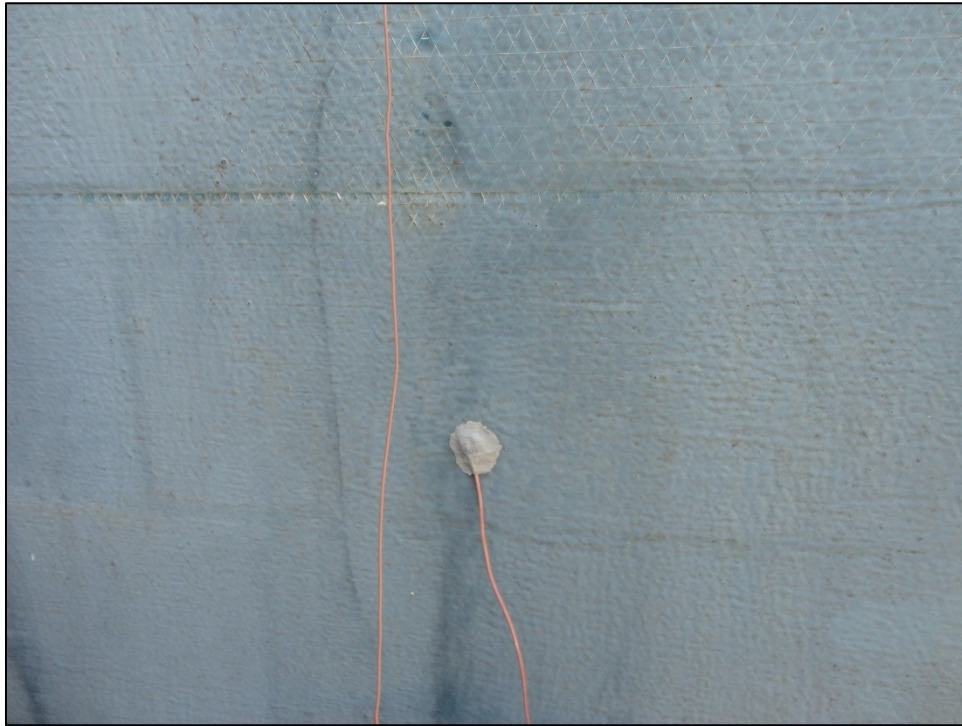


**Figure A33: Photo at Location 10 (North Side of Wall 2)**

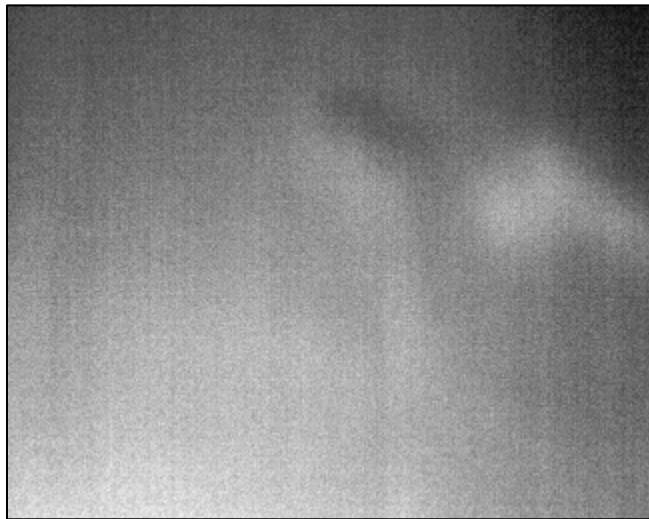


**Figure A34: Thermal Image at Location 11 at 10:47 AM (North Side of Wall 2)**



**Appendix A (Continued)**

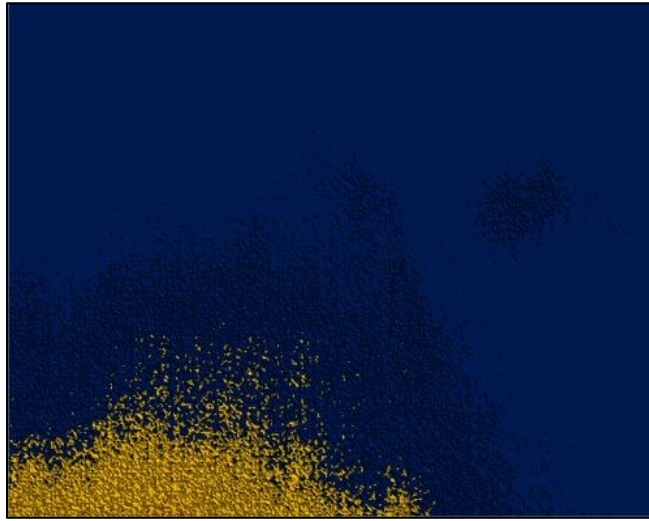


**Figure A35: Color Thermal Image at Location 11**



**Figure A36: Photo at Location 11 (North Side of Wall 2)**

**Appendix A (Continued)**

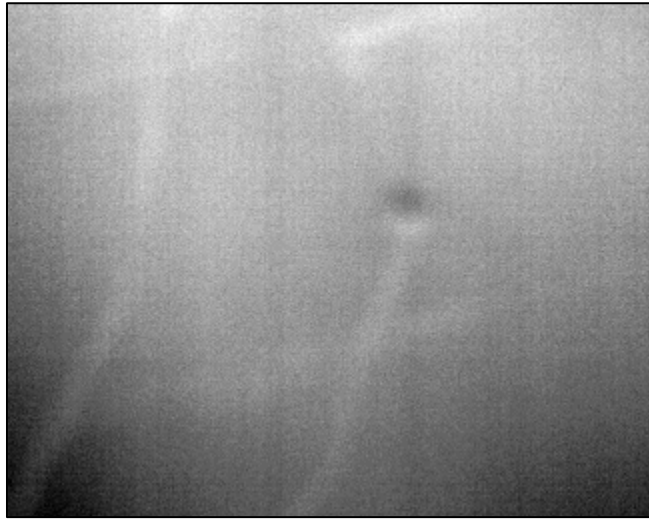


**Figure A37: Thermal Image at Location 12 at 11:07 AM (North Side of Wall 2)**

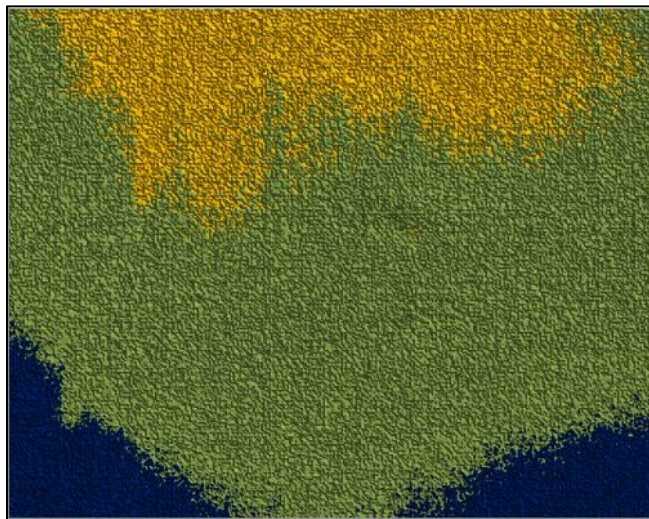


**Figure A38: Color Thermal Image at Location 12**

**Appendix A (Continued)**

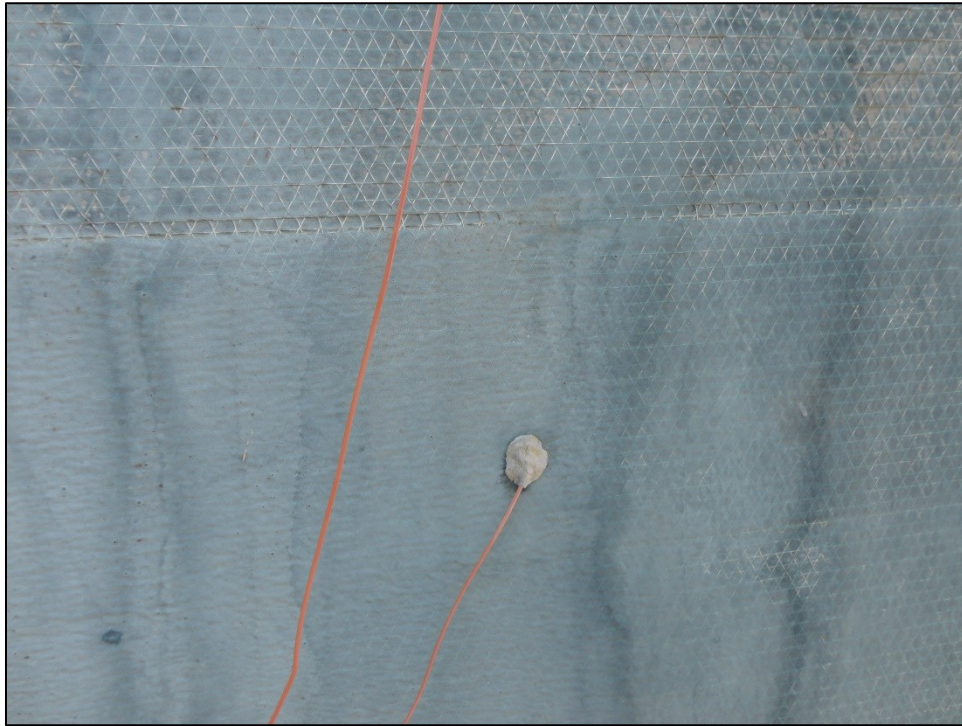


**Figure A39: Photo at Location 12 (North Side of Wall 2)**



**Figure A40: Thermal Image at Location 13 at 1:02 PM (North Side of Wall 2)**



**Appendix A (Continued)**

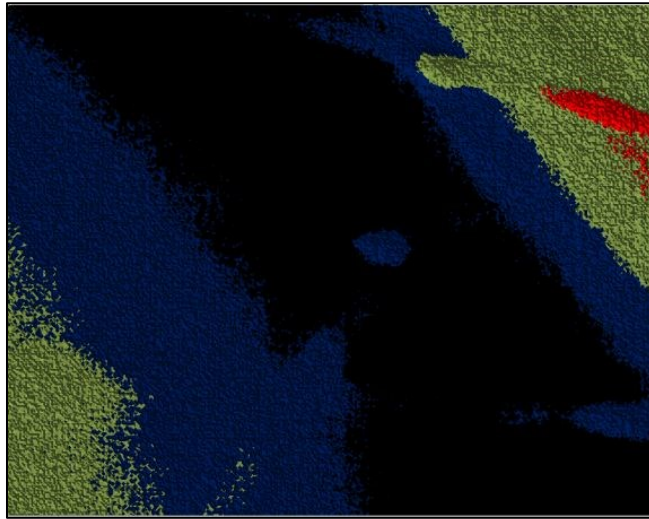


**Figure A41: Color Thermal Image at Location 13**

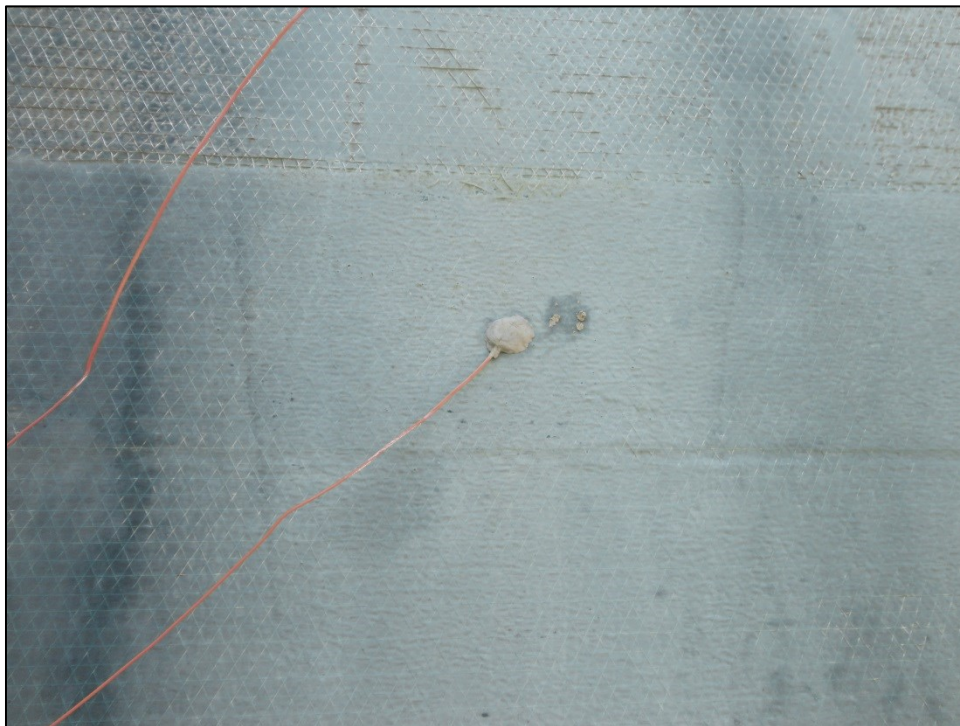


**Figure A42: Photo at Location 13 (North Side of Wall 2)**

**Appendix A (Continued)**



**Figure A43: Thermal Image at Location 14 at 1:23 PM (North Side of Wall 2)**

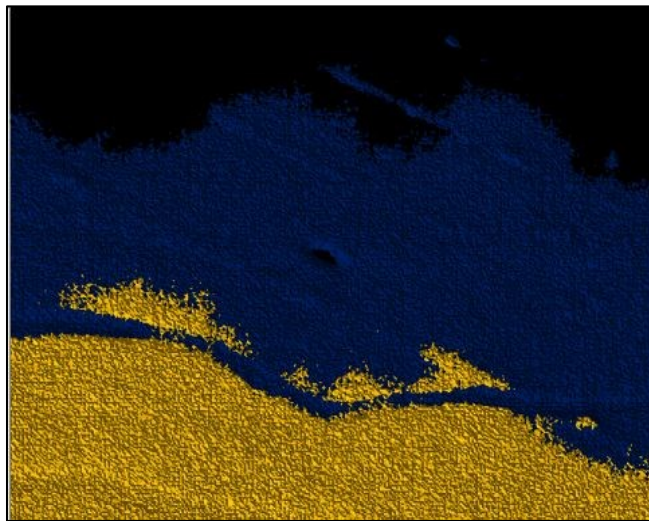


**Figure A44: Color Thermal Image at Location 14**



**Appendix A (Continued)**

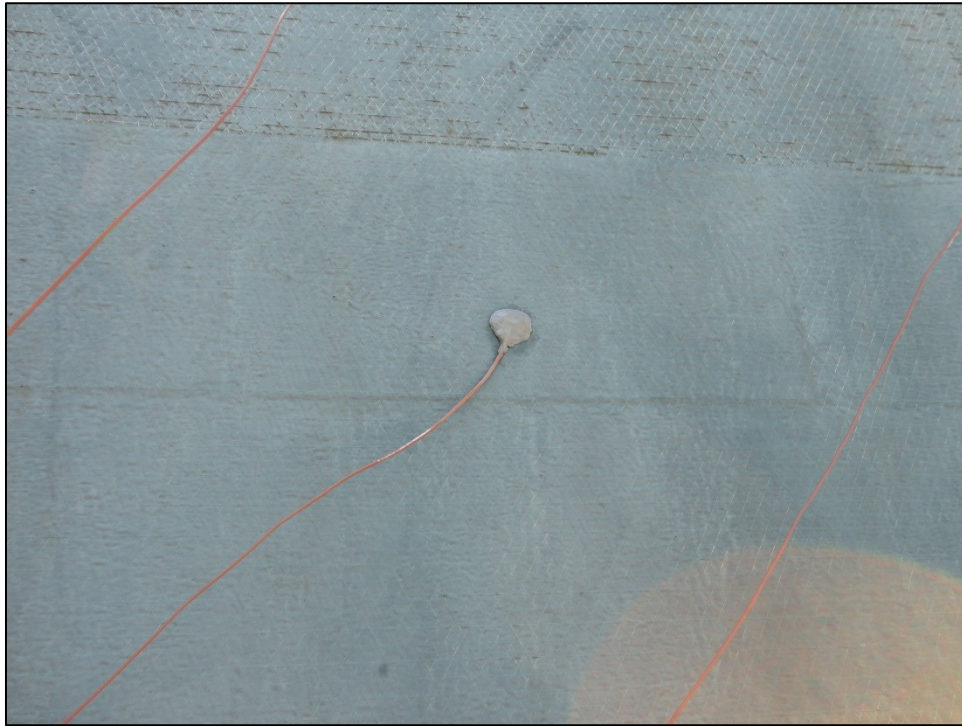


**Figure A45: Photo at Location 14 (North Side of Wall 2)**

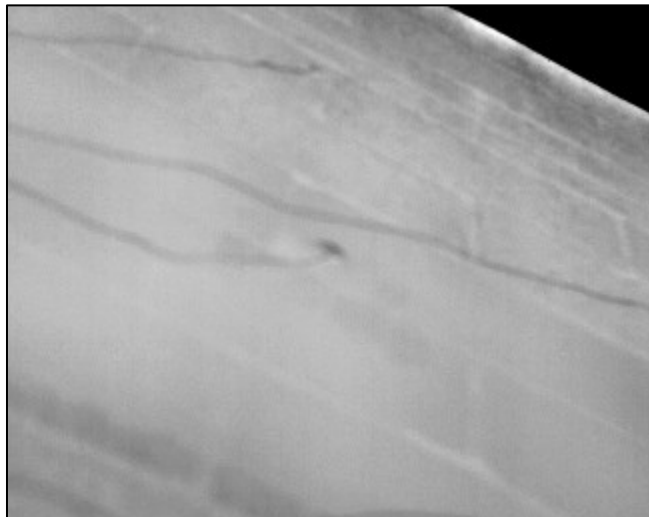


**Figure A46: Thermal Image at Location 15 at 1:44 PM (North Side of Wall 2)**

**Appendix A (Continued)**

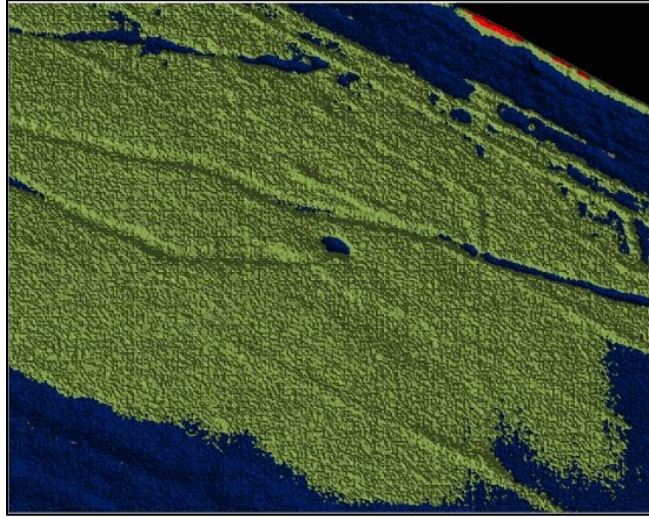


**Figure A47: Color Thermal Image at Location 15**

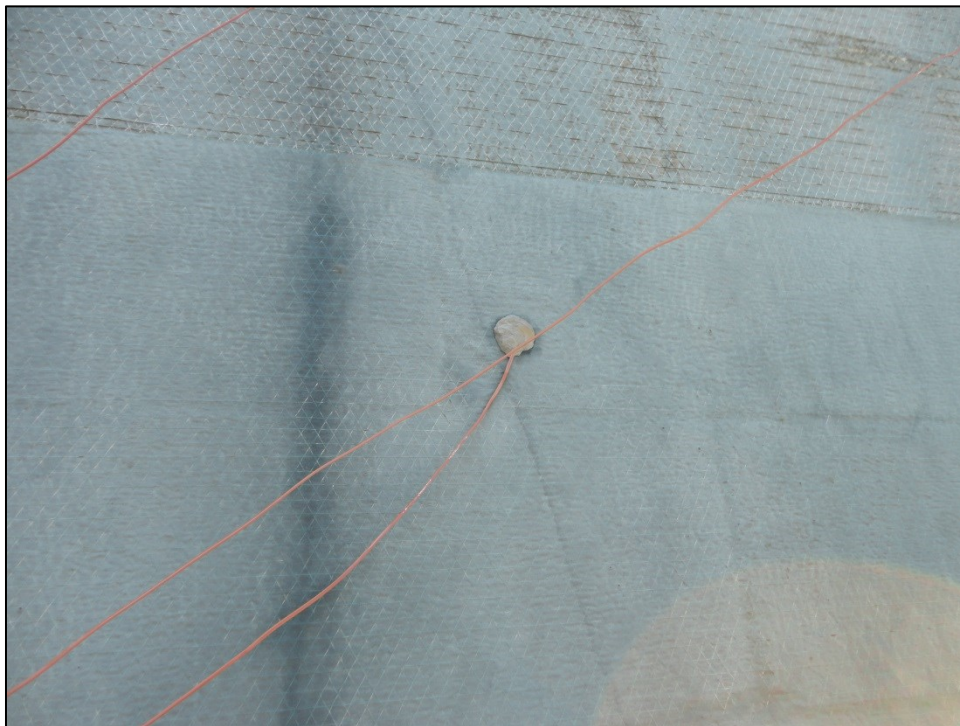


**Figure A48: Photo at Location 15 (North Side of Wall 2)**

**Appendix A (Continued)**

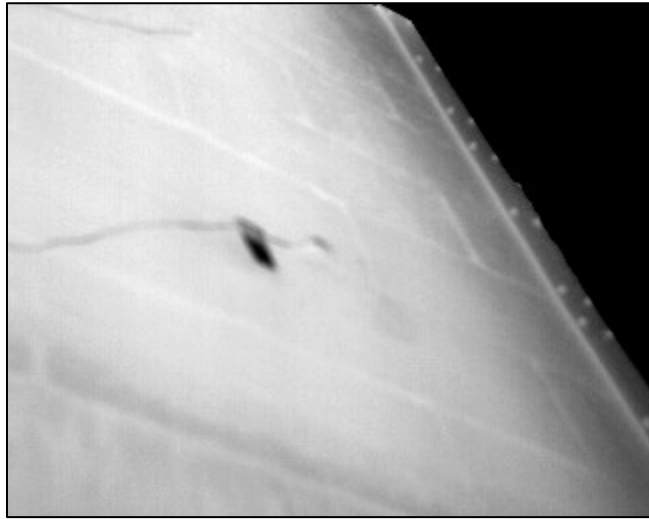


**Figure A49: Thermal Image at Location 16 at 1:54 PM (North Side of Wall 2)**

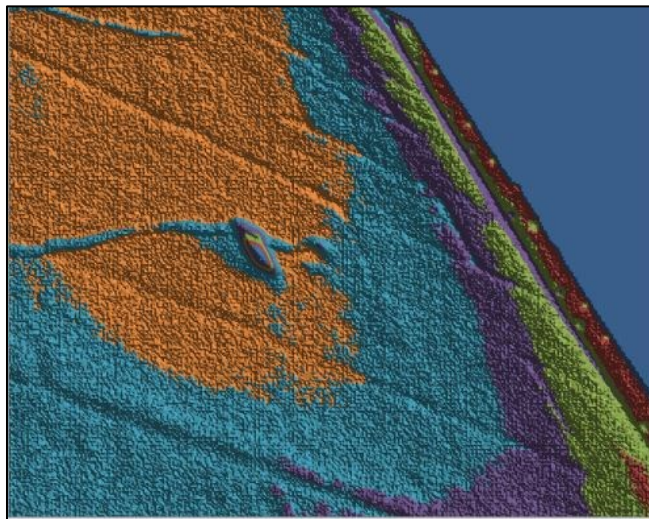


**Figure A50: Color Thermal Image at Location 16**



**Appendix A (Continued)**



**Figure A51: Photo at Location 16 (North Side of Wall 2)**

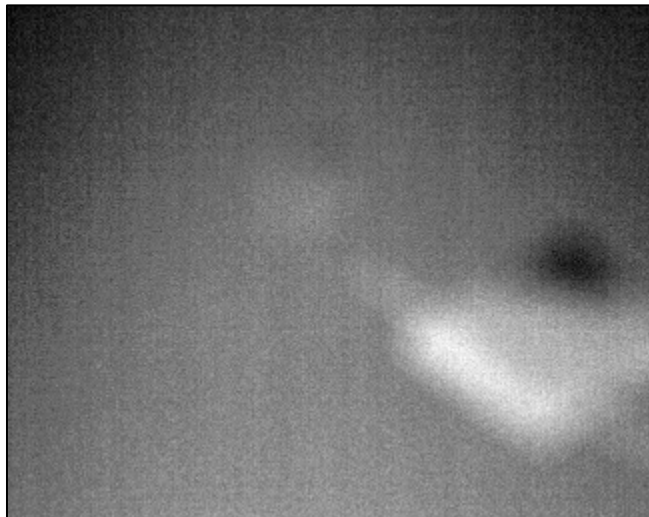


**Figure A52: Thermal Image at Location 17 at 10:30 AM (North Side of Wall 2)**

**Appendix A (Continued)**

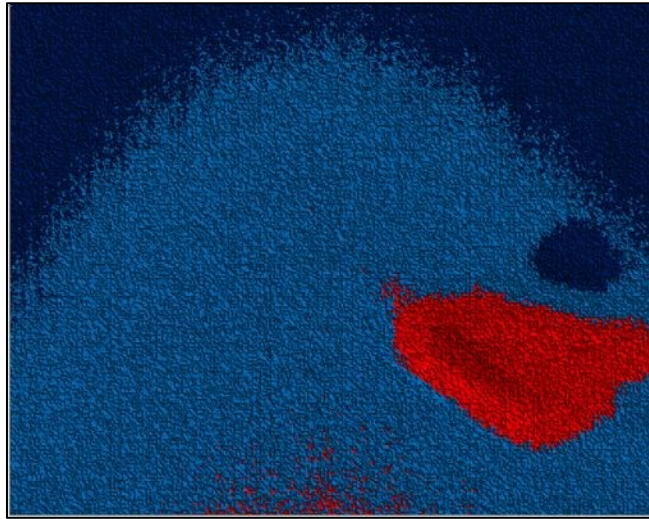


**Figure A53: Color Thermal Image at Location 17**



**Figure A54: Photo at Location 17 (North Side of Wall 2)**



**Appendix A (Continued)**

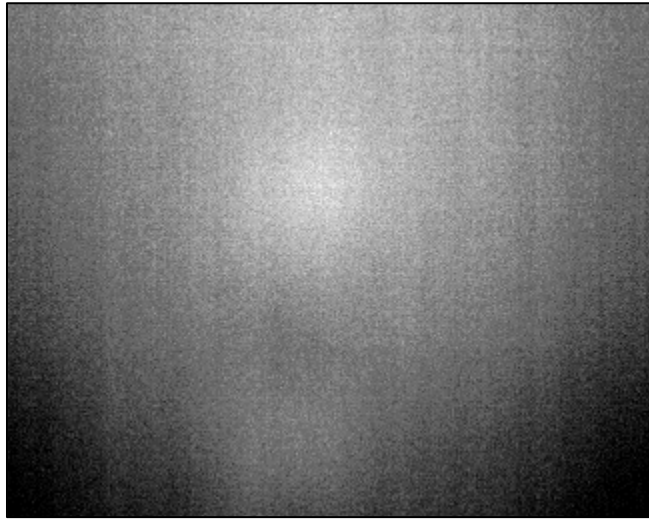


**Figure A55: Thermal Image at Location 18 at 10:39 AM (North Side of Wall 2)**

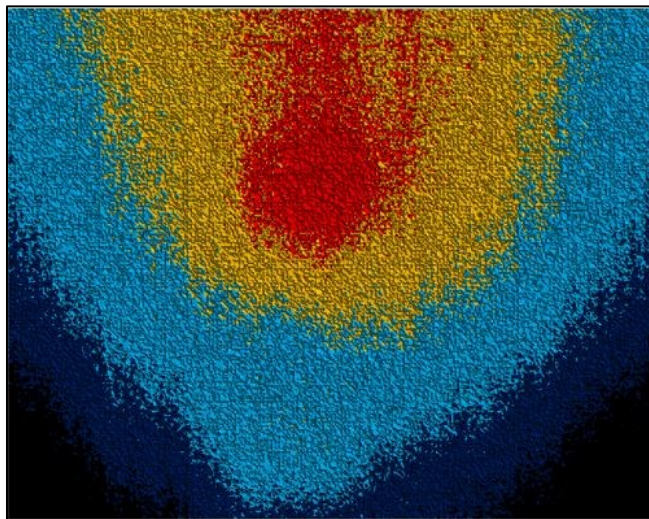


**Figure A56: Color Image at Location 18**

**Appendix A (Continued)**



**Figure A57: Photo at Location 18 (North Side of Wall 2)**



**Figure A58: Thermal Image at Location 19 at 10:51 AM (North Side of Wall 2)**



Appendix A (Continued)

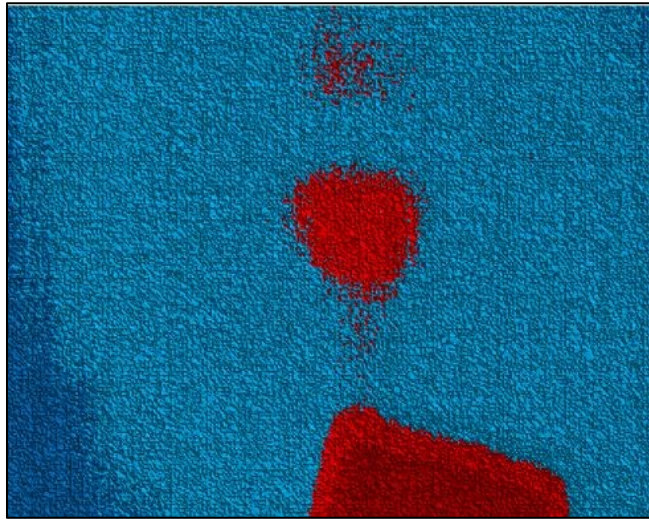
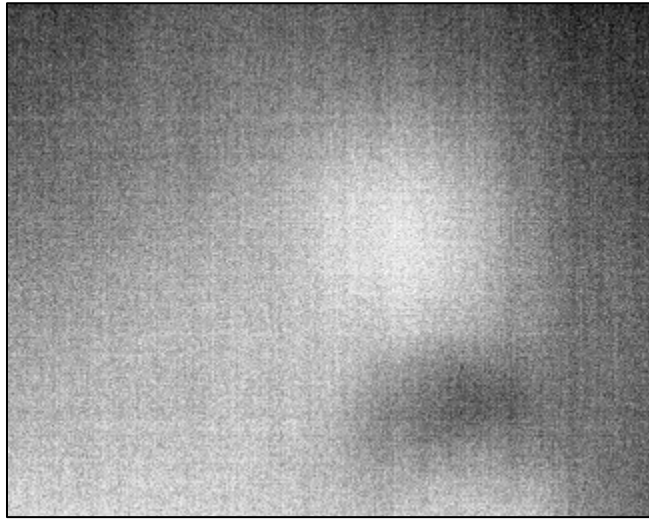


Figure A59: Color Image at Location 19

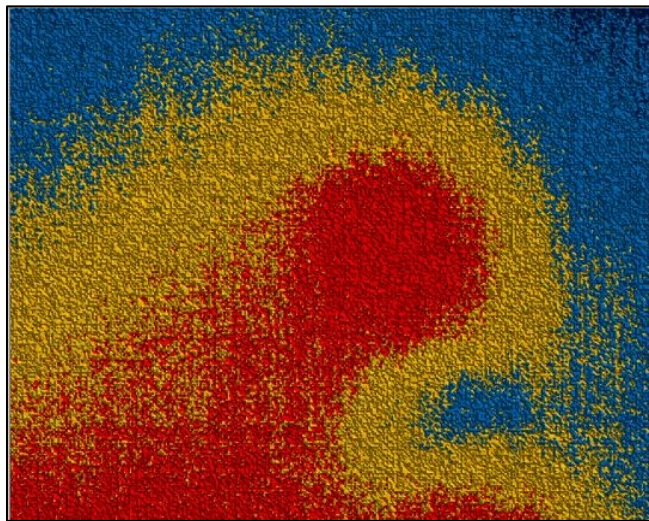


Figure A60: Photo at Location 19 (North Side of Wall 2)

**Appendix A (Continued)**



**Figure A61: Thermal Image at Location 20 at 11:10 AM (North Side of Wall 2)**



**Figure A62: Color Thermal Image at Location 20**



**Appendix A (Continued)**



**Figure A63: Photo at Location 20 (North Side of Wall 2)**



**Figure A64: Thermal Image at Location 21 at 1:06 PM (North Side of Wall 2)**

**Appendix A (Continued)**

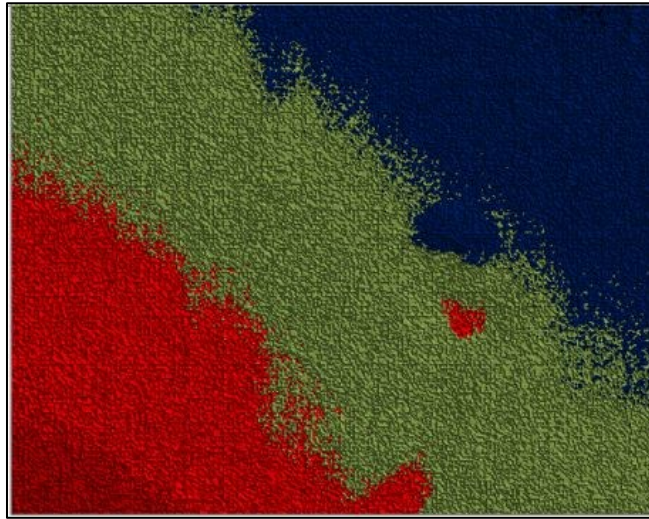


**Figure A65: Color Thermal Image at Location 21**



**Figure A66: Photo at Location 21 (North Side of Wall 2)**



**Appendix A (Continued)**

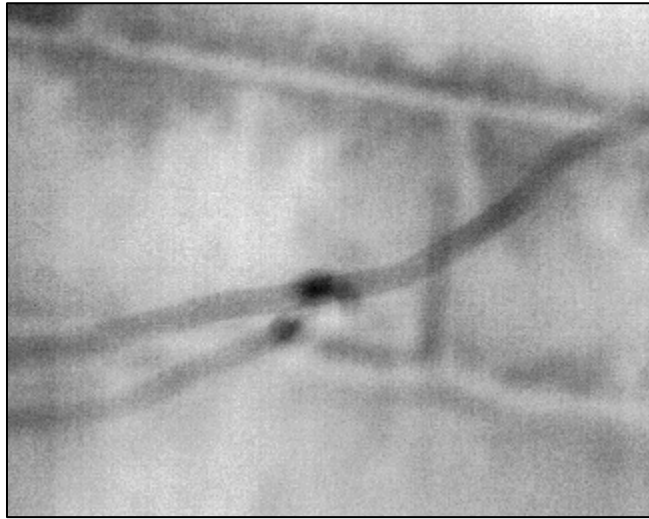


**Figure A67: Thermal Image at Location 22 at 1:34 PM (North Side of Wall 2)**

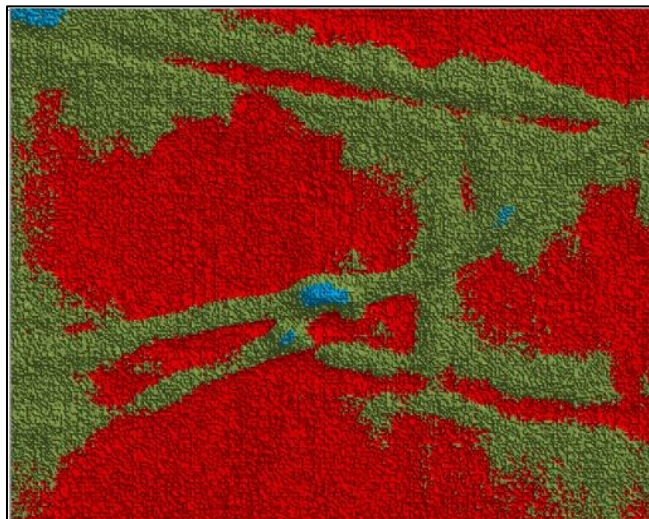


**Figure A68: Color Thermal Image at Location 22**

**Appendix A (Continued)**



**Figure A69: Photo at Location 22 (North Side of Wall 2)**

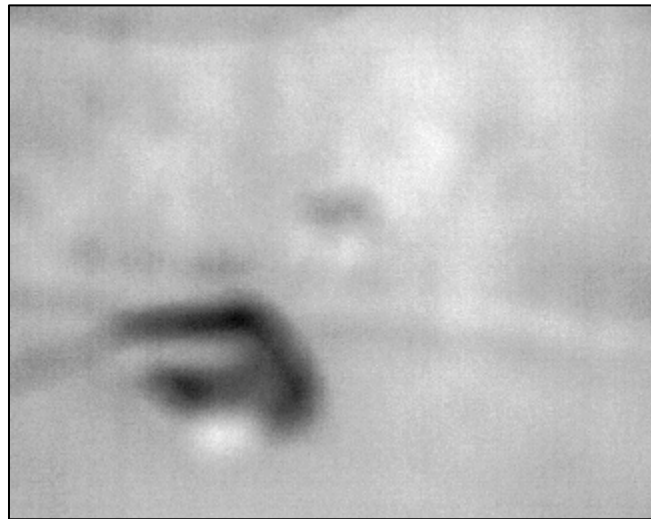


**Figure A70: Thermal Image at Location 23 at 1:47 PM (North Side of Wall 2)**



Appendix A (Continued)

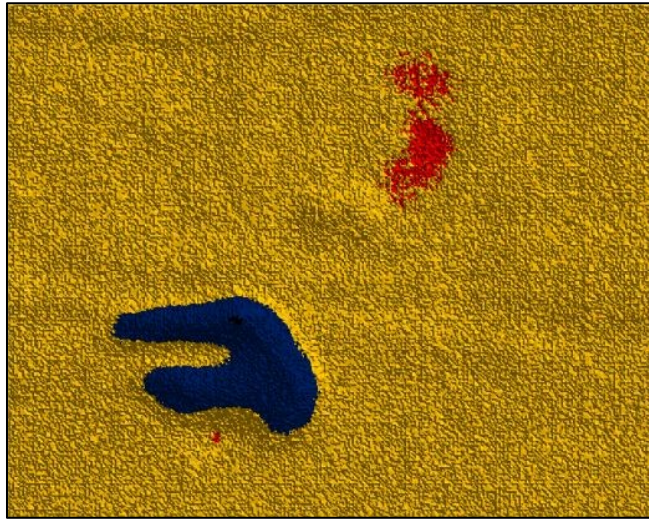
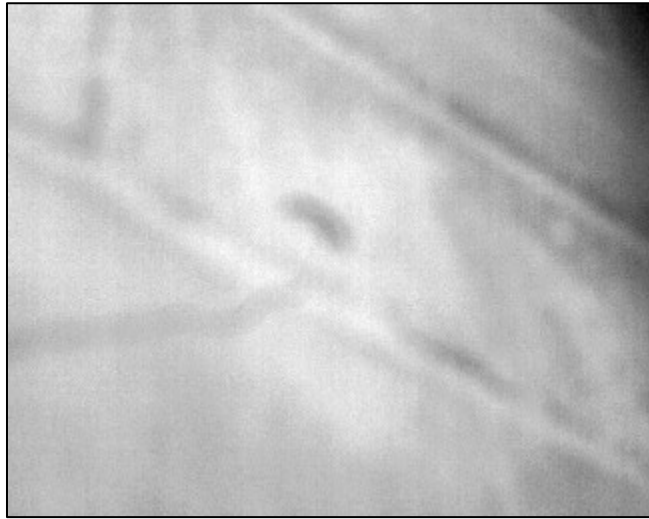


Figure A71: Color Thermal Image at Location 23

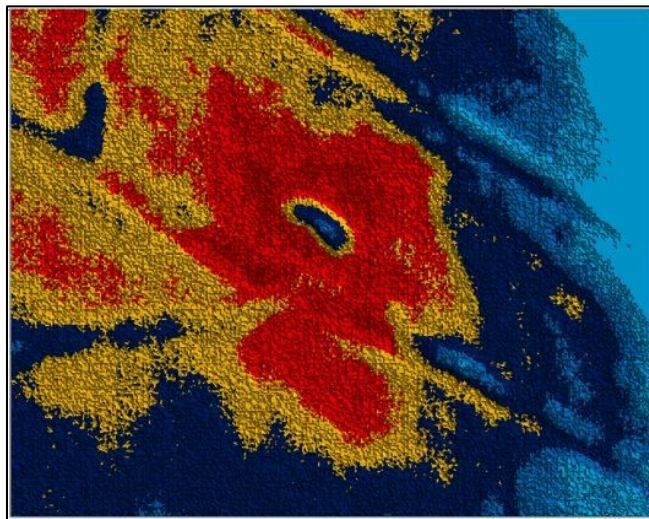


Figure A72: Photo at Location 23 (North Side of Wall 2)

**Appendix A (Continued)**



**Figure A73: Thermal Image at Location 24 at 1:58 PM (North Side of Wall 2)**



**Figure A74: Color Thermal Image at Location 24**



**Appendix A (Continued)**



**Figure A75: Photo at Location 24 (North Side of Wall 2)**

**Appendix B: Wall 2 Thermocouple Temperature Contours**

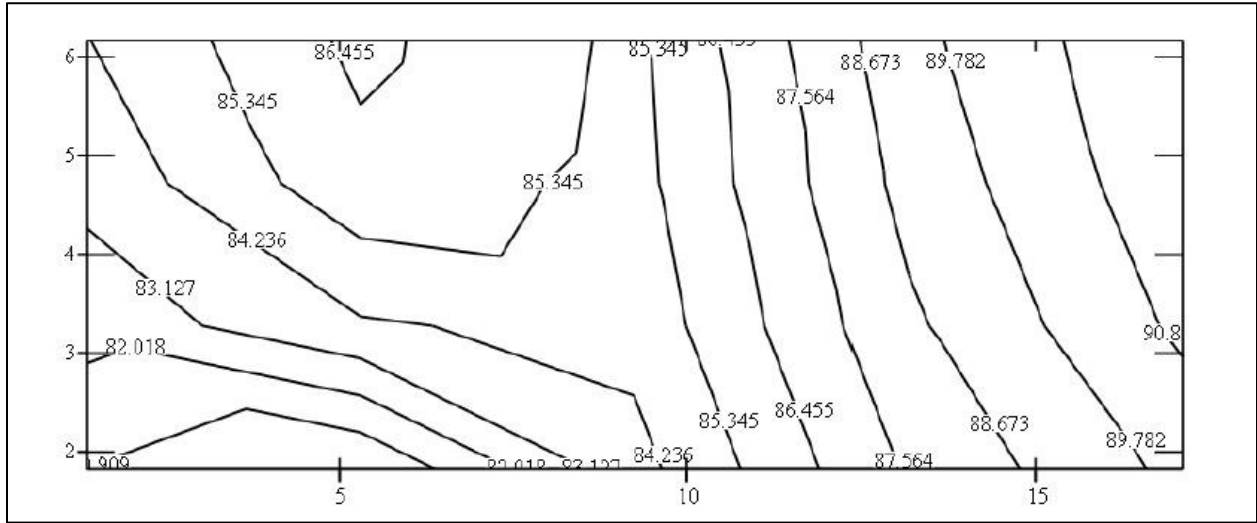


**Figure A76: Detailed Contour of Wall 2 North Side 4/4/12 at 1:00 PM (Looking South)**

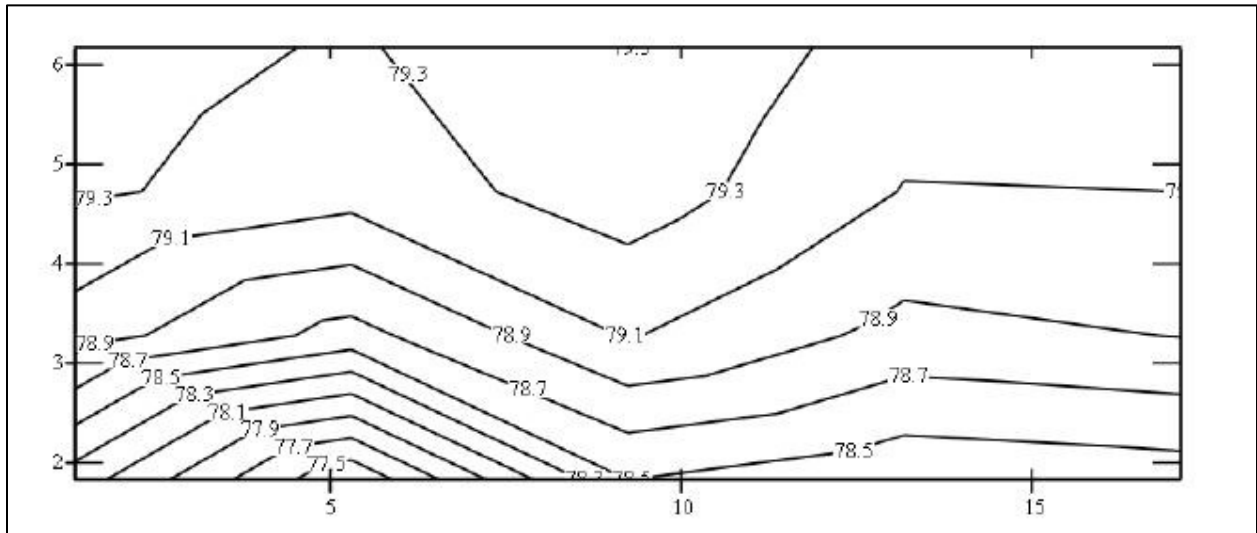


**Figure A77: Wall 2 North Side Mean Contour 3/31/12 to 4/7/12 (Looking South)**

Appendix B (Continued)

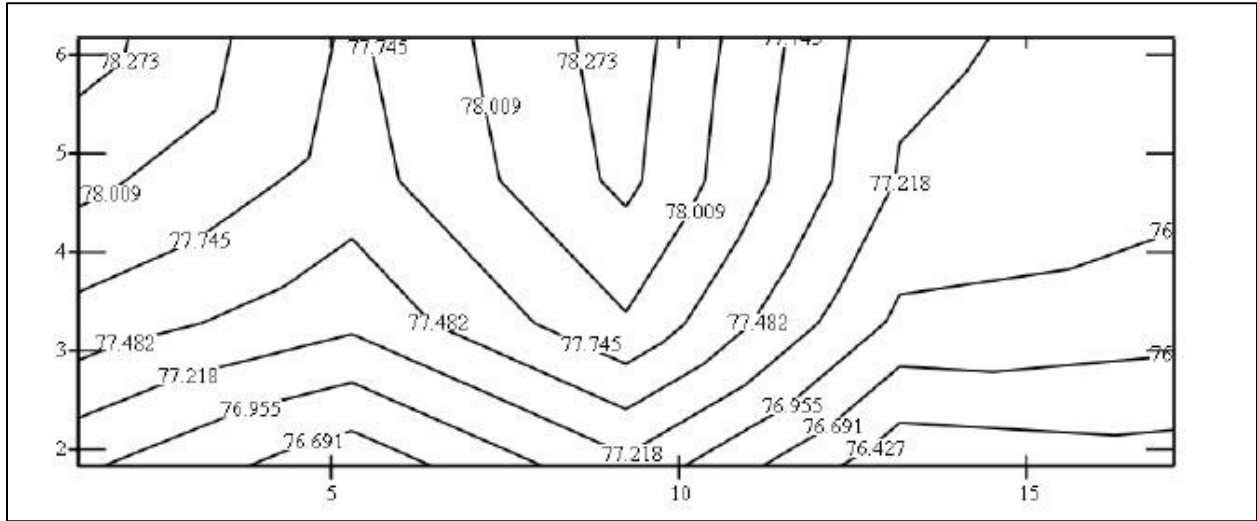


Figure A78: Wall 2 North Side Median Contour 3/31/12 to 4/7/12 (Looking South)

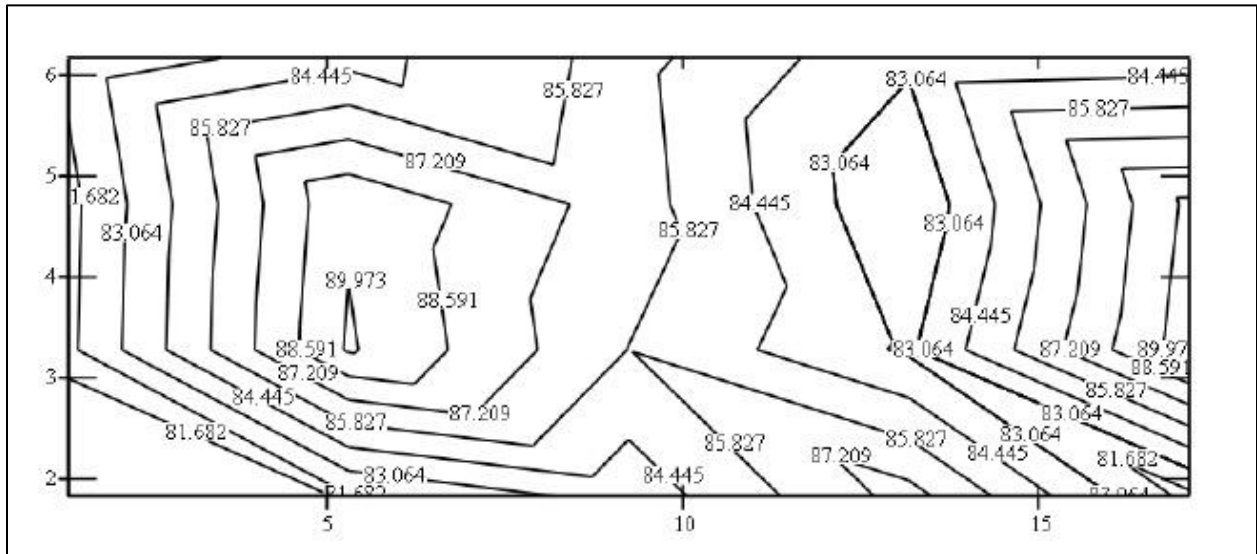
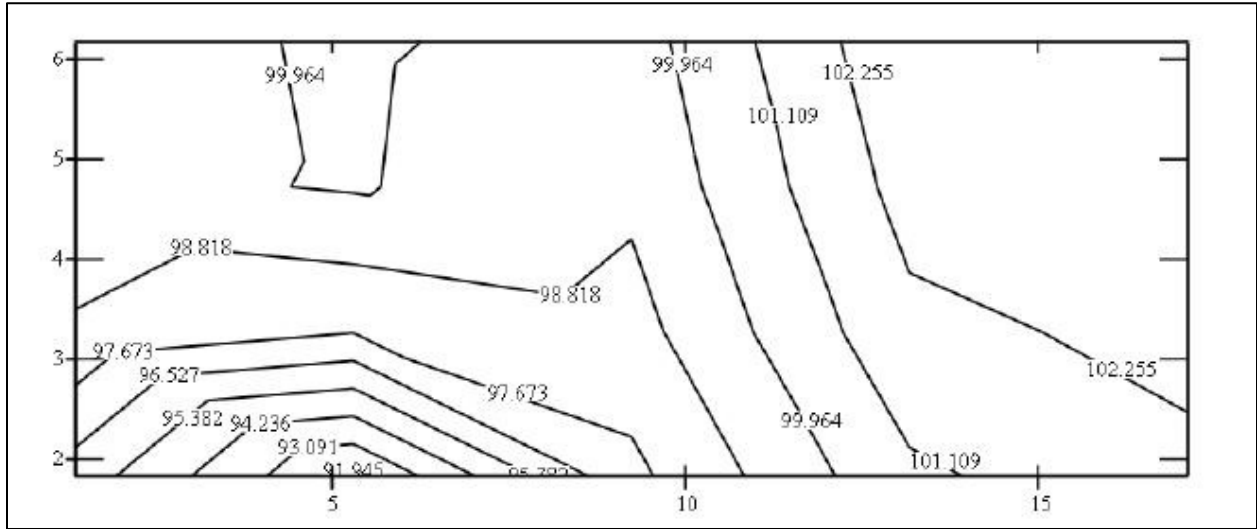


Figure A79: Wall 2 North Side Mode Contour 3/31/12 to 4/7/12 (Looking South)



**Appendix B (Continued)**



**Figure A80: Wall 2 North Side Max Contour 3/31/12 to 4/7/12 (Looking South)**

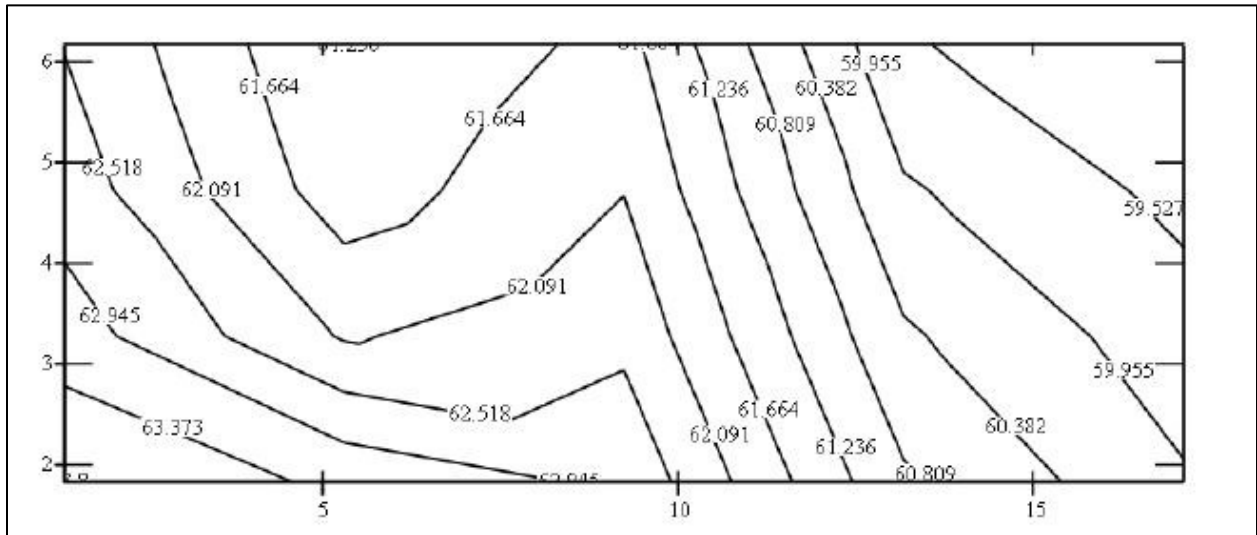


**Figure A81: Wall 2 North Side Min Contour 3/31/12 to 4/7/12 (Looking South)**

Appendix B (Continued)

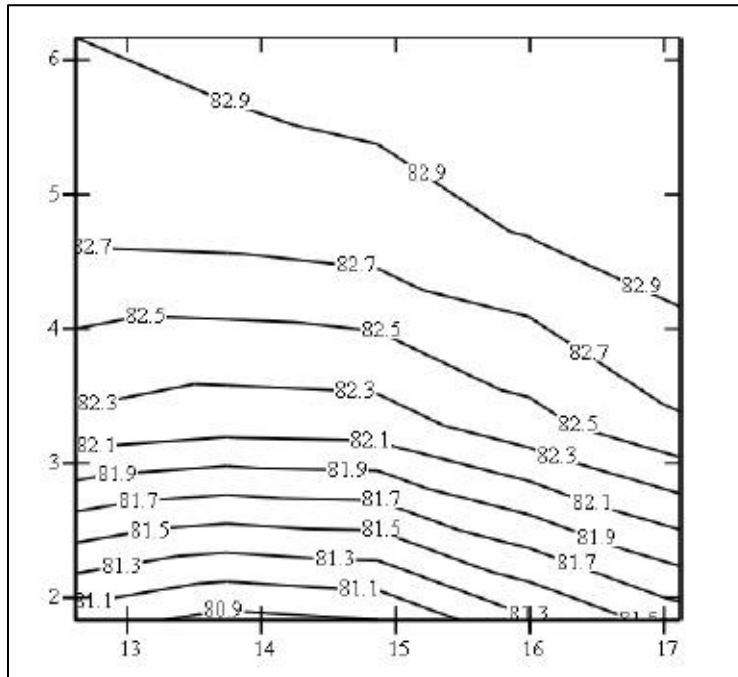


Figure A82: Wall 2 North Side Average Contour 8/11/12 to 8/18/12 (Looking South)

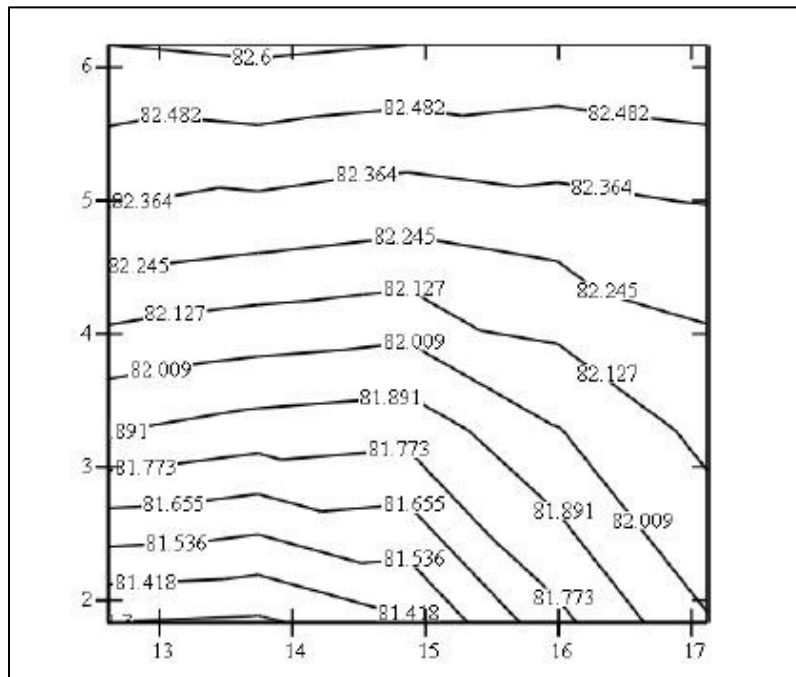


Figure A83: Wall 2 South Side Average Contour 8/11/12 to 8/18/12 (Looking South)

Appendix B (Continued)

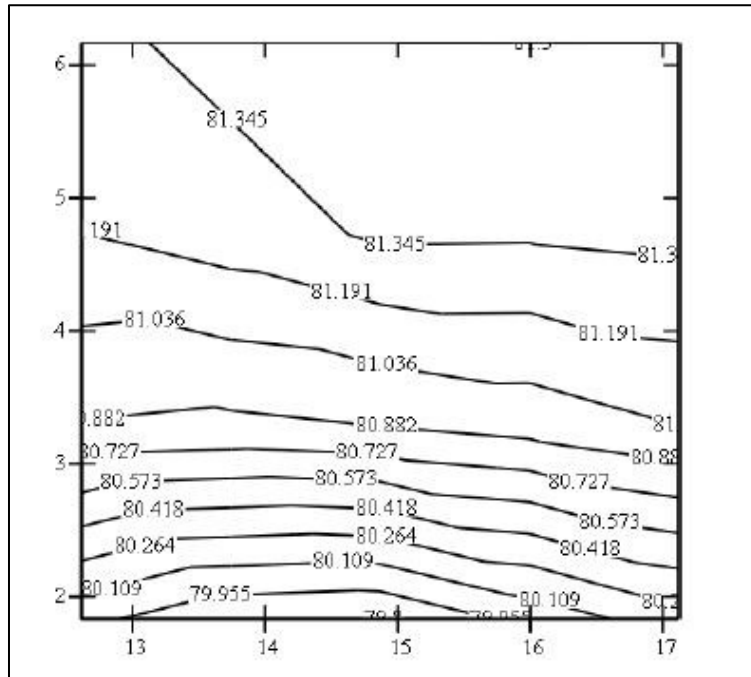


Figure A84: Wall 2 North Side Median Contour 8/11/12 to 8/18/12 (Looking South)

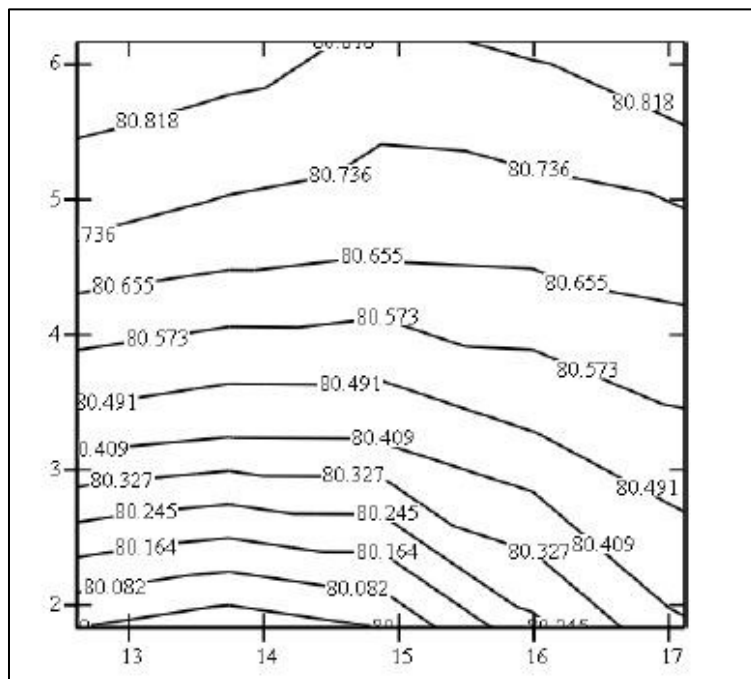


Figure A85: Wall 2 South Side Median Contour 8/11/12 to 8/18/12 (Looking South)

Appendix B (Continued)

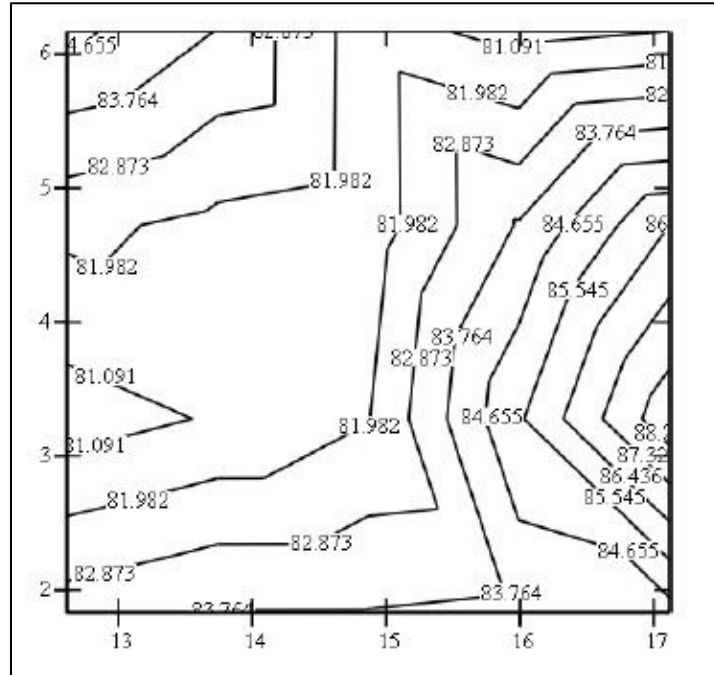


Figure A86: Wall 2 North Side Mode Contour 8/11/12 to 8/18/12 (Looking South)

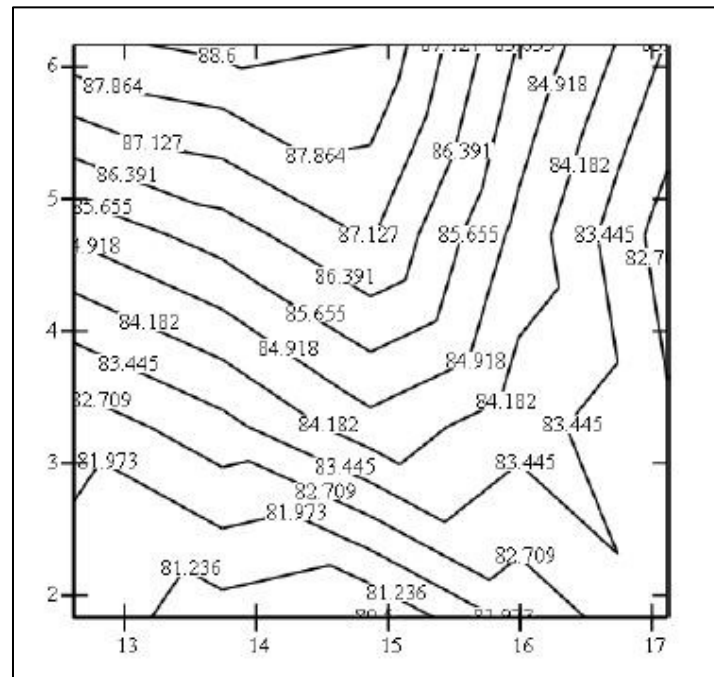


Figure A87: Wall 2 South Side Mode Contour 8/11/12 to 8/18/12 (Looking South)

Appendix B (Continued)

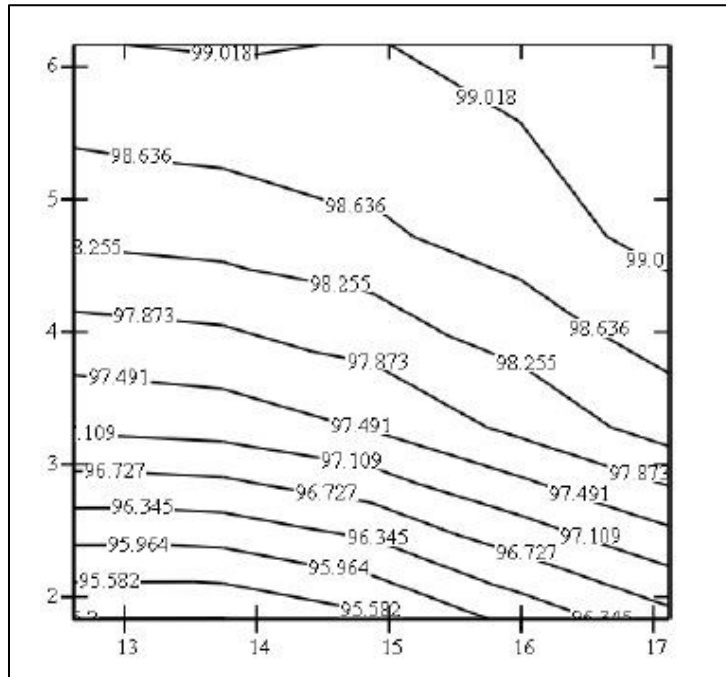


Figure A88: Wall 2 North Side Max Contour 8/11/12 to 8/18/12 (Looking South)

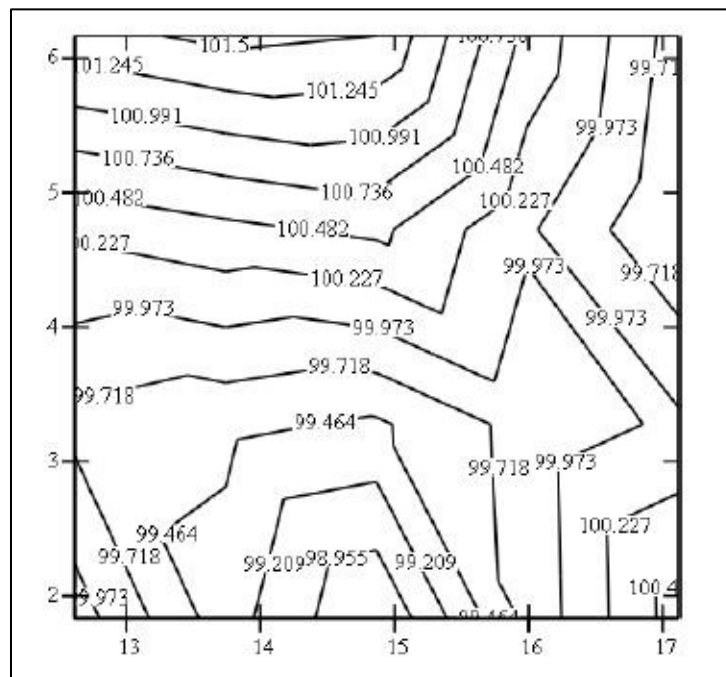
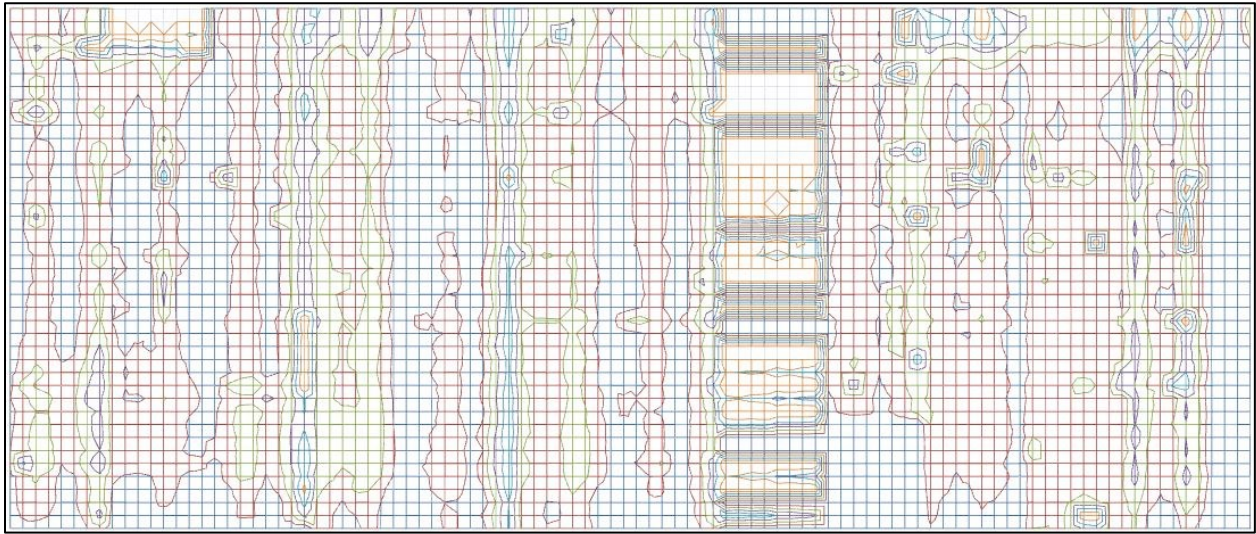


Figure A89: Wall 2 South Side Max Contour 8/11/12 to 8/18/12 (Looking South)





## Appendix C: Scanner Contours



**Figure A92: Contour of Thermal Scanner Data (Wall 2)**

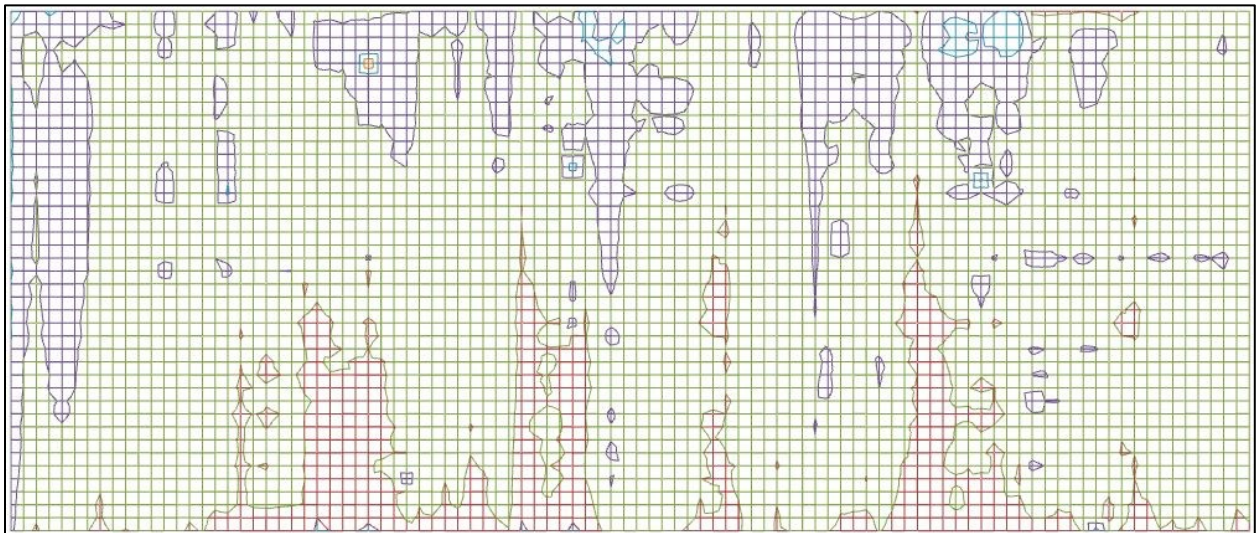


**Figure A93: Contour of Thermal Scanner Data (Wall 3)**

## Appendix D: Historical Thermal Stresses

The following calculation provides the details of the thermal stresses experienced by the walls. The subscripts e, m, and c stand for epoxy, masonry, and CFRP, respectively. The following material properties are used in the calculation:

$$f'_m = 1900 \text{ psi}$$

$$E_e = 500,000 \text{ psi}$$

$$\alpha_m = 0.0000060/^\circ\text{F}$$

$$\alpha_e = 0.0000300/^\circ\text{F}$$

$$\alpha_c = -0.0000006/^\circ\text{F}$$

where  $\alpha$  is the coefficient of thermal expansion. From the historical data, the following temperature information is available:

$$T_0 = 86^\circ\text{F}$$

$$T_1 = 98^\circ\text{F}$$

$$T_2 = 25^\circ\text{F}$$

where  $T_0$  is the average temperature on the installation date of the CFRP (8/14/1995),  $T_1$  is the historical maximum and  $T_2$  is the historical minimum temperature.

$$\Delta T_{\max} = 86^\circ\text{F} - 25^\circ\text{F} = 61^\circ\text{F}$$

Any length can be used, but assuming a 5ft length and calculating the change in length for each of the respective materials due to the temperature change, we have the following:

$$L = 5\text{ft} = 60\text{in.}$$

$$\Delta L = \Delta T_{\max} L \alpha \quad (1)$$

$$\Delta L_m = (61^\circ\text{F})(60\text{in})(0.000006/^\circ\text{F}) = 0.02196\text{in.}$$

## Appendix D (Continued)

$$\Delta L_e = (61^\circ\text{F})(60\text{in})(0.00003/^\circ\text{F}) = 0.1098\text{in.}$$

$$\Delta L_c = (61^\circ\text{F})(60\text{in})(-0.0000006/^\circ\text{F}) = -0.002196\text{in.}$$

Next, the difference in change between epoxy / masonry and epoxy / CFRP is obtained:

$$\Delta L_{me} = 0.1098\text{in.} - 0.02196\text{in.} = 0.08784\text{in.}$$

$$\Delta L_{ec} = 0.1098\text{in.} + 0.002196\text{in.} = 0.111996\text{in.}$$

The strain can now be calculated:

$$\varepsilon = \Delta L/L \quad (2)$$

$$\varepsilon_{me} = 0.08784\text{in.}/60\text{in.} = 0.001464$$

$$\varepsilon_{ec} = 0.111996\text{in.}/60\text{in.} = 0.0018666$$

And finally, the stresses are obtained:

$$\sigma = E\varepsilon \quad (3)$$

$$\sigma_{me} = (0.001464)(500,000\text{psi}) = 732 \text{ psi}$$

$$\sigma_{ec} = (0.0018666)(500,000\text{psi}) = 933 \text{ psi}$$

Both of these stresses are less than 1 ksi and are negligible to the epoxy bond. These stresses are not additive and so the larger one controls.

## Appendix E: Correction Factors

The following is a symbolic representation of how the correction factors were obtained.

The first correction factor was the scan rate correction factor:

$r_n$  = average scan rate for scan n

$t_n$  = average temperature for scan n

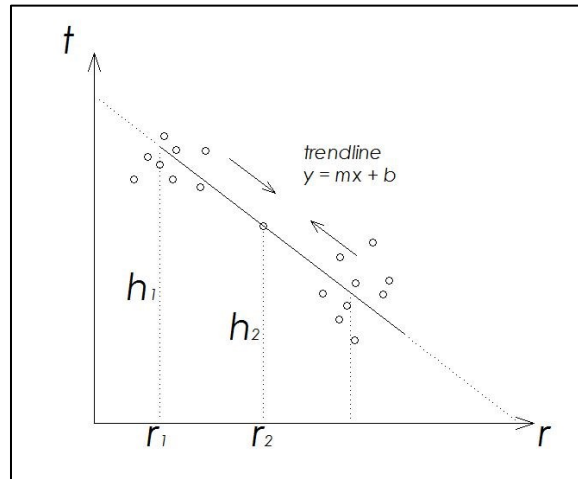


**Figure A94: Scan Rate Corrections**

Wall temperatures were averaged across all sensors for each scan. These temperatures were then averaged again along the length of the scan to obtain one overall temperature for each scan. These average wall temperatures and average scan rates were plotted for each scan and a trend line was drawn. Data generally fell into a faster scan or slower scan. The parameter  $h_1$  represents the temperature given by the trend line equation at the average rate for that scan. This value is unique for each scan. The trend line was obtained in excel. The parameter  $h_2$  is a constant for all scans and represents the temperature given by the trend line equation at the rate temperatures are being normalized to. This is a common scan rate to help normalize the temperatures on the wall.



## Appendix E (Continued)

The correction factor was then found by the following relationship:

$$c_r = \frac{h_2}{h_1} \quad (4)$$

The second correction factor was the calibration correction factor:

A term was also needed to correct for variance in calibration. This was done by finding  $s_n$ . This is the average temperature detected by a sensor  $n$ . The entire data from each of the twelve scans was used to calculate this average. All sensors were then normalized to IR1. The following relationship was used:

$$t_c = s_n - s_1 \quad (5)$$

This corrective term was then used to correct the data along with the rate correction factor. The temperatures that were actually graphed into thermal images were obtained by:

$$t_n = t_i c_r - t_c \quad (6)$$

The corrections were tailored to the specific data of each wall, and those data sets were kept separate for purposes of calibration.

## Appendix F: Wall Scan Overlays

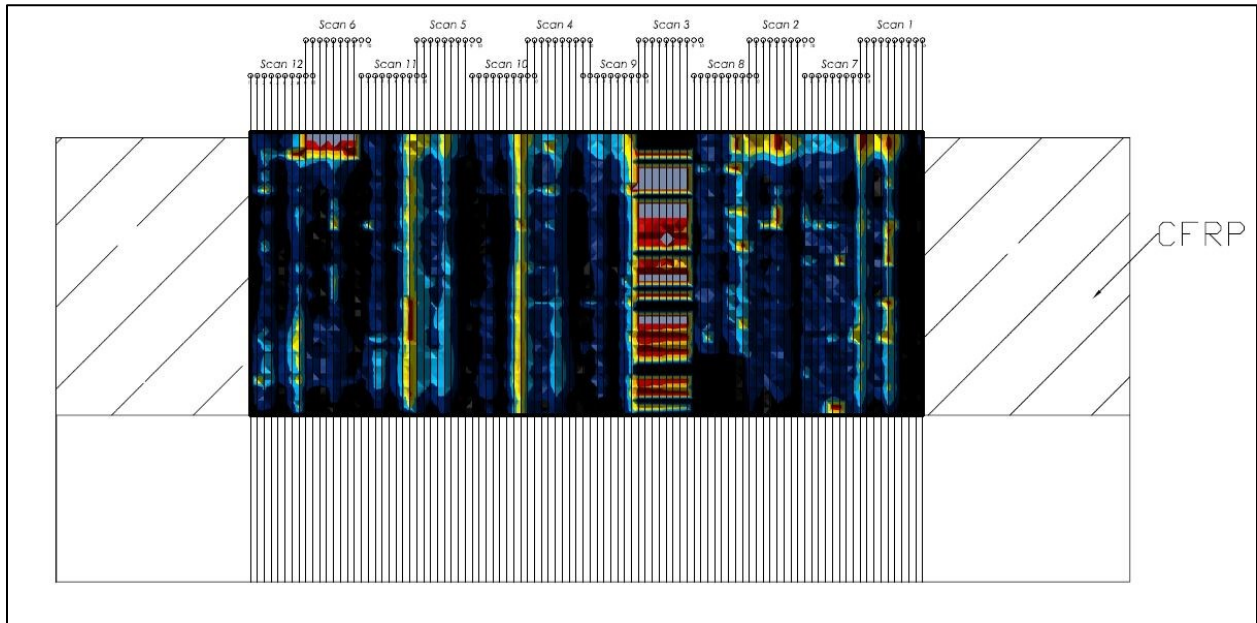


**Figure A95: Wall 2 Scan Overlay (Looking South)**

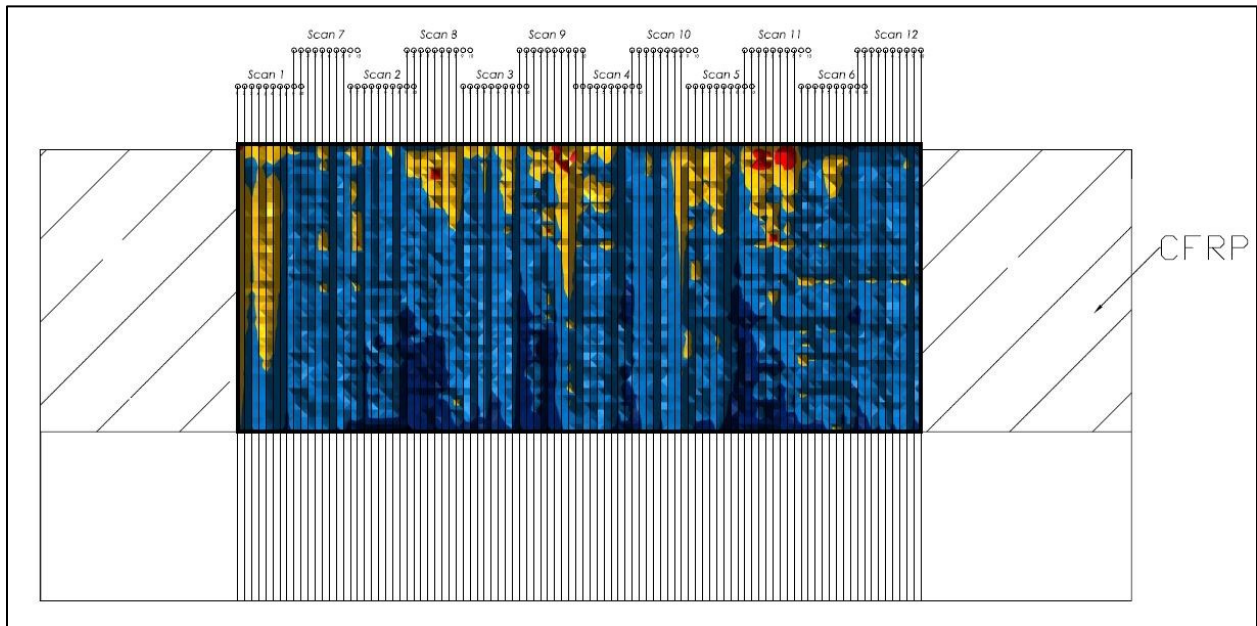


**Figure A96: Wall 3 Scan Overlay (Looking South)**

## ABOUT THE AUTHOR

Joseph Ross completed a Bachelor of Science in Civil Engineering degree at the University of South Florida in May 2010. During and since his undergraduate experience, Joseph has worked with several civil engineering companies. While still working on his undergraduate degree, Joseph worked as an intern with Professional Service Industries, Inc. (PSI) in their geotechnical department. He later worked as an intern at The Structures Group, Inc. The work done with The Structures Group consisted mainly of structural design of residential and light commercial buildings, as well as some forensic structural engineering. Currently Joseph works for Hatch Ltd. in their structural engineering department and works on designing industrial steel structures for use in the mining, metals, and energy sectors. Joseph is currently registered as an Engineer Intern with the Florida Board of Professional Engineers.